

Archive ouverte UNIGE

https://archive-ouverte.unige.ch

Thèse 2016

Open Access

This version of the publication is provided by the author(s) and made available in accordance with the copyright holder(s).

The fate of mercury species from the shallow to the deep waters of a large lake

Gascon Diez, Elena

How to cite

GASCON DIEZ, Elena. The fate of mercury species from the shallow to the deep waters of a large lake. Doctoral Thesis, 2016. doi: 10.13097/archive-ouverte/unige:86030

This publication URL: https://archive-ouverte.unige.ch/unige:86030

Publication DOI: <u>10.13097/archive-ouverte/unige:86030</u>

© This document is protected by copyright. Please refer to copyright holder(s) for terms of use.

Docteur Jean-Luc Loizeau

The Fate of Mercury Species from the Shallow to the Deep Waters of a Large Lake

THÈSE

présentée à la Faculté des Sciences de l'Université de Genève pour obtenir le grade de Docteur ès Sciences, mention Sciences de l'Environnement

par

Elena Gascón Díez

de

Madrid (Espagne)

Thèse N° 4917

GENÈVE Atelier d'impression ReproMail 2016



Doctorat ès sciences Mention sciences de l'environnement

Thèse de Madame Elena GASCÓN DIEZ

intitulée :

"The Fate of Mercury Species from the Shallow to the Deep Waters of a Large Lake"

La Faculté des sciences, sur le préavis de Monsieur J.-L. LOIZEAU, docteur et directeur de thèse (Institut F.-A. Forel), Monsieur D. ARIZTEGUI, professeur associé (Département des sciences de la Terre), Monsieur H.-R. PFEIFER, professeur honoraire (Institut des dynamiques de la surface terrestre, Institut des sciences de la Terre, Université de Lausanne, Suisse), Madame Andrea GARCIA BRAVO, docteure (Department of Ecology and Genetics, Limnology, Uppsala University, Sweden) et Madame Rocío MILLÁN GOMEZ, docteure (Departemento de Medio Ambiente, Unidad de Conservación y recuperación de suelos, Centro de Investigaciónes Energéticas, Medioambientales y Tecnológicas, Madrid, España), autorise l'impression de la présente thèse, sans exprimer d'opinion sur les propositions qui y sont énoncées.

Genève, le 4 avril 2016

Thèse - 4917 -

Le Doyen

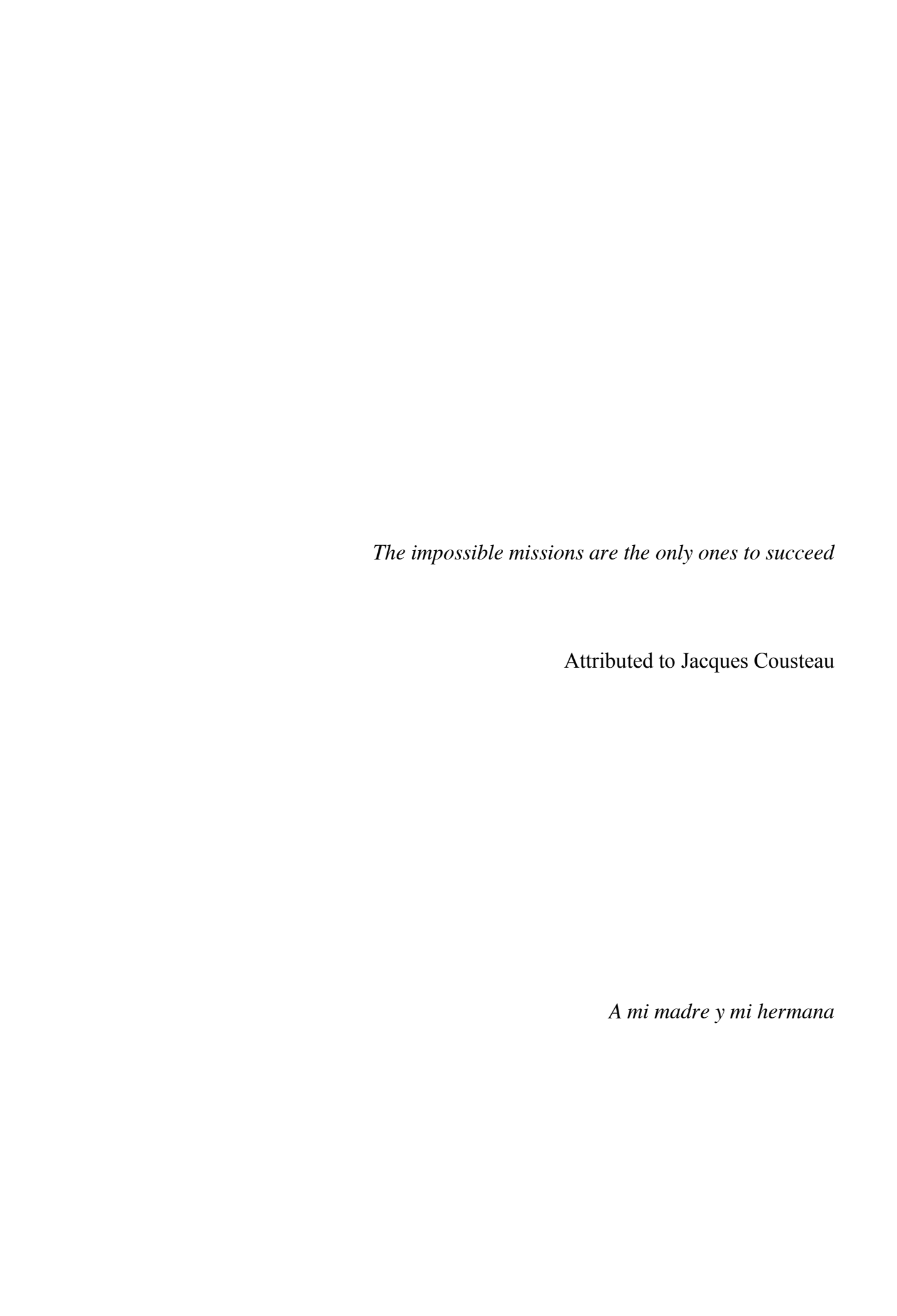


Table of Contents

List of Figures	xi
List of Tables	.xiii
Acknowledgements	XV
French Summary – Résumé en Français	xvii
Abstract	.xix
CHAPTER I	1
1. Introduction	3
1.1. Project context and objectives	
1.2. State of the art	
1.2.1. Natural releases of mercury to the atmosphere	6
1.2.2. Anthropogenic Hg releases to the atmosphere	7
1.2.3. Anthropogenic releases to the aquatic system	8
1.2.4. Mercury global cycle	9
1.3. Research objectives and approach	12
1.3.1. Study case: Vidy Bay, Lake Geneva	14
References	17
CHAPTER II	23
Abstract	27
1. Introduction	28
1.1. Settings	29
1.2. Important dates for the WWTP	30
2. Materials and methods	31
2.1. Sampling and subsampling	
2.2. Volume magnetic susceptibility, freeze-drying and sediment grain size distribution	
2.3. Dating	
2.4. Total organic carbon, mineral carbon, Hydrogen Index and Oxygen Index	

2.5. Total nitrogen analysis	33
2.6. Mercury analyses	33
2.7. Trace elements	33
2.8. Enrichment factor calculations	34
2.9. Statistics	35
3. Results	35
3.1. Stratigraphic units	35
3.2. Age model	38
3.3. Geochemistry	39
3.3.1. Geogenic elements	40
3.3.2. Anthropogenic trace elements	41
4. Discussion	45
4.1. Physico-chemical parameters	45
4.2. Total organic carbon and mineral carbon	46
4.3. Hydrogen Index, Oxygen Index and C/N ratio	46
4.4. Detrital composition of the sediment	47
4.5. Historical reconstruction of pollutants in Vidy Bay in the 20th century	48
5. Conclusions	52
Acknowledgements	53
Supporting information	54
References	55
CHAPTER III	61
Abstract	65
1. Introduction	66
2. Methods	67
2.1. Direct sediment observation.	67
2.2. Core sampling and sediment processing	71
2.3. Sedimentological and chemical analyses	72
2.4. Statistical analyses	73
3 Results and discussion	74

3.1. Surface sediment analyses	74
3.2. THg _{sed} : an indicator of the contamination from the WWTP	77
3.3. Hg speciation in pore water	78
3.4. Hg speciation in overlying waters	79
3.5. Influence of sediment types on Hg forms	80
4. Summary	82
Acknowledgments	82
References	83
CHAPTER IV	87
Abstract	91
1. Introduction	92
2. Materials and methods.	94
2.1. Sediment and settling particles sampling	94
2.2. Geochemical analyses	96
2.3. Sediment dating and mercury flux in sediments at NG2	96
2.4. Statistical analyses	97
3. Results	98
3.1. Grain-size distribution evolution	98
3.2. THg concentrations and fluxes	99
3.3. MeHg concentrations and fluxes	101
4. Discussion	103
4.1. Grain-size distribution	103
4.2. The fate of THg	103
4.3. The fate of MeHg	106
5. Summary	107
Acknowledgements	108
Supporting information	109
References	111

CHAPTER V	115
Abstract	119
1. Introduction	120
2. Materials and methods	121
2.1. Study site and sampling strategy	121
2.2. Hg-methylation and demethylation rate constants in sediments and settlin particles	_
2.3. Laboratory analyses	123
2.3.1. THg and MeHg concentrations in sediments and settling particles	123
2.3.2. Sulfate-reduction rates	124
2.3.3. Total organic carbon, mineral carbon, Hydrogen Index and Oxygen Index	124
2.3.4. Total nitrogen analyses	125
2.4. Mineral composition analyses	125
2.5. Statistical analyses	125
3. Results and discussion	126
3.1. Temporal trends of THg and MeHg concentrations in sediments and settling particles	126
3.2. THg and MeHg sources for Lake Geneva	128
3.3. Hg species transformation rates in sediments and settling particles	129
3.4. Bacterial anaerobic metabolism contributes to Hg methylation in oxic water column	131
3.5. Organic matter quality favors Hg-methylation in particles compared to sediments	132
3.6. Environmental perspectives	135
Acknowledgments	136
Supporting information	137
References	145
CHAPTER VI	151
1. General discussion	153
1.1. Historical and current THg accumulation and fate in sediments and settling particles	153

	1.2. MeHg distribution and production in lake compartments	157
2.	Conclusions	159
3.	Perspectives	160
Re	eferences	163

List of Figures

CHAPTER I Introduction

Figure 1. Main sources of mercury of the global Hg budget to the atmosphere	6
Figure 2. Natural releases to the atmosphere	7
Figure 3. Anthropogenic releases to the atmosphere.	8
Figure 4. Hg cycle: reactions, transformations and transfers	10
Figure 5. Schematic role of bacteria on Hg methylation	11
Figure 6. Location of Lake Geneva and map of Vidy Bay	15
CHAPTER II History of contamination of the 20th century	
Figure. 1. Bathymetric map of Vidy Bay of the study area in Lake Geneva	30
Figure 2a. EGD3 core image; sedimentary units and physico-chemical parameters.	36
Figure 2b. EGD3 core age-depth model.	37
Figure 3. Principal Component Analysis of lithological elements and trace metals	40
Figure 4. Geogenic elements.	41
Figure 5. Concentration of trace metals	43
Figure 6. Enrichment factor profiles of anthropogenic elements	45
Figure 7. Hydrogen Index versus Oxygen Index	47
Figure S1. Geogenic element concentrations measured by XRF and ICP-MS	54
CHAPTER III Mercury contamination in sediments	
Figure 1. Map of Vidy Bay and sediment type distribution.	70
Figure 2. Photos of the different types of sediments surfaces.	71
Figure 3. Concentration ranges of THg in surface sediments by sediment types	78
CHAPTER IV Mercury distribution from the shore to the deep waters	
Figure 1. Map of the study area and scheme of the chain of traps	95
Figure 2. Mean grain size distribution of settling particles at NG2 and NG3	98
Figure 3. Spatial variability of THg in surface sediment concentration in Vidy Bay	99
Figure 4. THg concentrations and fluxes in settling particles and sediments	100

Figure 5. MeHg concentrations and fluxes in settling particles and sediments 102
Figure S1. Precipitation at the Pully weather station and flow data of the
Venoge River
CHAPTER V Mercury methylation in settling particles
Figure 1. Concentrations THg, MeHg and %MeHg/THg
Figure 2. Hg methylation and MeHg demethylation rate constants and net MeHg
formation in settling particles and surface sediments of Lake
Figure 3. Inhibition of Hg methylation and SO_4^{2-} consumption
Figure 4. C/N ratio and Hydrogen Index versus Oxygen Index
Figure S1. Sampling site location and scheme of the sampling set up
Figure S2. MeHg concentration on a map of the study area
Figure S3. Dissolved oxygen, temperature and redox
Figure S4. Electronic microscopy images
Figure S5. Mineralogical distribution in settling particles and sediments141-142
Figure S6. Calcite abundance in settling particles and sediments
CHAPTER VI Discussion and Conclusions
Figure 1. Location of the reference site, SHL2, in Lake Geneva
Figure 2. Schema of particle transport from the shore to the deep lake

List of Tables

CHAPTER II History of contamination of the 20th century
Table 1. Mean metal concentrations per stratigraphic unit
CHAPTER III Mercury contamination in sediments
Table 1. Sediment core locations and corresponding sediment type
Table 2. Mercury species, sulphate and iron concentrations in lake sediments 75-76
Table 3. Correlation p-values between the measured parameters
Table 4. Independence Mann-Whitney-Wilcoxon test for non-distance correlated
variables
CHAPTER IV Mercury distribution from the shore to the deep waters
Table 1. Comparative table of Sediment Accumulation Rates, Organic Matter, and
CaCO ₃ fluxes per sampling site and year
Table S1. Sampling dates, Sediment Accumulation Rates, Organic Matter and CaCO ₃
data collected at NG2 and NG3
CHAPTER V Mercury methylation in settling particles
Table S1. Correlation matrix between minerals settling particles and sediments 144

Acknowledgements

I would like to thank all those persons that have been at my side day by day during this special journey.

First of all I want to express all my gratitude to my supervisor Jean-Luc Loizeau who believed in me and gave me the extraordinary opportunity to realize this PhD and sharing his knowledge and experience. It was a pleasure to work with such a motivated and involved and patient person.

I also thank the members of the jury, Andrea G. Bravo, Rocío Millán, Daniel Ariztegui and Hansuedi Pfeifer for their time their advises sharing their scientific knowledge.

I thank Guillermo Díaz del Río and Mary-Lou Tercier-Weaber, for being the firsts persons trusting in my scientific career. Janusz Dominik, Walter Wildi, Raffaele and Sandro Peduzzi for their interest in my work.

A special thank goes the co-authors of the papers published in the context of this work. Without them this could not have been possible.

Thank to all my colleagues of the Forel Institute, especially Arnaud, Anh-Dao, Eric, Sonia, Claudia, Philippe, Daniel, Serge and John for their patience and good humor.

My Swiss families The Fulliquet and The Hakistar, and also my flatmates Matthieu and Fabrice. My Spanish friends in Switzerland Thaïs, Carolina, Chelo, Nani, Javi, Luis, Dani and Isa. Finally my lifelong friends Rafa, Raúl, Pablo and Elena.

I am of course especially grateful to my family, my mom and my sister, for their support anytime and anywhere, for taking care of me despite of the distance, for believing in me and for the love they always give me. And my father for the legacy he left here. You all did a great job ¡Muchas Gracias!

My heartfelt thanks to all of them and to those I could forget in this list.

French Summary – Résumé en Français

Le but de cette thèse est de caractériser les sources et la distribution spatio-temporelle du mercure particulaire depuis la côte jusqu'au large d'un grand lac. Le cas d'étude est la Baie de Vidy, qui a été reconnu par des études précédentes comme l'endroit le plus contaminé du Léman à cause du rejet des eaux usées préalablement traitées ou non par une station d'épuration. Une étude sur l'historique à haute résolution du mercure, d'autres métaux traces toxiques ainsi que sur la matière organique, dans des sédiments situés près de l'exutoire des eaux usées, a permis de déterminer les périodes pendant lesquelles la contamination était la plus importante dans la Baie de Vidy. La pollution de cette zone a commencé au début des années 1930. Après l'installation de la station d'épuration en 1964 dans la baie, une augmentation concomitante de la contamination a été observée pour certains métaux (plomb, cadmium, cuivre, zinc et mercure). Cependant, un pic important de pollution a été enregistré en 1986 pour le mercure (11µg g⁻¹). De nos jours, la valeur de contamination du mercure oscille entre 0.32 et 10.1 µg g⁻¹ en fonction de la distance par rapport à l'exutoire. Dans la couche néphéloïde près de l'interface eau-sédiments, la concentration totale en mercure est plus forte pour l'eau non filtrée comparée à celle de l'eau filtrée. D'autres propriétés basées sur la couleur, la texture et la structure de la surface des sédiments ont été étudiées. Une relation entre ces caractéristiques et la contamination en mercure a été établie, sans pour autant trouver une corrélation statistique entre le type de sédiment et cette pollution. Les flux et les concentrations en mercure total et méthylmercure sur des sédiments et des particules qui sédimentent (settling particles) ont été également étudiés pendant deux ans, principalement sur deux sites pour deux profondeurs de la colonne d'eau au large de la Baie de Vidy. Les résultats de cette étude ont montré, tout d'abord, l'existence d'une resuspension du mercure total particulaire du sédiment dans la colonne d'eau, cinq mètres au-dessus de la surface de sédiment. Mais également une diminution des apports en mercure total particulaire, dépendant de la distance par rapport à la source initiale de mercure provenant de la rive. Cette diminution pourrait s'expliquer par un mélange d'advection entre le bassin principal et la zone côtière.

Finalement, les taux de sédimentation des particules et de la matière organique, pour les deux sites échantillonnés (situés à 1,900 et 2,800 mètres depuis la côte), restent élevés comparés aux données précédemment acquises pour le site SHL2 situé au centre du lac (point le plus profond). Concernant les résultats pour le méthylmercure, de plus fortes concentrations et flux ont été mesurés dans les particules de la colonne d'eau que dans les sédiments. A l'inverse du mercure total, la distance par rapport à la zone cotière n'affecte pas clairement la concentration et le flux en méthylmercure. Cela suggère que la source principale ne provient pas de la côte mais d'une méthylation au sein même des particules. Pour mieux comprendre ces potentielles méthylations dans les particules, des incubations avec des traceurs isotopiques (méthylmercure, mercure inorganique) ont été effectuées en parallèle dans les particules en suspension et dans les sédiments. La production potentielle de méthylmercure dans les particules de la colonne est dix fois plus élevée que dans les sédiments. Ces résultats confirment l'hypothèse possible d'une méthylation in situ. La forte méthylation déterminée dans les particules est attribué essentiellement à la qualité de la matière organique, plus algale ou fraîche que dans les sédiments, permettant une assimilation plus aisée pour les micro-organismes responsables de la méthylation du mercure. Ici, ces organismes sont principalement des bactéries sulfatoréductrices anaérobiques, suggérant la présence de micro-gradient d'oxygène dans les particules de la colonne d'eau oxique du Léman. Cette découverte ouvre la voie à des recherches sur une meilleure compréhension des processus de méthylation du mercure dans un milieu jusqu'alors considéré comme non propice à la transformation de ce polluant en une forme plus toxique pour la biocénose lacustre.

Abstract

The aim of this study was to characterize the sources and the spatio-temporal distribution of particulate mercury in and around a contaminated area of a freshwater lake. The study case was Vidy Bay, which is the most contaminated area of Lake Geneva, due to the sewage effluents of a wastewater treatment plant.

A high-resolution reconstruction of mercury, other toxic trace metals and organic matter in sediments nearby the effluent of the wastewater treatment plant allowed determining the most important periods of contamination in the bay. Although the contamination in the lake started early and slowly increased along with the industrial evolution in Europe, the highest values of Hg were recorded in Vidy Bay, reaching a maximum of 11 µg g⁻¹, in 1986. This contamination was clearly related to the wastewater treatment plant effluents that also modified the organic matter quality. Nowadays, the contamination of mercury in sediments within the bay varies between 0.32 and 10.1 µg g⁻¹ as a function of the distance to the outlet pipe. Total mercury was also observed to be important in the non-filtered water of the nephloid layer in the contaminated bay. Moreover, different visual characteristics were observed in sediments of the bay. No statistical correlation was found between the visual characteristics of sediments and the mercury contamination. Total mercury and methylmercury concentration and fluxes were also studied over almost two years in sediments and settling particles, mainly at two sites and two depths near Vidy Bay. The results of this study suggested that (i) particulate total mercury is resuspended at the bottom of the lake (5m), (ii) there is an input of particulate total mercury into the lake from the shore to the deep lake that disappears with distance, probably due to the mixing of advection between the main basin and the coastal zone, and (iii) mercury in studied settling particles at the two sites (1,900 m and 2,800 m from the shore) were still affected by the littoral inputs. Regarding the methylmercury results, higher concentrations and fluxes in settling particles than in sediments were found. Slightly more MeHg was observed in concentrations and fluxes at both sites. However, not a clear decrease of these values with the distance to the shore was observed. Thus, it is suggested that an internal methylation was taking place on settling particles. In order to demonstrate this potential methylation in settling particles, isotopic-mercury incubations in surface sediments and settling particles were carried out. Methylation yields in settling particles were 10-fold higher than methylation yields in sediments. These results strongly supported the hypothesis of possible methylation in settling particles. The reason of this high methylation in settling particles pointed to the quality of the organic matter, which was more algal or fresh type in settling particles than in sediments. As mercury methylation is an anaerobic microbiological process, anoxic microzones are suggested to exist inside the settling particles.

CHAPTER I

Introduction

1. Introduction

1.1. Project context and objectives

This thesis forms part of a major collaborative project in which nine research groups, from different Swiss institutions were involved. Léman 21 is a project conceived to prevent the negative influences that humans can cause to large lakes. The sustainable management of these ecosystems passes by scientific investigation fields such as chemistry, microbiology, or physical dynamics. As most contaminants enter in lakes from the shore through runoff, wastewater treatment plant effluents or diffuse sources, Léman 21 aimed at understanding the water dynamics and contaminant transfer processes from shallow to deep waters. Four different issues had been raised for the global understanding on pollutants brought into mid-sized lakes by the demographic pressure of the catchment area:

<u>Module 1:</u> Water dynamics and contaminant transfers from the shallow to the deep waters of a mid-sized lake.

<u>Module 2</u>: The origin of micropollutants in the catchment and their transport to a mid-sized lake.

<u>Module 3:</u> Micropollutant degradation in a mid-sized lake: Coupling degradation and dilution processes with lake dynamics.

<u>Module 4:</u> Microbial resistance, ecotoxicological impact, and risk assessment of micropollutants in a mid-sized lake.

These four projects helped to understand and quantify aquatic contaminants transfer from the shoreline to deeper parts of Lake Geneva as a case study.

Contaminants in aquatic systems are often particle-bound, in particular hazardous metals such as mercury. For this reason, within the Module 1, major processes involving the transport of sediments from the shallow to deeper areas of the lake were studied. Vidy Bay (near the city of Lausanne), was a suitable area of Lake Geneva to characterize anthropogenic contaminant from the coast. Previous studies investigated

wind, tides, and wave influences on currents of Vidy Bay (Lemmin et al., 2005; Graf et al., 1979). In the frame of this project, numeric simulations were used to study current influences between the main basin of Lake Geneva and Vidy Bay showing the existence of a near-shore gyre and the limit of the bay using the zero vorticity line was modeled (Razmi et al., 2013). Residence time was calculated using particle tracking, providing important information about the contaminant transport. The particularity of Vidy Bay is, that due to significant gyres, the residence time varies between 50 to 100 hours depending on wind and current regimes. Other models have been developed to determine the fate of micropollutants in aquatic environments (such as the spreading of the wastewater plume), but never integrating 3D-hydrodynamics with depth dependant degradation processes. As a result of the Léman 21 project, a coupled Hydrodynamic-Photolysis model could be used to simulate the zone of ecotoxicological risk in Vidy Bay, which extends over 300 m horizontally from the wastewater treatment plant (Bonvin et al., 2013). In addition, other studies pointed to a persistent loading of particle-bound contaminants in the bay (Graham, 2015).

Heavy metals are hazardous to the aquatic ecosystem and human health. They can be present either in organic or inorganic forms. Cadmium, copper, nickel, lead, and zinc are toxic trace metals widely found in the environment (Wang et al., 2009). Of special concern is mercury (Hg), a toxic trace metal which is the only one found in liquid state at standard conditions of temperature and pressure. Hg naturally occurs in the environment and the most common natural forms are metallic mercury, mercury salts (mercury sulfide and mercuric chloride) and organic mercury (methylmercury). This toxic trace element has the particularity to accumulate over time in organisms (bioaccumulation) and along the food chain (biomagnification) when present as its organic form, methylmercury (MeHg), causing nerve damage, muscle tremors, distorted speech, dizziness and blurred vision and hallucinations.

The objective of this work is to determine the fate of mercury derived from the shore as the most contaminated areas and its potential dispersal towards the deeper areas of the lake throughout the measurements of total mercury (THg) and methylmercury (MeHg) attached to particles.

1.2. State of the art

Mercury is ubiquitous in the environment and is unique among metals due to its high volatility. Natural Hg ore is found forming rocks surrounding geologically recent volcanic activity as a toxic mercury sulfide mineral, cinnabar (HgS). Other Hg-rich materials are often burned, as in coal combustion or waste incineration. Mercury is released to the atmosphere as a gas either in elemental form, Hg(0), or oxidized divalent form, Hg(II). The oxidized form is water-soluble and usually found as HgCl₂ that is promptly deposited nearby the emission source. Hg(0) is not water-soluble and it is oxidized to Hg(II) to be deposited. This oxidation takes place in the atmosphere on a time scale of one year, during this time the emitted Hg can be easily transported to other areas of the world by atmospheric circulation and deposited, contributing to global pollution problems (Minamata Convention Report). Once Hg(II) is deposited in waters, soils and mostly in sediments, it is likely methylated monomethylmercury, CH₃Hg⁺, which is the most toxic form of mercury, together with dimethylmercury, (CH₃)₂Hg. Their thermal instability and photodegradation keep the concentrations of both methylmercury's (MeHg) generally low. However the degradation of aquatic MeHg may represent a source of Hg(II). Of major concern are Hg anthropogenic releases, considerably raising Hg levels in the biosphere, and in terrestrial and water systems. This accumulation is evident from sediment cores that provide historical records of mercury deposition for the last several centuries.

The major sources of mercury in the environment can be classified into:

- Natural Hg releases to the atmosphere
- Anthropogenic Hg releases to the atmosphere
- Anthropogenic releases to aquatic systems

In this thesis, especial awareness is given to freshwater ecosystems, impacted by the releases of dry and wet Hg depositions caused in an anthropic littoral zone.

1.2.1. Natural releases of mercury to the atmosphere

Natural emissions of gaseous elemental mercury to the atmosphere from geogenic releases are a continuous source of elemental Hg (80-600 t y⁻¹; Mason et al., 2012; Ferrara et al., 2000). Biomass burning (Friedli et al., 2009), soil and vegetation, together with oceanic evasions are the main sources of Hg to the atmosphere (Figures 1 and 2). Similarly, the majority of loads to oceans come from wet and dry atmospheric deposition (Mason et al., 2012; Mason et al., 1994; Soerensen et al., 2010). In lakes with high dissolved organic carbon and Hg content, evasion rates can reach 130 ng m⁻² d⁻¹ (Boudala et al., 2000).

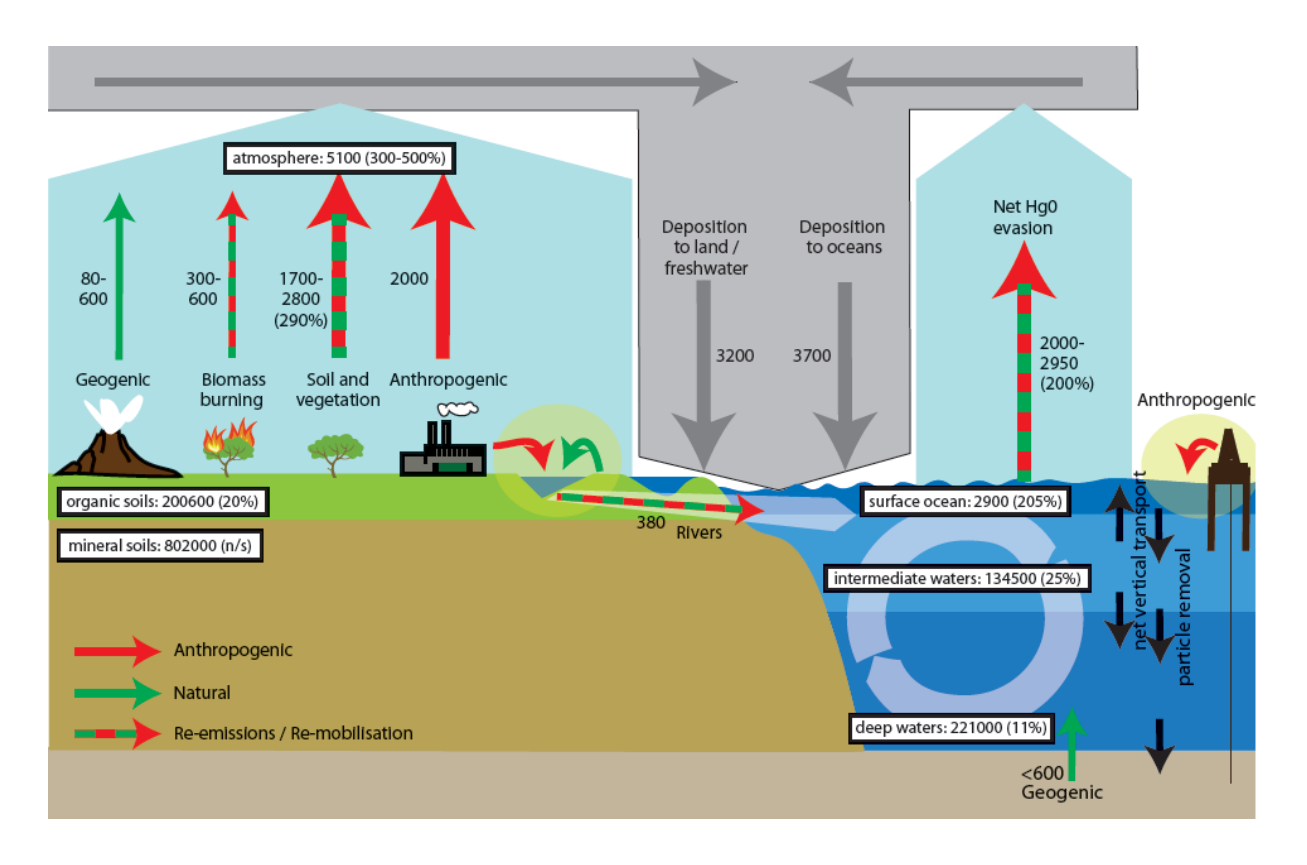


Figure 1. Main sources of mercury of the global Hg budget to the atmosphere.

Mason et al. (2012) and AMAP/UNEP (2013).

In 2000, mercury emissions (including re-emissions) from natural processes, was estimated at $5,207 \text{ Mg y}^{-1}$, this is 70% of the global mercury emission budget. Oceans were the most important sources (52%) followed by biomass burning (13%), desert/metalliferous/non-vegetated zones (10%), tundra / grassland / savannah /

prairie / chaparral (9%), forests 7 (%) (Figure 2). Evasion after mercury depletion events represented 4% of the total emissions and volcanoes and geothermal areas; agricultural areas and lakes represented 2% each.

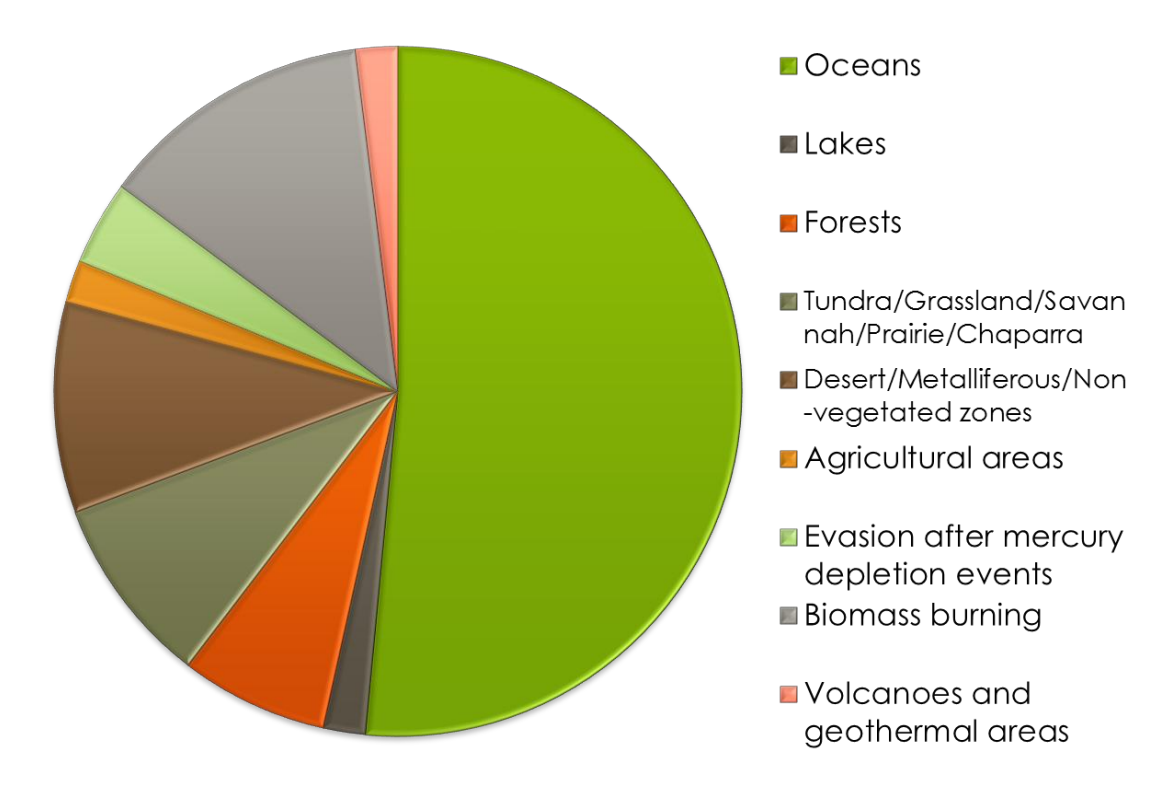


Figure 2. Natural releases to the atmosphere. Adapted from Pirrone et al. (2010).

Although land, water, and other surfaces can regularly re-emit mercury into the atmosphere after its initial release into the environment, atmospheric mercury nowadays can also be the results of reminiscences from past emission.

1.2.2. Anthropogenic Hg releases to the atmosphere

Anthropogenic Hg emissions significantly contribute to the global pool of mercury in the environment. Different anthropogenic activities promote Hg releases due to the ability of mercury to form amalgams; it has been largely used in gold mining activities (37.1%) and gold production or in dental amalgams in the past. Coal combustion (24.2%), metal production (9.9%), cement production (8.8%), waste water (4.9%), and contaminated sites contribute (4.2%) as well to the Hg atmospheric pollution (Figure 3). Paradoxically, mercury production "only" releases 0.6% of the total antropogenic Hg-inputs in the atmosphere.

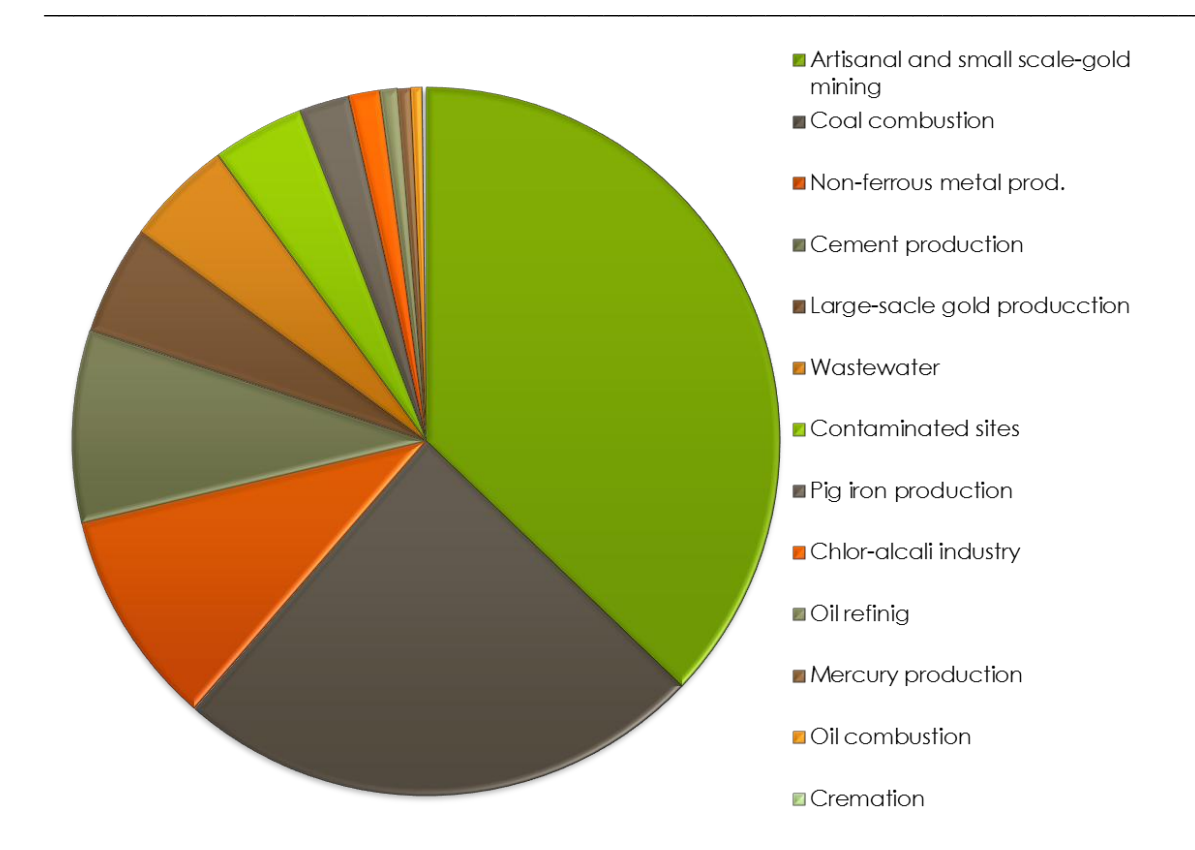


Figure 3. Anthropogenic releases to the atmosphere.

Adapted from AMAP/UNEP (2013).

Mercury emissions are closely related to industrial and energy sources primarily affecting the United States, Canada, Australia and EU members (AMAP/UNEP, 2013). Cremation is estimated to contribute 0.2% of the total anthropogenic emissions. Asia is the region that releases the highest amount of Hg (around 500 tons in 2010) principally through cremation from human remains. Fortunately, major emitting countries are reducing their emanations using new mitigating policies.

1.2.3. Anthropogenic releases to the aquatic system

Large amounts of Hg can reach water systems throughout anthropogenic additions. However, these releases are poorly reported and only past stock-take can be found. Distribution factors have been used to estimate the releases of point source releases to water (AMAP/UNEP, 2013). Hg releases to continental waters are mainly from non-ferrous production industries, oil refineries, chlor-alkali plants, and other waste activities such as wastewater treatments plants (Muller et al., 2000; Wihlborg and

Danielsson, 2006; Bravo et al., 2009; Karageorgis et al., 2009). Urban Wastewater Treatment Plants (WWTP) have historically been significant contributors of Hg to receiving waters, however, these discharges of mercury have sharply decreased in the last 30 years (Balogh et al., 1999). Although some studies focused on the transformations of Hg within a WWTP or the effects of domestic sewage treatment on THg and MeHg concentrations (Bodaly et al. 1998; Gbondo-Tugbawa et al. 2010), they do not assess the impact that WWTP effluents can have on sediments or the behaviour of mercury-bound settling particles.

Even though the volume of continental waters is small compared to the oceans, lacustrine environment have characteristic geochemical processes (Salomons and Förstner, 1984). Hg can be introduced in lakes either in solution or in particulate form. The allochthonous particles will partially settle to the bottom and the dissolved Hg is subject to removal processes such as sorption, uptake by biota and incorporation in authigenic phases. Because natural processes occur within the aquatic ecosystems, covering the speciation of this metal, it is important to understand mercury's aquatic pathways and fate.

1.2.4. Mercury global cycle

As mentioned above, Hg enters aquatic ecosystems through several ways, including atmospheric deposition, natural runoff, point source emission from industry or leaching from contaminated areas (Figure 4). Divalent mercury Hg(II), from the oxidation of volatile elemental mercury, Hg(0), in the atmosphere, reaches the aquatic surfaces via wet or dry depositions. Once in surface water, it can be reduced to Hg(0) through photochemical processes (Fitzgerald et al., 1991; Rolfhus and Fitzgerald, 2004). The amount of Hg(II) reduced by this process depends on the intensity of solar radiation received in the escosystem (Lanzillotta and Ferrara, 2001; Fantozzi et al., 2007; O'Driscoll et al., 2007). The remaining Hg(II) within the water column likely binds to suspended particles and then its fate depends on the particle transformation, transport and deposition. This Hg adsorbed to particles in the sediments can be either buried by younger sediments, and thus sediments are a sink of mercury; or resuspeded,

in which case, sediments are a secondary source of mercury (Blasco et al., 2000; Bale, 2000, Figure 4).

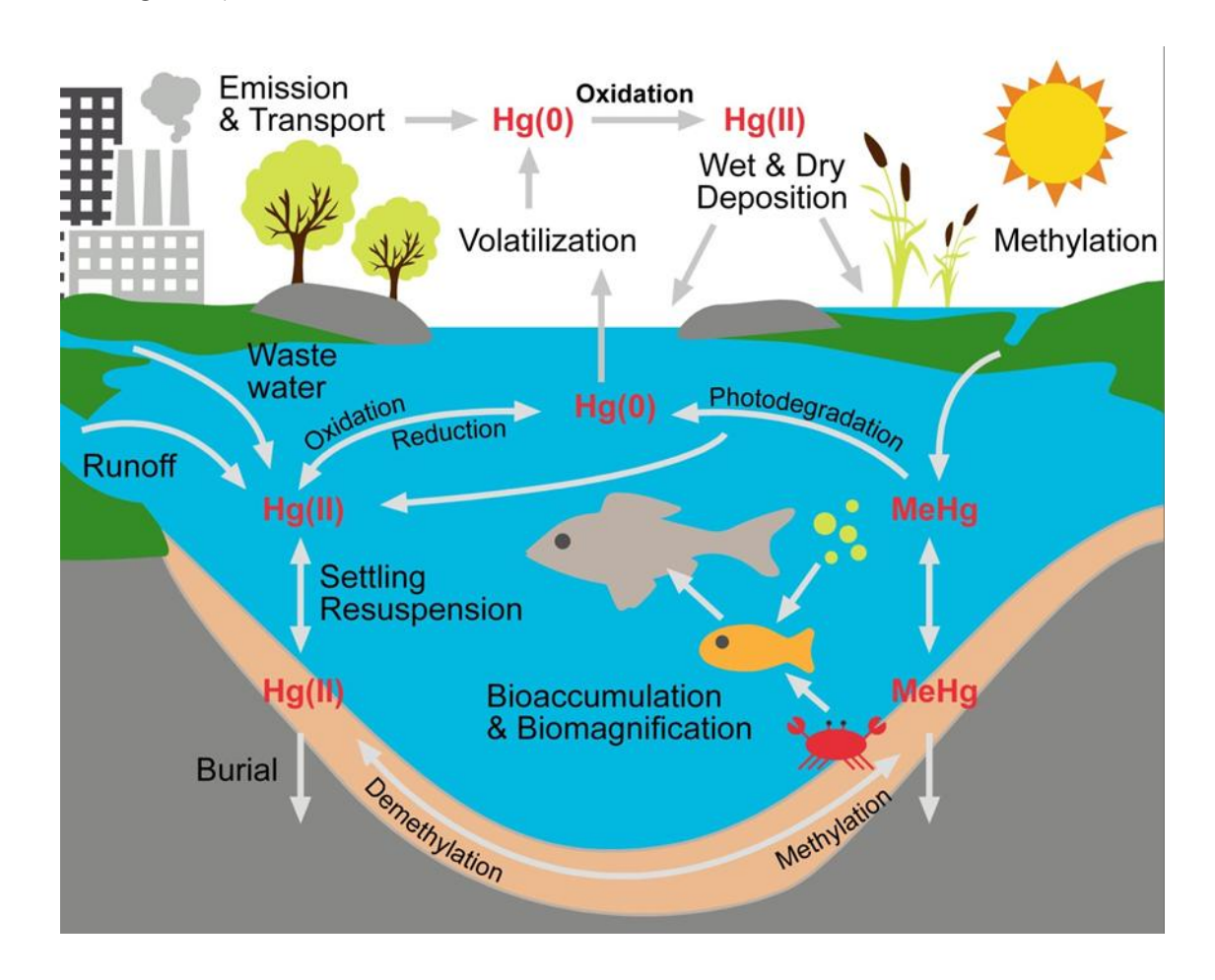


Figure 4. Hg cycle: reactions, transformations and transfers.

Adapted from Engstrom (2007).

Inorganic Hg(II) in sediments can be methylated, forming methylmercury (MeHg) which is a potent neurotoxin that is biomagnified in food chains of aquatic systems and can damage the wild life (Scheulhammer et al., 2007), depending on the concentration and the compunds. Due to its chemical properties, Hg(II) it forms stable complexes with ligands such as thiols, HS⁻, and CN⁻ (Pearson, 1963; Hepler and Olofsson, 1975). These complexes are important since inorganic Hg can be methylated by heterotrophic bacteria under sub-oxic conditions. Certain microorganisms with anaerobic metabolisms absorb Hg(II). The best suited organisms to methylate mercury are specific strains of sulfate-reducing bacteria (SRB) (Compeau and Bartha, 1985;

Gilmour and Henry, 1992; Gilmour et al., 2013; Parks et al., 2013; Podar et al., 2015) and iron-reducing bacteria (IRB) (Fleming et al., 2006; Kerin et al., 2006; Schaefer and Morel, 2009; Si et al., 2015) (Figure 5). To a lesser extent, methanogens and firmicutes (Yu et al., 2013) have been also reported to methylate.

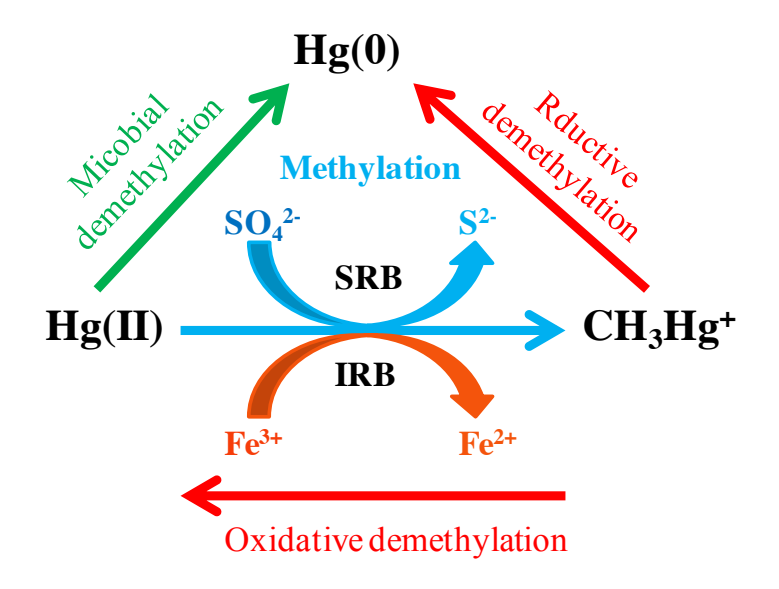


Figure 5. Schematic role of bacteria on Hg methylation (Yu et al., 2012).

To date, Hg-methylation is known to primarily occur at the oxic-anoxic boundary of stratified water columns and lake sediments (Figure 4) (Malcolm et al., 2010). Only a few works report Hg-methylation in oxygenated environments, where most of them showed Hg-methylation in marine oxic waters (Cossa et al., 2009; Lehnherr et al., 2011; Monperrus et al., 2007a; Sunderland et al., 2009). Only one work suggested the possible Hg-methylation on settling particles in the lake waters (Eckley et al., 2005).

Abiotic methylation is also possible only if suitable methyl donors are present. Small organic molecules such as methyl iodide and dimethylsulfide, and larger organic components of dissolved organic matter such as fulvic and humic acids are thought to produce abiotic methylmercury. Organometallic complexes such as methylcobalamin, methyllead and methyltin compounds have also been considered to induce chemical Hg-methylation pathways in the aquatic environment. However, these processes have not been much described in the literature (Weber, 1993; Celo et al., 2006).

Although MeHg is a stable molecule, it can be degraded producing Hg(II) or Hg(0). The MeHg decomposition can be abiotically induced by photodegradation in the water column (Sellers et al., 1996). On the other hand, certain microorganisms are able of demethylate MeHg in sediments by reductive or oxidative pathways, depending on the level of Hg contamination (Marvin-DiPasquale et al., 2000; Hines et al., 2006). The methylated form is the main form of Hg transfer and accumulation along the food chain.

Finally, bioaccumulation in living aquatic organisms depends on the bioavailability of MeHg. Thus, MeHg produced in the water column is suggested to bioaccumulate in marine food webs via direct uptake by phytoplankton and pelagic feeding, whereas MeHg produced in sediments can be taken up through either benthic or pelagic pathways (Mason and Lawrence, 1999; Monperrus et al., 2007b). After bioaccumulation in fish and shellfish, MeHg can easily reach humans through seafood consumption. A clear example of this biomagnification of MeHg along the food cahin is the Minamata disase in 1956. More than 2,000 people were victims of MeHg poisoning, showing ataxia, deadness in the hands and feet, general muscle weakness, loss of peripheral vision, damage to hearing and speech and death (Minamata Convention Report).

1.3. Research objectives and approach

The present work aims to understand contaminant behavior from the shore to the deepest part of a mid-sized lake, using mercury released from an urban WWTP as a tracer of contamination. This thesis, encompasses four scientific papers. The historical evolution of lake sediment contamination resulting from the release of industrial/domestic sewage waters is Chapter II. The interactions between anthropogenic trace metals, lithogenic elements and organic matter in sediments influenced by this kind of effluent, and their recovery when the harmful activity cease, will be described.

The study presented in chapter III, determined the influence of THg releases from the WWTP in different types of sediments reflecting both, sedimentological and

biogeochemical processes. Surface sediments were visually described, and mercury concentrations measured searching for correlations between sediment types. THg partition coefficients ($logK_d$) were studied in each type of sediment, the ratio of THg concentrations between sediments and the pore waters. In addition, an overview of the interaction between the Hg contamination in sediments and the filtered and non-filtered overlying water is given. THg and MeHg concentrations measured in overlying waters suggested that Hg in the water column is likely related to settling particles.

Chapter IV concentrates in long-term Hg-bound suspended sediment shift trends in the bottom boundary layer of the lake. To be able to identify THg and MeHg in vertical and lateral transport paths from the shallow to the deep lake, sediments traps were deployed at two sites and at two depths near Vidy Bay. Settling particles collected over two years in sediments traps were geochemically measured and results were compared with existing data of the center of the lake. This permitted to better constrain the Hg pathways from the shoreline.

Chapter V provides a closer look to possible MeHg formation on settling particles studied in chapter IV. In the light of the results of MeHg/THg ratio measured in settling particles as a proxy for Hg-methylation, incubation experiments were carried out. These experiments permitted a better estimation of methylation rates, which explain the processes that occur in settling particles deposited in sediment traps during the exposition time in the lake in comparison to sediments. Moreover, this chapter explains the biological implication of the Hg-methylation in this environment, and finally the possible environmental drivers of the process.

Chapter VI discuss the findings on this thesis and summarize the general conclusions found in the studies of the different aspects discussed in each individual chapter.

This introduction provides a general view of the study while each chapter includes a specific introduction as well as the used materials and methods.

1.3.1. Study case: Vidy Bay, Lake Geneva

Lake Geneva (Switzerland-France) is a mid-sized lake at global scale, but belongs to the large freshwater systems in Western Europe (Figure 6). It has a volume of 89 km³, a surface area of 580.1 km², a maximum depth of 309 m and a mean residence time of 11.3 years. Lake hydrodynamics are controlled by environmental and meteorological conditions, along with two principal wind regimes that dominate the area (Razmi et al., 2013). Lake Geneva has several WWTP outfalls discharge effluents along the shore (Condamines, 2015). The WWTP of Vidy Bay is one of the most important ones and discharges more than 100,000 m³ day⁻¹ of treated wastewater from the city of Lausanne (Hoerger et al., 2014; Margot et al., 2013). Vidy Bay has been the object of several studies pointing to its contamination by trace metals (Monna et al., 1999; Loizeau et al., 2003; Loizeau et al., 2004; Pote et al., 2008; Thevenon et al., 2011; Bravo et al., 2011; Masson and Tercier-Waeber, 2014, Bravo et al., 2015), organic micropollutants (Perazzolo et al., 2010; Morasch et al., 2010; Bonvin et al., 2013) and fecal indicator bacteria (Haller et al., 2009; Pote et al., 2009), presenting a potential ecotoxicological risk. Some works proposed a spatial extent of the zone bearing an ecotoxicological risk due to the spreading of the micropollutant plume from the WWTP outlet in the water column (Bonvin et al., 2013; Razmi et al., 2014). In addition, suspended colloids and particles at the sediment-water interface, vertical and lateral sedimentation pathways, and hydrodynamic conditions affecting the bottom boundary layer of the bay have been investigated (Graham, 2015). However, dynamics of a particle-bound contaminant such as mercury was not studied yet.

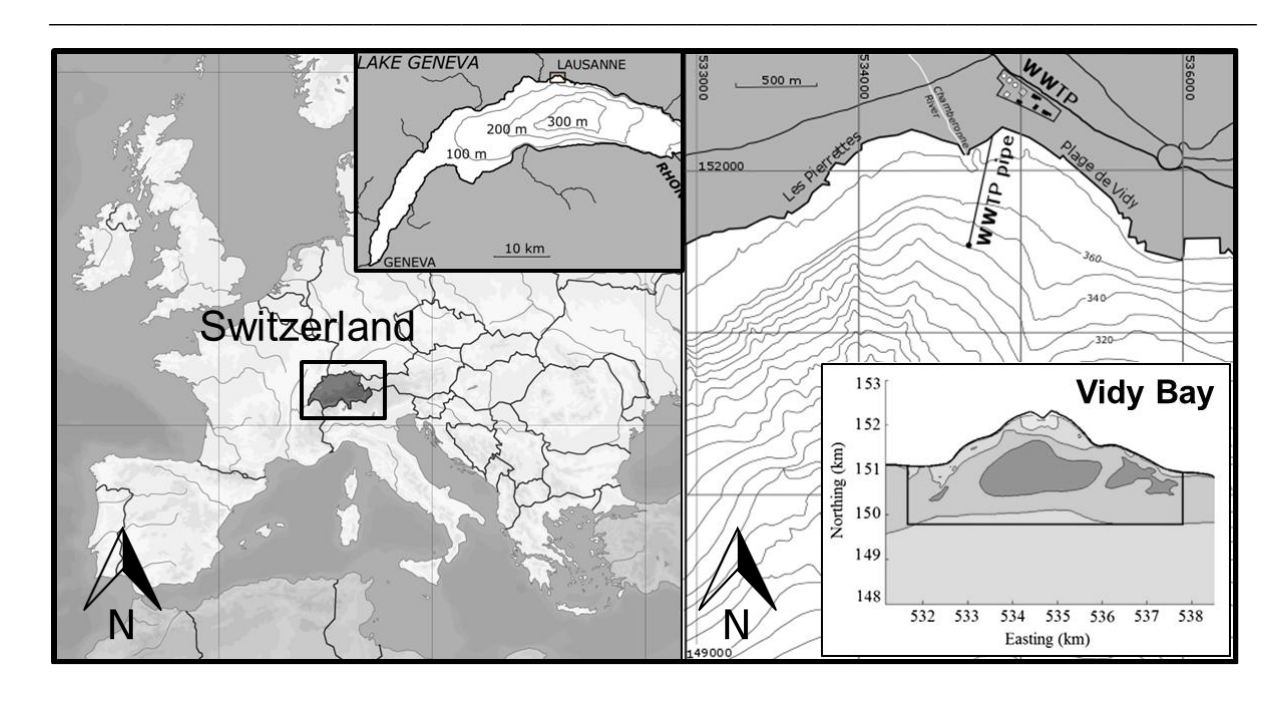


Figure 6. Location of Lake Geneva and map of Vidy Bay indicating the outfall pipe of the WWTP is indicated. Delimitation of Vidy Bay as a function of currents, from Razmi et al. (2013), using the Swiss coordinate system (CH1903).

References

- AMAP/UNEP 2013. Technical Background Report for the Global Mercury Assessment 2013, Arctic Monitoringand Assessment Programme, Oslo, Norway/UNEP ChemicalsBranch, Geneva, Switzerland.
- AMYOT, M., MIERLE, G., LEAN, D. & MCQUEEN, D. J. 1997. Effect of solar radiation on the formation of dissolved gaseous mercury in temperate lakes. *Geochimica Et Cosmochimica Acta*, 61, 975-987.
- BALE, A. E. 2000. Modeling aquatic mercury fate in Clear Lake, Calif. *Journal of Environmental Engineering-Asce*, 126, 153-163.
- BALOGH, S. J., ENGSTROM, D. R., ALMENDINGER, J. E., MEYER, M. L. & JOHNSON, D. K. 1999. History of mercury loading in the Upper Mississippi River reconstructed from the sediments of Lake Pepin. *Environmental Science & Technology*, 33, 3297-3302.
- BLASCO, J., SAENZ, V. & GOMEZ-PARRA, A. 2000. Heavy metal fluxes at the sediment-water interface of three coastal ecosystems from south-west of the Iberian Peninsula. *Science of the Total Environment*, 247, 189-199.
- BODALY, R. A., RUDD, J. W. M. & FLETT, R. J. 1998. Effect of urban sewage treatment on total and methyl mercury concentrations in effluents. *Biogeochemistry*, 40, 279-291.
- BONVIN, F., RAZMI, A. M., BARRY, D. A. & KOHN, T. 2013. Micropollutant Dynamics in Vidy Bay-A Coupled Hydrodynamic-Photolysis Model to Assess the Spatial Extent of Ecotoxicological Risk. *Environmental Science & Technology*, 47, 9207-9216.
- BOUDALA, F. S., FOLKINS, I., BEAUCHAMP, S., TORDON, R., NEIMA, J. & JOHNSON, B. 2000. Mercury flux measurements over air and water in Kejimkujik National Park, Nova Scotia. *Water Air and Soil Pollution*, 122, 183-202.
- BRAVO, A. G., BOUCHET, S., AMOUROUX, D., POTE, J. & DOMINIK, J. 2011. Distribution of mercury and organic matter in particle-size classes in sediments contaminated by a waste water treatment plant: Vidy Bay, Lake Geneva, Switzerland. *Journal of Environmental Monitoring*, 13, 974-982.
- BRAVO, A. G., BOUCHET, S., GUÉDRON, S., AMOUROUX, D., DOMINIK, J. & ZOPFI, J. 2015. High methylmercury production under ferruginous conditions in sediments impacted by sewage treatment plant discharges. *Water Research*, 80, 245-255.
- BRAVO, A. G., LOIZEAU, J. L., ANCEY, L., UNGUREANU, V. G. & DOMINIK, J. 2009. Historical record of mercury contamination in sediments from the Babeni Reservoir in the Olt River, Romania. *Environmental Science and Pollution Research*, 16, 66-75.
- CANARIO, J. & VALE, C. 2004. Rapid release of mercury from intertidal sediments exposed to solar radiation: A field experiment. *Environmental Science & Technology*, 38, 3901-3907.
- CELO, V., LEAN, D. R. S. & SCOTT, S. L. 2006. Abiotic methylation of mercury in the aquatic environment. *Science of the Total Environment*, 368, 126-137.
- COMPEAU, G. C. & BARTHA, R. 1985. Sulfate-Reducing Bacteria Principal Methylators of Mercury in Anoxic Estuarine Sediment. *Applied and Environmental Microbiology*, 50, 498-502.
- CONDAMINES, M. 2015. Contrôle des stations d'épuration (STEP). Annual monitoring of waste water treatment plants (WWTP). *Rapport Commission internationale pour la protection des eaux du Léman*, campagne 2014, 173-194.
- COSSA, D., AVERTY, B. & PIRRONE, N. 2009. The origin of methylmercury in open Mediterranean waters. *Limnology and Oceanography*, 54, 837-844.

- ECKLEY, C. S., WATRAS, C. J., HINTELMANN, H., MORRISON, K., KENT, A. D. & REGNELL, O. 2005. Mercury methylation in the hypolimnetic waters of lakes with and without connection to wetlands in northern Wisconsin. *Canadian Journal of Fisheries and Aquatic Sciences*, 62, 400-411.
- ENGSTROM, D. R. 2007. Fish respond when the mercury rises. *Proceedings of the National Academy of Sciences of the United States of America*, 104, 16394-16395.
- FANTOZZI, L., FERRARA, R., FRONTINI, F. P. & DINI, F. 2007. Factors influencing the daily behaviour of dissolved gaseous mercury concentration in the Mediterranean Sea. *Marine Chemistry*, 107, 4-12.
- FERRARA, R., MAZZOLAI, B., LANZILLOTTA, E., NUCARO, E. & PIRRONE, N. 2000. Volcanoes as emission sources of atmospheric mercury in the Mediterranean basin. *Science of the Total Environment*, 259, 115-121.
- FITZGERALD, W. F., MASON, R. P. & VANDAL, G. M. 1991. Atmospheric Cycling and Air-Water Exchange of Mercury over Midcontinental Lacustrine Regions. *Water Air and Soil Pollution*, 56, 745-767.
- FLEMING, E. J., MACK, E. E., GREEN, P. G. & NELSON, D. C. 2006. Mercury methylation from unexpected sources: Molybdate-inhibited freshwater sediments and an iron-reducing bacterium. *Applied and Environmental Microbiology*, 72, 457-464.
- FRIEDLI, H. R., ARELLANO, A. F., CINNIRELLA, S. & PIRRONE, N. 2009. Initial Estimates of Mercury Emissions to the Atmosphere from Global Biomass Burning. *Environmental Science & Technology*, 43, 3507-3513.
- GBONDO-TUGBAWA, S. S., MCALEAR, J. A., DRISCOLL, C. T. & SHARPE, C. W. 2010. Total and methyl mercury transformations and mass loadings within a wastewater treatment plant and the impact of the effluent discharge to an alkaline hypereutrophic lake. *Water Research*, 44, 2863-2875.
- GILMOUR, C. C. & HENRY, E. A. 1992. Mercury Methylation by Sulfate-Reducing Bacteria Biogeochemical and Pure Culture Studies. *Abstracts of Papers of the American Chemical Society*, 203, 140-GEOC.
- GILMOUR, C. C., PODAR, M., BULLOCK, A. L., GRAHAM, A. M., BROWN, S. D., SOMENAHALLY, A. C., JOHS, A., HURT, R. A., BAILEY, K. L. & ELIAS, D. A. 2013. Mercury Methylation by Novel Microorganisms from New Environments. *Environmental Science & Technology*, 47, 11810-11820.
- GRAF, W. H., PERRINJAQUET, C., BAUER, S. W., PROST, J. P. & GIROD, H. 1979. Measuring on lake Geneva* (Le Leman). *In:* WALTER, H. G. & CLIFFORD, H. M. (eds.) *Developments in Water Science*. Elsevier.
- GRAHAM, N. 2015. The fate of sediment-bound contaminants: a case study of Vidy Bay (Lake Geneva, Switzerland).
- HALLER, L., POTE, J., LOIZEAU, J. L. & WILDI, W. 2009. Distribution and survival of faecal indicator bacteria in the sediments of the Bay of Vidy, Lake Geneva, Switzerland. *Ecological Indicators*, 9, 540-547.
- HEPLER, L. G. & OLOFSSON, G. 1975. Mercury Thermodynamic Properties, Chemical-Equilibria, and Standard Potentials. *Chemical Reviews*, 75, 585-602.
- HINES, M. E., FAGANELI, J., ADATTO, I. & HORVAT, M. 2006. Microbial mercury transformations in marine, estuarine and freshwater sediment downstream of the Idrija Mercury Mine, Slovenia. *Applied Geochemistry*, 21, 1924-1939.
- HOERGER, C. C., AKHTMAN, Y., MARTELLETTI, L., RUTLER, R., BONVIN, F., GRANGE, A., AREY, J. S. & KOHN, T. 2014. Spatial extent and ecotoxicological risk assessment of a micropollutant-contaminated wastewater plume in Lake Geneva. *Aquatic Sciences*, 76, S7-S19.

- KARAGEORGIS, A. P., KATSANEVAKIS, S. & KABERI, H. 2009. Use of Enrichment Factors for the Assessment of Heavy Metal Contamination in the Sediments of Koumoundourou Lake, Greece. *Water Air and Soil Pollution*, 204, 243-258.
- KERIN, E. J., GILMOUR, C. C., RODEN, E., SUZUKI, M. T., COATES, J. D. & MASON, R. P. 2006. Mercury methylation by dissimilatory iron-reducing bacteria. *Applied and Environmental Microbiology*, 72, 7919-7921.
- LANZILLOTTA, E. & FERRARA, R. 2001. Daily trend of dissolved gaseous mercury concentration in coastal seawater of the Mediterranean basin. *Chemosphere*, 45, 935-940.
- LEMMIN, U., MORTIMER, C. H. & BAUERLE, E. 2005. Internal seiche dynamics in Lake Geneva. *Limnology and Oceanography*, 50, 207-216.
- LEHNHERR, I., ST LOUIS, V. L., HINTELMANN, H. & KIRK, J. L. 2011. Methylation of inorganic mercury in polar marine waters. *Nature Geoscience*, 4, 298-302.
- LOIZEAU, J.-L., PARDOS, M., MONNA, F., PEYTREMANN, C., GLASS-HALLER, L. & DOMINIK, J. 2004. The impact of a sewage treatment plant's effluent on sediment quality in a small bay in Lake Geneva (Switzerland–France). Part 2: Temporal evolution of heavy metals. *Lakes & Reservoirs*, 9, 53-63.
- LOIZEAU, J. L., ROZE, S., PEYTREMANN, C., MONNA, F. & DOMINIK, J. 2003. Mapping sediment accumulation rate by using volume magnetic susceptibility core correlation in a contaminated bay (Lake Geneva, Switzerland). *Eclogae Geologicae Helvetiae*, 96, S73-S79.
- MALCOLM, E. G., SCHAEFER, J. K., EKSTROM, E. B., TUIT, C. B., JAYAKUMAR, A., PARK, H., WARD, B. & MOREL, F. M. M. 2010. Mercury methylation in oxygen deficient zones of the oceans: No evidence for the predominance of anaerobes. *Marine Chemistry*, 122, 11-19.
- MARGOT, J., KIENLE, C., MAGNET, A., WEIL, M., ROSSI, L., DE ALENCASTRO, L. F., ABEGGLEN, C., THONNEY, D., CHEVRE, N., SCHARER, M. & BARRY, D. A. 2013. Treatment of micropollutants in municipal wastewater: Ozone or powdered activated carbon? *Science of the Total Environment*, 461, 480-498.
- MARVIN-DIPASQUALE, M., AGEE, J., MCGOWAN, C., OREMLAND, R. S., THOMAS, M., KRABBENHOFT, D. & GILMOUR, C. C. 2000. Methyl-mercury degradation pathways: A comparison among three mercury-impacted ecosystems. *Environmental Science & Technology*, 34, 4908-4916.
- MASON, R. P., CHOI, A. L., FITZGERALD, W. F., HAMMERSCHMIDT, C. R., LAMBORG, C. H., SOERENSEN, A. L. & SUNDERLAND, E. M. 2012. Mercury biogeochemical cycling in the ocean and policy implications. *Environmental Research*. 119, 101-117.
- MASON, R. P., FITZGERALD, W. F. & MOREL, F. M. M. 1994. The Biogeochemical Cycling of Elemental Mercury Anthropogenic Influences. *Geochimica Et Cosmochimica Acta*, 58, 3191-3198.
- MASON, R. P. & LAWRENCE, A. L. 1999. Concentration, distribution, and bioavailability of mercury and methylmercury in sediments of Baltimore Harbor and Chesapeake Bay, Maryland, USA. *Environmental Toxicology and Chemistry*, 18, 2438-2447.
- MASSON, M. & TERCIER-WAEBER, M. L. 2014. Trace metal speciation at the sediment-water interface of Vidy Bay: influence of contrasting sediment characteristics. *Aquatic Sciences*, 76, S47-S58.
- MINAMATA CONVENTION ON MERCURY. 2013. www.mercuryconvention.org
- MONNA, F., DOMINIK, J., LOIZEAU, J. L., PARDOS, M. & ARPAGAUS, P. 1999. Origin and evolution of Pb in sediments of Lake Geneva (Switzerland-France). Establishing a stable Pb record. *Environmental Science & Technology*, 33, 2850-2857.

- MONPERRUS, M., TESSIER, E., AMOUROUX, D., LEYNAERT, A., HUONNIC, P. & DONARD, O. F. X. 2007a. Mercury methylation, demethylation and reduction rates in coastal and marine surface waters of the Mediterranean Sea. *Marine Chemistry*, 107, 49-63.
- MONPERRUS, M., TESSIER, E., POINT, D., VIDIMOVA, K., AMOUROUX, D., GUYONEAUD, R., LEYNAERT, A., GRALL, J., CHAUVAUD, L., THOUZEAU, G. & DONARD, O. F. X. 2007b. The biogeochemistry of mercury at the sediment-water interface in the Thau Lagoon. 2. Evaluation of mercury methylation potential in both surface sediment and the water column. *Estuarine Coastal and Shelf Science*, 72, 485-496.
- MORASCH, B., BONVIN, F., REISER, H., GRANDJEAN, D., DE ALENCASTRO, L. F., PERAZZOLO, C., CHEVRE, N. & KOHN, T. 2010. Occurrence and Fate of Micropollutants in the Vidy Bay of Lake Geneva, Switzerland. Part Ii: Micropollutant Removal between Wastewater and Raw Drinking Water. *Environmental Toxicology and Chemistry*, 29, 1658-1668.
- MULLER, J., RUPPERT, H., MURAMATSU, Y. & SCHNEIDER, J. 2000. Reservoir sediments a witness of mining and industrial development (Malter Reservoir, eastern Erzgebirge, Germany). *Environmental Geology*, 39, 1341-1351.
- NRIAGU, J. O., KEMP, A. L. W., WONG, H. K. T. & HARPER, N. 1979. Sedimentary record of heavy metal pollution in Lake Erie. *Geochimica Et Cosmochimica Acta*, 43, 247-258
- O'DRISCOLL, N. J., POISSANT, L., CANARIO, J., RIDAL, J. & LEAN, D. R. S. 2007. Continuous analysis of dissolved gaseous mercury and mercury volatilization in the upper St. Lawrence River: Exploring temporal relationships and UV attenuation. *Environmental Science & Technology*, 41, 5342-5348.
- PARKS, J. M., JOHS, A., PODAR, M., BRIDOU, R., HURT, R. A., SMITH, S. D., TOMANICEK, S. J., QIAN, Y., BROWN, S. D., BRANDT, C. C., PALUMBO, A. V., SMITH, J. C., WALL, J. D., ELIAS, D. A. & LIANG, L. Y. 2013. The Genetic Basis for Bacterial Mercury Methylation. *Science*, 339, 1332-1335.
- PEARSON, R. G. 1963. Hard and Soft Acids and Bases. *Journal of the American Chemical Society*, 85, 3533-&.
- PERAZZOLO, C., MORASCH, B., KOHN, T., MAGNET, A., THONNEY, D. & CHEVRE, N. 2010. Occurrence and Fate of Micropollutants in the Vidy Bay of Lake Geneva, Switzerland. Part I: Priority List for Environmental Risk Assessment of Pharmaceuticals. *Environmental Toxicology and Chemistry*, 29, 1649-1657.
- PIRRONE, N., CINNIRELLA, S., FENG, X., FINKELMAN, R. B., FRIEDLI, H. R., LEANER, J., MASON, R., MUKHERJEE, A. B., STRACHER, G. B., STREETS, D. G. & TELMER, K. 2010. Global mercury emissions to the atmosphere from anthropogenic and natural sources. *Atmospheric Chemistry and Physics*, 10, 5951-5964.
- PODAR, M., GILMOUR, C. C., BRANDT, C. C., SOREN, A., BROWN, S. D., CRABLE, B. R., PALUMBO, A. V., SOMENAHALLY, A. C. & ELIAS, D. A. 2015. Global prevalence and distribution of genes and microorganisms involved in mercury methylation. *Science Advances*, 1.
- POTE, J., HALLER, L., KOTTELAT, R., SASTRE, V., ARPAGAUS, P. & WILDI, W. 2009. Persistence and growth of faecal culturable bacterial indicators in water column and sediments of Vidy Bay, Lake Geneva, Switzerland. *Journal of Environmental Sciences-China*, 21, 62-69.
- POTE, J., HALLER, L., LOIZEAU, J. L., BRAVO, A. G., SASTRE, V. & WILDI, W. 2008. Effects of a sewage treatment plant outlet pipe extension on the distribution of

- contaminants in the sediments of the Bay of Vidy, Lake Geneva, Switzerland. *Bioresource Technology*, 99, 7122-7131.
- RAZMI, A. M., BARRY, D. A., BAKHTYAR, R., LE DANTEC, N., DASTGHEIB, A., LEMMIN, U. & WUEST, A. 2013. Current variability in a wide and open lacustrine embayment in Lake Geneva (Switzerland). *Journal of Great Lakes Research*, 39, 455-465.
- RAZMI, A. M., BARRY, D. A., LEMMIN, U., BONVIN, F., KOHN, T. & BAKHTYAR, R. 2014. Direct effects of dominant winds on residence and travel times in the wide and open lacustrine embayment: Vidy Bay (Lake Geneva, Switzerland). *Aquatic Sciences*, 76, S59-S71.
- ROLFHUS, K. R. & FITZGERALD, W. F. 2004. Mechanisms and temporal variability of dissolved gaseous mercury production in coastal seawater. *Marine Chemistry*, 90, 125-136.
- SALOMONS, W. & FÖRSTNER, U. 1984. Metals in the hydrocycle, Springer-Verlag.
- SCHAEFER, J. K. & MOREL, F. M. M. 2009. High methylation rates of mercury bound to cysteine by Geobacter sulfurreducens. *Nature Geoscience*, 2, 123-126.
- SCHEULHAMMER, A. M., MEYER, M. W., SANDHEINRICH, M. B. & MURRAY, M. W. 2007. Effects of environmental methylmercury on the health of wild birds, mammals, and fish. *Ambio*, 36, 12-18.
- SELLERS, P., KELLY, C. A., RUDD, J. W. M. & MACHUTCHON, A. R. 1996. Photodegradation of methylmercury in lakes. *Nature*, 380, 694-697.
- SI, Y. B., ZOU, Y., LIU, X. H., SI, X. Y. & MAO, J. D. 2015. Mercury methylation coupled to iron reduction by dissimilatory iron-reducing bacteria. *Chemosphere*, 122, 206-212.
- SOERENSEN, A. L., SUNDERLAND, E. M., HOLMES, C. D., JACOB, D. J., YANTOSCA, R. M., SKOV, H., CHRISTENSEN, J. H., STRODE, S. A. & MASON, R. P. 2010. An Improved Global Model for Air-Sea Exchange of Mercury: High Concentrations over the North Atlantic. *Environmental Science & Technology*, 44, 8574-8580.
- SUNDERLAND, E. M., KRABBENHOFT, D. P., MOREAU, J. W., STRODE, S. A. & LANDING, W. M. 2009. Mercury sources, distribution, and bioavailability in the North Pacific Ocean: Insights from data and models. *Global Biogeochemical Cycles*, 23
- THEVENON, F., GRAHAM, N. D., CHIARADIA, M., ARPAGAUS, P., WILDI, W. & POTE, J. 2011. Local to regional scale industrial heavy metal pollution recorded in sediments of large freshwater lakes in central Europe (lakes Geneva and Lucerne) over the last centuries. *Science of the Total Environment*, 412, 239-247.
- WANG, L. K., CHEN, J. P., HUNG, Y.-T. & SHAMMAS, N. K. 2009. *Heavy Metals in the Environment*, Taylor & Francis Group, LLC.
- WEBER, J. H. 1993. Review of Possible Paths for Abiotic Methylation of Mercury(Ii) in the Aquatic Environment. *Chemosphere*, 26, 2063-2077.
- WIHLBORG, P. & DANIELSSON, A. 2006. Half a century of mercury contamination in Lake Vanern (Sweden). *Water Air and Soil Pollution*, 170, 285-300.
- YU, R. Q., FLANDERS, J. R., MACK, E. E., TURNER, R., MIRZA, M. B. & BARKAY, T. 2012. Contribution of Coexisting Sulfate and Iron Reducing Bacteria to Methylmercury Production in Freshwater River Sediments. *Environmental Science & Technology*, 46, 2684-2691.
- YU, R. Q., REINFELDER, J. R., HINES, M. E. & BARKAY, T. 2013. Mercury Methylation by the Methanogen Methanospirillum hungatei. *Applied and Environmental Microbiology*, 79, 6325-6330.

CHAPTER II

History of contamination in the 20th century

This chapter provides a temporal high-resolution reconstruction of the contaminants in Vidy Bay. Trace metals are good candidates for binding to particles. The historical records of these elements and the kind of organic matter are needed to understand geochemical interactions in sediments as a result of contamination periods. This is the first approach to understand particle-bound behaviour in this work.

High-resolution reconstruction of the 20th century history of trace metals and major elements in sediments in a contaminated area of Lake Geneva, Switzerland

Elena Gascón Díez^{1,2}, Juan Pablo Corella^{3,4}, Thierry Adatte⁵, Florian Thevenon¹, Jean–Luc Loizeau^{1,2}

An article of similar form to this chapter is under review in *Applied Geochemistry* for publishing.

¹ Institut F.-A. Forel , University of Geneva, Boulevard Carl-Vogt 66, 1211 Geneva, Switzerland

² Institute for Environmental Sciences, University of Geneva, Boulevard Carl-Vogt 66, 1211 Geneva, Switzerland

³ Department of Earth Sciences, University of Geneva, rue des Maraîchers 13, 1211 Geneva 4, Switzerland.

⁴ Institute of Physical Chemistry Rocasolano (IQFR/CSIC), C/ Serrano 117, 28006 Madrid, Spain

⁵ Institute of Earth Sciences (ISTE), University of Lausanne, 1015 Lausanne, Switzerland

Abstract

Toxic trace metals in lacustrine sediments are of major concern because they can be hazardous to biota and human health. A high-resolution multiproxy study, including trace metals, major elements, total organic carbon, mineral carbon, Hydrogen Index, Oxygen Index, and C/N ratios, was performed on a sediment core from Vidy Bay in Lake Geneva. This bay has been affected by hazardous compounds released via the sewage effluent of a major wastewater treatment plant (WWTP). Anthropogenic trace metals, such as Pb, Cd, Cu, Zn, and Hg, increased following the industrial revolution in Europe. The highest amounts of these toxic metals, together with Ni, Cr, Co, Ag, Bi, and Fe, were recorded in sediments from 1964, the date of the WWTP implementation. During this period, all trace elements exceeded the sediment quality guideline "probable concentration effect" (PEC), with the following maximum concentrations (in mg kg⁻¹): Pb 3,977; Cd 23, Cu 1,166; Zn 8,586; Hg 11; Ni 143; Cr 265; Ag 126; and Bi 309. The geochemistry of detrital elements (Al, Si, Ca, Ti, Zr, Rb, and Sr), as well as S, Fe, P, and the nature and quality of organic matter were clearly also affected by the effluent. The sedimentary record also revealed that, after some improvements in the wastewater treatment processes and the relocation of the outlet pipe, the sediments tended to return to concentrations similar to those prevailing before the WWTP implementation. However, despite the reduction in the contamination load from the WWTP, which could be reinforced with the construction of a new plant in the near future, the sediments deposited in the Vidy Bay represent a major contaminant legacy that constitutes a potential threat to the lake biota in the case of sediment remobilization.

Keywords: Heavy metals, trace metals, wastewater, sediment contamination, organic matter.

1. Introduction

Lake sediments are archives of climatic variations and pollution in the environment. Trace, minor and major element signals recorded in sediments allow the reconstruction of historical events, both natural and anthropogenic in origin. Geogenic trace metals are discharged through watershed runoff (directly or from fluvial inputs) into lakes. Heavy metal emissions by anthropogenic activities have been shown to increase local, regional, and global fluxes to the atmosphere since the beginning of metallurgy (Nriagu, 1996; Vesely, 2000). Thus, trace metals are widely distributed in the environment. Nevertheless, sewage waters and sludge directly discharged by wastewater treatment plants (WWTP) also represent major sources of contamination in lakes. Heavy metals accumulate in sediments via several mechanisms, such as adsorptive attachment to fine-grained particles (Sholkovitz and Price, 1980), precipitation of discrete metal compounds, coprecipitation of metals by Mn- and Feoxyhydroxides and carbonates, and association with organic molecules (Forstner, 1982). The mobility and bioavailability of trace metals in lake sediments depend on their speciation and stability (Calmano et al., 1993), which are controlled by chemical conditions such as the sediment redox potential, pH, organic matter content, and Mnand Fe-oxyhydroxides. Sediment contamination can harm benthic infauna and epifauna through superficial contact with polluted sediments and pore water, as well through direct ingestion of sediments and detritus (Lawrence and Mason, 2001; Reynoldson, 1987). Moreover, in case of sediment remobilization, trace metals are likely released into the water column and may enter the aquatic life, which is deleterious to organisms because they accumulate in food, leading to damage in human organs and severe diseases (Alissa and Ferns, 2011; Hu, 2000; Ibrahim et al., 2006). In particular, mercury is a toxic trace metal that has gradually increased in concentration in sediments due to anthropogenic activities. Since the industrial revolution (late 18th century), the burning of fossil fuels, nonferrous-metal industry, wood combustion, chlor-alkali industries, and waste incineration have been the principal sources of Hg to the atmosphere (AMAP/UNEP, 2013) and, consequently, to the aquatic environments and soils via deposition (Wang et al., 2004) all over the globe.

The present study aims to reconstruct the trace element history during the last century in the sediments of Vidy Bay, a fresh water bay in Lake Geneva (Switzerland). Recent sediments contain approximately fifty times more Hg and Pb than pre-industrial sediment measured in the deepest part of the lake (Thevenon et al., 2011). This area has been the object of several studies that found that it is the most contaminated site in the lake due to the discharge of local WWTP effluent. Trace metal contamination (Hg, Pb, Cd, Cu, Zn and Mn), fecal indicator bacteria activity, and antibiotic-resistant bacteria genes in Vidy Bay sediments increased since the implementation of the WWTP in 1964 (Loizeau et al., 2004; Monna et al., 1999; Thevenon and Pote, 2012). Nevertheless, no detailed chronology of contamination events before and after the WWTP outlet pipe emplacement in the bay has been conducted. Moreover, very few published studies exist on lake sediment contaminated by urban wastewater. To start to fill this gap, we studied anthropogenic trace element contents of Pb, Cd, Cu, Zn, Ni, Cr, Co, Ag, Bi, Hg, S, P and Fe, the geogenic trace elements Al, Si, Ca, Ti, K, Zr, Rb, and Sr, and organic matter in the contaminated Vidy Bay sediments.

1.1. Settings

Lake Geneva is a warm monomictic peri-alpine lake in central Europe, located at the border between Switzerland and France (Fig. 1). It is the largest freshwater reservoir in Western Europe, with a surface area of 580.1 km², a volume of 89 km³ and an average depth of 152.7 m (maximum depth: 309 m). The Lake Geneva catchment area (including the lake) is 7,999 km², and the Rhône River is the major tributary (75% of the total water input), with a mean inflow of 185 m³ s⁻¹ and a mean outflow of 250 m³ s⁻¹. Complete vertical mixing does not occur every year at the end of the winter (Loizeau and Dominik, 2005). A main drinking water pumping station is located in St. Sulpice, approximately 4 km west of Vidy Bay. Since 1964, the bay has received domestic and industrial sewage water from (1) the outlet pipe of a wastewater treatment plant (WWTP), which initially discharged into the lake 300 m distance from shore and at 12 m depth; (2) the Flon River, which collects surface water and wastewater from the west side of the city during floods (when discharge is greater than 4 - 5 m³ s⁻¹) and discharges through a pipe at 12 m depth; and (3) the Chamberonne

River, which drains the watershed and also carries some urban runoff (Thevenon et al., 2011). The sewer system is only partially separated and collects a significant amount of urban runoff during rain events. The WWTP was conceived for 220,000 equivalent inhabitants and treats 1 - 3 m³ s⁻¹ of wastewater. The wastewater treatment consists of pre-treatments (grit removal and screening at 1 cm), primary clarifiers, biologically activated sludge treatment without nitrification, or, for 5% of the flow, a moving bed bioreactor (MBBR) with partial to complete nitrification (<1 mg N-NH4 L⁻¹) (Margot et al., 2013).

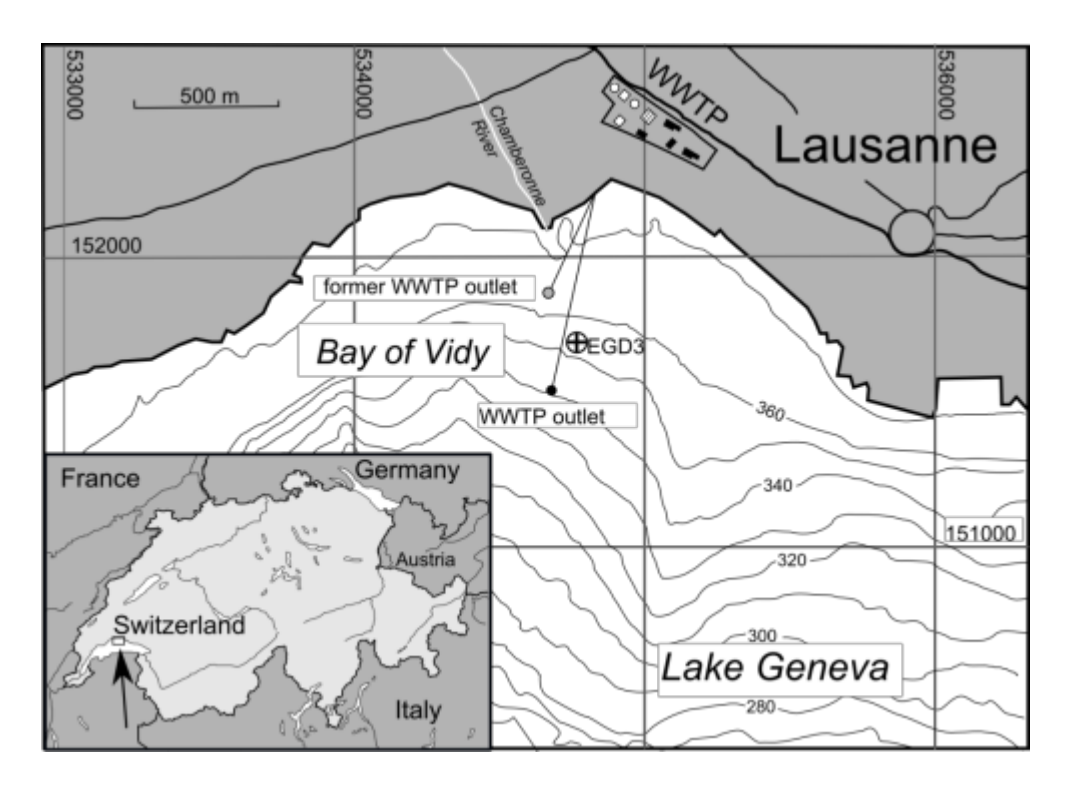


Figure 1. Location of Vidy Bay shown on a bathymetric map of the study area in Lake Geneva. EGD3 represents the site were the studied sediment core was retrieved.

1.2. Important dates for the WWTP

Since the late 1960s, the lake has featured meso-eutrophic conditions (Lang, 1985; Monod, 1983). For that reason, in 1971, ferric chloride (FeCl₃) was used to precipitate and eliminate the phosphorous present in wastewater as a measure to reduce the P load in the lake. The WWTP was extended in 1976, introducing a physico-chemical

treatment that increased the water treatment capacity by 1 m³ s⁻¹. A second chain of sludge incineration was put into operation in 1979. In 2001, the outlet pipe was extended to the present location, 700 m from shore and at 35 m depth (Fig. 1). A specific treatment of greasy residues was introduced in 2002 and new chemical deodorization washing facilities were introduced to complement the existing equipment in 2003. In 2005, road bag treatments began using filtering dumpsters. Finally, in September 2008, the new boiler furnace #2 started functioning, increasing the daily tonnage of incinerated sludge in Vidy. The Vidy WWTP facilities do not meet current standards in terms of the quality of the releases (Préavis N° 2010/65, 2010). Vidy Bay remains the most contaminated area in Lake Geneva because the WWTP effluent still contains pollutants that settle to surface sediments, such as Hg and other trace metals, fecal indicator bacteria and organic matter (Czekalski et al., 2014; Gascon Diez et al., 2014; Masson and Tercier-Waeber, 2014; Sauvain et al., 2014).

2. Materials and methods

2.1. Sampling and subsampling

A 103-cm-long sediment core (EGD3) was retrieved from a depth of 21 m on October 2010 between the current WWTP outlet and the old outlet (6°35'17.97'' E, 46°30'48.30'' N; Fig. 1) using a polyvinyl chloride liner in a UWITEC gravity corer and weight hammering while aboard the "La Licorne" scientific vessel.

2.2. Volume magnetic susceptibility, freeze-drying and sediment grain size distribution

A Volume Magnetic Susceptibility (VMS) profile was determined using a MS2 susceptibility meter (Bartington Instruments, England) at 1-cm resolution. Afterwards, the core was split lengthwise, photographed, sedimentologically described and subsampled down-core with 1-cm resolution. Particle grain size distributions were determined on wet sediments using a laser diffraction Coulter LS-100 analyzer following the procedure described by Loizeau et al. (1994). Sediments were freeze-

dried in a CHRIST BETA 1-8 K freeze-drying unit (-54 °C, 6 Pa) for a minimum of 48h. Dry samples were ground and homogenized with an agate mortar.

2.3. Dating

The age depth model was obtained by radiometric dating (¹³⁷Cs and ⁷Be) using a HPGe well gamma spectrometer (Ortec EG&G). Five time markers were used: the first occurrence of ¹³⁷Cs in 1954; two ¹³⁷Cs fallout peaks, one in 1964 (atmospheric nuclear weapon testing) and one in 1986 (the Chernobyl accident); the VMS maximum gradient in 1971 (Loizeau et al., 2003); and the surface sediment in 2010. Water content measurements and porosity calculations (Hankanson and Jansson, 1983) were necessary to estimate the *in situ* density of dry particles to obtain the mass of accumulated sediment per centimeter. The depth scale was converted to a mass scale to calculate sediment accumulation rates (SAR) [g cm⁻² y⁻¹].

2.4. Total organic carbon, mineral carbon, Hydrogen Index and Oxygen Index

Characterization and quantification of the organic matter were performed on powdered bulk sediment at the Institute of Earth Sciences at the University of Lausanne using Rock-Eval 6 following the method described by (Behar et al., 2001; Espitalie et al., 1985a; Espitalie et al., 1985b). The samples were placed in an oven and first heated to 300°C under an inert atmosphere then gradually pyrolyzed to 650 °C. After complete pyrolysis, samples were transferred into another oven and gradually heated to 850 °C in the presence of air. The determined parameters were total organic carbon (TOC), the Hydrogen Index (HI as mg HC g⁻¹ TOC) and the Oxygen Index (OI as mg CO₂ g⁻¹ TOC), which permit an overall characterization of the sedimentary organic matter. The HI and OI values are proportional to the H/C and O/C ratios of the organic matter, respectively, and can be used for OM classification in Van Krevelen-like diagrams (Espitalie et al., 1985a).

The standard used was IFP 160000 Rock-Eval, and the analyses were carried out on 50 - 100 mg of powdered dry sediment under standard conditions. Analytical precision was higher than 0.05 wt.% (1 σ) for TOC, 10 mg HC g⁻¹ TOC (1 σ) for HI, and 10 mg CO2 g⁻¹ TOC (1 σ) for OI.

2.5. Total nitrogen analysis

Total nitrogen concentration (% N) was analyzed in a CHN Elemental Analyzer (Carlo Erba Flash EA 1112 CHNS/MAS200) using approximately 10 mg of dry powdered sediment. The carbon/nitrogen (C/N) ratio was calculated as the weight ratio of the total organic carbon measured by the Rock-Eval pyrolysis (see above) and the N content analyzed by the CHN Elemental Analyzer. The precision was better than 1% based on an internal standard and replicate samples.

2.6. Mercury analyses

Total mercury was analyzed by Cold Vapor Atomic Absorption Spectrophotometry (CV-AAS) using an Advance Mercury Analyzer (Model AMA 254, Altec, Czech Republic) through dry mineralization and pre-concentration of Hg and amalgamation on a gold trap (Szakova et al., 2004). All analyses were run in triplicate. The detection limit and working range were 0.01 ng and 0.05-600 ng, respectively. The relative error was usually \pm 5% and always less than 10% (Roos-Barraclough et al., 2002). The concentrations obtained for repeated analyses of the certified reference material never exceeded the specified range of concentrations given for the MESS-3 reference material (National Research Council Canada).

2.7. Trace elements

Two analytical techniques were used to measure trace element concentrations. The first one is a quantitative method. Quadrupole-based inductively coupled plasma mass spectrometry (ICP-MS, model 7700 series, Agilent) was performed following sediment digestion in Teflon bombs heated to 150°C in analytical grade 2 M HNO₃. Multi-element standard solutions of different concentrations (0, 0.02, 1, 5, 20, 100 and 200 µg L⁻¹) were used for calibration. The total variation coefficients for triplicate sample measurements were less than 10%. The metal concentrations in the sediments are expressed in mg kg⁻¹ of dry weight sediment. The ICP-MS measurements were carried out with 1-cm resolution. The second technique is based on X-ray fluorescence (XRF) element scanning using a model AVAATECH XRF core scanner (2000 A, 10-30 kV and 20-50 s measuring time) that measured every 2 mm. Core images were

obtained using a high-resolution AVAATECH core scanner coupled camera. It is helpful to combine these two analytical techniques. On one hand, XRF is a higher-resolution, non-destructive technique but provides only semiquantitative geochemical information and measurements can be biased by humidity, porosity and particle grain size within the sediment (Hennekam and de Lange, 2012; Tjallingii et al., 2007). On the other hand, ICP-MS provides quantitative results, permitting more precise analysis of certain elements. As the resolutions employed were different for each technique, the XRF data were averaged every five measurements to compare the results from both instruments.

2.8. Enrichment factor calculations

Enrichment factors (EFs) are commonly used to identify and quantify human interference in natural element cycles. It has been shown that normalizing data with the average crustal value can be erroneous (Reimann and De Caritat, 2000; Reimann and de Caritat, 2005). A better approach is to use local non-contaminated sediments as a reference of pre-industrial conditions (Angelidis and Aloupi, 1995; Kersten and Smedes, 2002). In this study, EFs have been calculated and normalized using the average concentration of the bottommost 10 cm of the sediment core. These sediments were clearly weakly affected by human contamination because concentrations were very similar to the natural background reference values for Lake Geneva (Arbouille et al., 1988):

$$EF = \frac{{}^{M_{cm}}/{}_{Ti_{cm}}}{{}^{M_{bottom}}/{}_{Ti_{hottom}}}$$
(1)

where M_{cm} is the metal concentration for each centimeter of the sediment core; Ti_{cm} is the concentration of titanium at that cm; and M_{bottom} and Ti_{bottom} are the average metal and titanium concentrations, respectively, in the bottommost 10 cm of the core (94 - 103 cm).

All the anthropogenic trace elements were normalized to the conservative geogenic element Ti to confirm that the changes in concentrations of anthropogenic metals were not due to geogenic input variations.

2.9. Statistics

The data were statistically described using SigmaPlot 11.0 software. The data were not normally distributed; therefore, correlation coefficients were calculated using the Spearman rank order method. A statistical treatment of the geochemical dataset (Principal Component Analyses) was carried out using SPSS Statistics 23 software to investigate the end members that can help to infer the main environmental processes controlling sediment deposition (Corella et al., 2011a; Corella et al., 2011b; Giralt et al., 2008).

3. Results

3.1. Stratigraphic units

Stratigraphic units were defined according to visual variations in color, grain size, TOC, mineral carbon (MinC), HI and OI), water content, and C/N ratio (Fig. 2a). The sedimentary sequence was therefore divided into 5 main stratigraphic units, from the bottom to the top of the core:

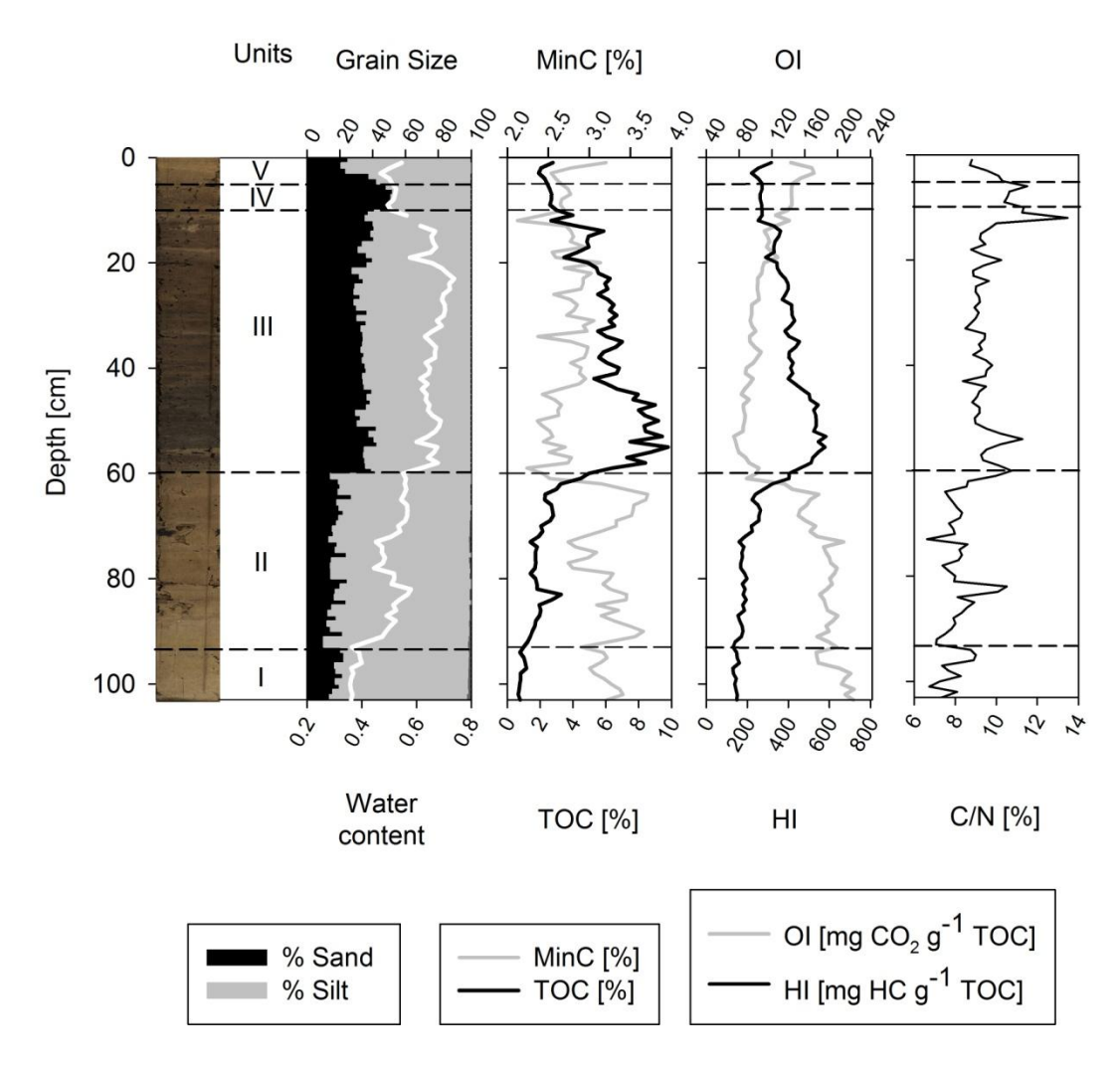


Figure 2a. From left to right: EGD3 core image; sedimentary units; grain size and water content; TOC: total organic carbon and MinC: mineral carbon; OI: Oxygen index and HI: Hydrogen index; and C/N ratio.

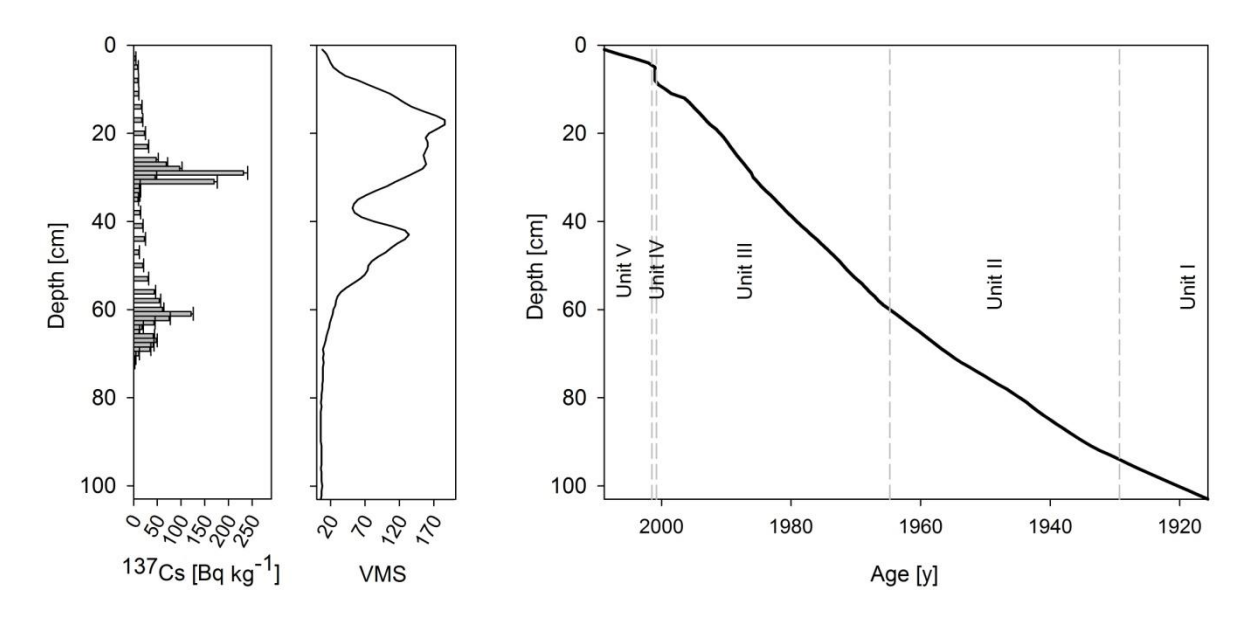


Figure 2b. The age-depth model based on ¹³⁷Cs radiometric dating and Volume Magnetic Susceptibility (VMS).

Unit I (103 - 94 cm) was composed of homogeneous light-brown organic-rich silts (TOC \sim 6% and of MinC \sim 3.20%). The OI values were the highest of the entire core (\sim 204 mg CO₂ g⁻¹ TOC), and the HI and C/N exhibited low values in this unit (\sim 145 mg HC g⁻¹ TOC; C/N \sim 7 - 9).

Unit II (94 - 60 cm) was composed of plain dark brown silts (average TOC values approximately 2.1% and MinC of $\sim 3.23\%$). In this unit, the HI showed an increasing trend at the top of the unit, while the OI decreased progressively. The C/N ratios were overall similar to unit I, although with greater variability.

Unit III was the thickest unit (60 - 10 cm) and was composed predominantly of black sandy silts punctuated by thin brown organic-rich layers. The TOC content reached the highest values (\sim 10%) in this unit, while the MinC values were the lowest (\sim 2%) for the entire core. The OI values decreased dramatically on average from 177 in unit II to 99 OI mg CO₂ g-1 TOC in unit III, with the lowest OI values at 56 - 53 cm. In contrast, the HI values increased progressively from 203 in unit II to 426 mg HC g-1 TOC in this unit, with maximum HI values observed at 55 - 53 cm. The C/N ratio was higher than those of units I and II (average value 9.5).

Unit IV (10 - 5 cm) was composed of dark brown silty sands. In this unit, the water content (50%) and TOC values (2.7%) were similar to unit II, and the TOC value was approximately half that measured in unit III. The MinC average values were similar to those in unit III (2.70%). The C/N average values were the highest in this unit (~11).

Finally, unit V, the uppermost sediments (from 5 cm to surface) featured light brown silts, with 73% silt, a water content of 50%, and 2.3% TOC (average values). The MinC increased again at the surface (uppermost cm), reaching a value of 3.2%. The HI and OI values continued to decrease and increase, respectively, without reaching the initial values recorded in unit I. The C/N ratio was low.

3.2. Age model

The chronology of the Vidy Bay sequence was based on ¹³⁷Cs and VMS dating. Two activity peaks were detected in the ¹³⁷Cs profile, reaching 121 and 231 Bq kg⁻¹ at 61 and 29 cm depth, respectively (Fig. 2b). These two peaks corresponded to the maximum ¹³⁷Cs deposition from radioactive fallout from nuclear weapon tests in the atmosphere (1963/64) and the Chernobyl accident (1986), respectively, allowing absolute dates to be assigned (Appleby, 2001). We also considered the first traces of ¹³⁷Cs deposition in 1954 for the age model. The first maximum gradient observed in VMS profile (Fig. 2b) is a reliable chronological marker because it corresponded to the implementation of the FeCl₃ treatment in the WWTP in 1971 (Loizeau et al., 2003). The detection of ⁷Be in the uppermost samples suggests that the water-sediment interface was preserved in the sediment core. The age model was based on the linear interpolation between these five tie points. Based on the sharp water content and grain size changes in unit IV (Fig. 2a), we assumed that the sediment deposited in centimeters 5 to 10 corresponded to resuspended or deposited particles from the transfer work of the WWTP outlet pipe, corresponding to the year 2001. Considering all this, the age model that we propose features four different SARs: in the 1954 - 1964 section, the SAR was 0.68 ± 0.13 g cm⁻² y⁻¹; in the 1964 - 1986 section, the SAR was 0.64 ± 0.04 g cm⁻² y⁻¹; in the 1986 - 2001 section, the SAR was 0.66 ± 0.08 g cm⁻² y⁻¹; and in the 2001 - 2010 section, the SAR was 0.33 ± 0.07 g cm⁻² y⁻¹ (Fig. 2b). From extrapolation of the older SAR, the bottom of the sediment core is estimated to correspond to 1915.

Following the age model, unit I (103 - 94 cm) corresponded to years ~1915 to ~1929; unit II (94 - 60 cm) to years ~1929 to 1964; unit III (60 - 10 cm) to years 1964 to 2001; unit IV (10 - 5 cm) to 2001; and unit I (5 - 0 cm) to between 2001 and 2010. However, the dating corresponding to the bottom ~10 cm is doubtful due to the lack of time markers older than 1954. Moreover, the sharp transition in water content between unit I and unit II (Fig. 2a) may suggest a sediment hiatus between these two units. For the purpose of this study, this uncertainty is not an issue because this section clearly remains at background levels with respect to Lake Geneva sediment contamination, and no detailed discussion focuses on this time period in the sediment core.

3.3. Geochemistry

A principal component analysis (PCA) carried out using the large geochemical dataset (21 variables) shows the multi-element relationships related to the main environmental conditions (Fig. 3). The two first eigenvectors of the PCA accounted for 71% of the total variance. The first eigenvector (PCA1) represented 52% of the total variance, and it was mainly controlled by anthropogenic-related elements (Cu, Bi, Zn, Cr, Co, Ni, Pb, Ni, Cd, Ag, Fe, Hg and P) at the positive end (Fig. 3). TOC was related to these elements because organic matter favors adsorption of trace metals (Tribovillard et al., 2006). PCA1 (Fig. 5) displayed low values between 1915 and 1929 (unit I) and increased slightly from 1929 to 1964 (unit II). The highest values were recorded between 1964 and 1979, the base of unit III, and values progressively decreased towards the top of the unit, resulting in low values since 2001 (units IV and V). The second eigenvector (PCA2, 19% of the total variance) was characterized by geogenic elements, i.e., Ca, Sr Ti, Si, Rb, K and Al (Fig. 3). It showed high variability related to sewage water inputs, exhibited an overall decreasing trend since between 1929 and 2001 (units II and III), and featured an abrupt increase since 2001 (units IV and V).

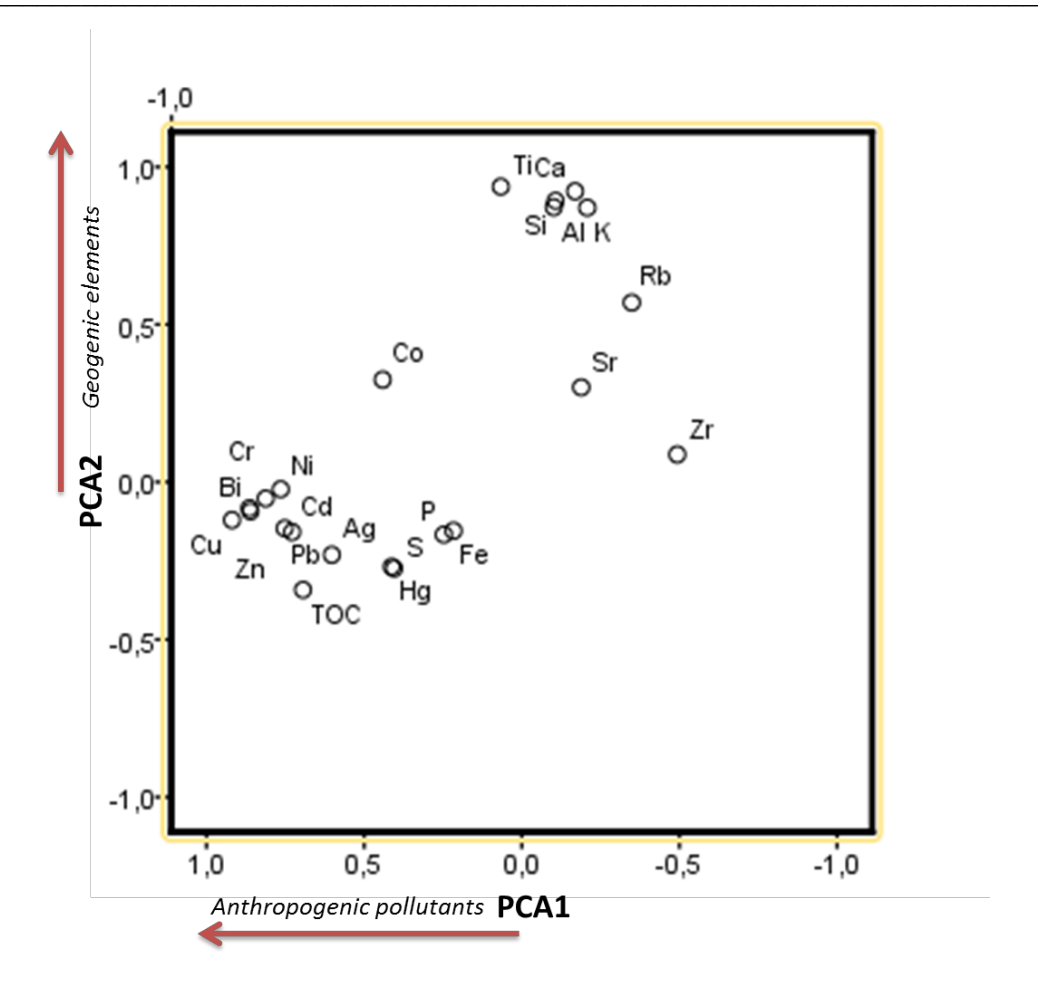


Figure 3. Principal Component Analysis (PCA) with XRF-normalized data for lithological elements and ICP-MS-normalized data for trace metals. TOC is also taken in account.

3.3.1. Geogenic elements

Depth profiles for all geogenic elements were measured using the XRF technique (Fig. 4), and some were also measured via ICP-MS. The elements measured by the two techniques showed similar patterns (Fig. S1 in supplementary material), and the large variations were comparable for both methods. However, high-frequency variations were not correlated. Typical geogenic element values were normalized with Ti (Fig. 4). Some trace-elements (Zr, Rb and Sr) exhibited significant fluctuations between ca. 10 and 20 cm. Major elements, such as Al, Si and K, showed similar trends, with the highest values in units I, II and V. The Ca/Ti profile did not show any particular trend. Zr and Sr were detrital elements, and the normalized values of these

elements were quite constant throughout the sediment core, excluding the disturbance at the top of unit III. Rb/Ti values were constant in units I and II, whereas Zr and Sr slightly decreased along with Al, Si and K from ca. 60 cm (Fig. 4).

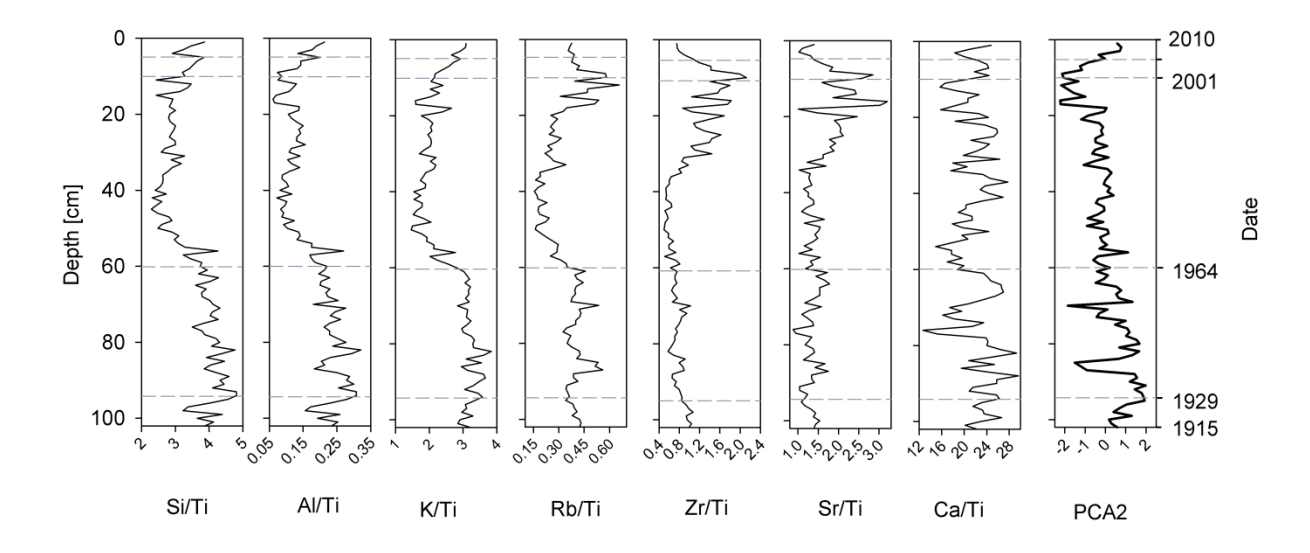


Figure 4. Geogenic elements measured using X-ray fluorescence (XRF) and normalized relative to Ti. PCA2 represents the lithological input. Horizontal short gray dashes represent the limits between lithological units I to V from bottom to top.

3.3.2. Anthropogenic trace elements

The concentration profiles of Pb, Cu, Zn, Cd, Ni, Cr, Co, Ag, Bi, Hg, Fe, P, and S are shown in Fig. 5, and the data are described in Table 1 by stratigraphic unit. Considering that the aim of this study was to highlight the direct impact of the WWTP in sediments, the non-normalized data faithfully reflected the contamination of heavy metals in the sediment. The trends in anthropogenic trace metal concentrations measured by either XRF or ICP-MS were similar. However, only the ICP-MS data are shown in Fig. 5 because this technique provided data on a longer list of trace metals. Some metals presented similar behavior along the sediment core; consequently, they are described together. Pb, Cd, Cu and Zn showed the lowest values in unit I (1915 - 1929 ca.), followed by a progressive increase in unit II (Fig. 5 and table 1). The highest values occurred in 1964 and 1979. Since 1979, concentrations of these

elements decreased gradually, reaching values similar to those observed before 1964 in unit IV (2001). The Ni, Cr, and Co concentration profiles differed from the four previously described. Although Ni, Cr, and Co also reached the highest values in unit III, their general increase was more gradual. Recent values have decreased, reaching levels similar to the oldest concentrations in ~1979. The Ag and Bi concentrations did not show any increasing trend until 62 cm (~1964), where they increased dramatically (Fig. 5 and Table 1). High concentrations were observed over a longer time interval in the Ag profile than in the Bi profile, although in both profiles, recent sediments also approached initial values. The Hg concentration in the sediment core did not closely follow the same trend as the other trace metals. In unit I, Hg concentrations were 10 times lower than the current concentration (top of the sediment core) (Table 1). Up to 63 cm, the concentration gradually increased, following a trend similar to those of Pb, Cd, Cu, and Zn. Before 1964, the sediments were already contaminated, with 2.6 mg kg⁻¹ of Hg, rising to 4.6 mg kg⁻¹ in 1964. Then, these concentrations remained quite stable with small-scale fluctuations up to 33 cm. The highest Hg value was observed at 32 cm (1986), whereas the other metals did not peak at this depth (Fig. 5). Since the 1990s, the concentration of Hg has gradually decreased. Fe concentrations in the sediments of Vidy Bay recorded different events than the other metals. No increase in Fe was observed from the bottom of the core, 1915 ca., up to 53 cm. Between 53 and 55 cm (1971), Fe concentration suddenly increased, reaching its highest values (Fig. 5). Finally, S exhibited a slight increase from 60 cm up to the top of unit IV.

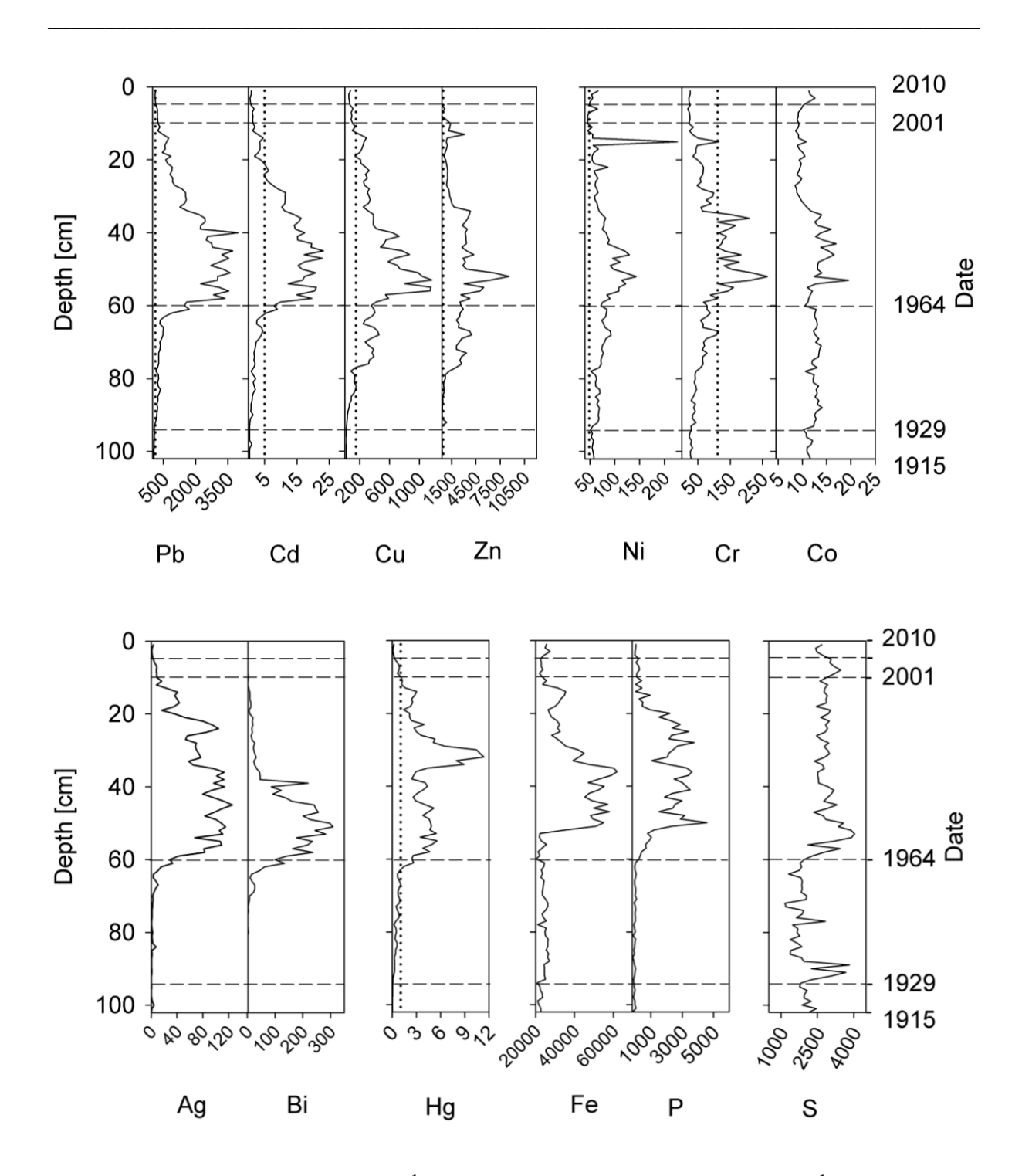


Figure 5. Trace metals in mg kg⁻¹ (analyzed by ICP-MS); Hg in mg kg⁻¹ (analyzed by CV-AAS); and S and P in cps (analyzed by XRF). Horizontal short gray dashes represent the limits between stratigraphic units I to V from bottom to top. Vertical dotted gray lines represent the probable effect concentration (PEC) for each element (MacDonald et al., 2000).

Table 1. Mean metal concentrations \pm standard error and the concentration ranges per stratigraphic unit.

Units		Pb (mg kg ⁻¹)	Cu (mg kg ⁻¹)	Zn (mg kg ⁻¹)	Cd (mg kg ⁻¹)	Ni (mg kg ⁻¹)	Cr (mg kg ⁻¹)	Co (mg kg ⁻¹)	Ag (mg kg ⁻¹)	Bi (mg kg ⁻¹)	Hg (mg kg ⁻¹)	Fe (mg kg ⁻¹)
V	mean	140 ± 18	63 ± 4	200 ± 12	0.75 ± 0.08	55 ± 3	24.5 ± 0.9	11.4 ± 0.4	2.3 ± 0.5	1.6 ± 0.1	0.21 ± 0.04	24903 ± 806
	range	118 - 160	53 - 76	175 - 234	0.50 - 0.94	49 - 66	21.9 - 26.4	10.1 - 12.6	1.2 - 3.5	1.2 - 2.1	0.12 - 0.32	22431 - 27367
IV	mean	235 ± 6	95 ± 5	679 ± 197	1.42 ± 0.09	50 ± 4	23 ± 1	9.2 ± 0.1	8.1 ± 0.6	2.8 ± 0.2	0.84 ± 0.09	22916 ± 304
	range	222- 253	83 - 110	279 - 1348	1.17 - 1.75	45 - 65	18 - 25	8.9 - 9.7	5.7 - 9.0	2.4- 3.8	0.66 - 1.12	21904 - 23662
III	mean	1913 ± 155 236 - 3977	469 ± 40 99 - 1166	2579 ± 246 543 - 8586	11.6 ± 0.9 1.3 - 23.2	83 ± 4 45 - 226	104 ± 8 24 - 265	11.7 ± 0.4 8.5 - 19.5	76 ± 4 8 - 126	99 ± 14 2 - 309	4.2 ± 0.3 1.2 - 11.4	38231 ± 1753 20374 - 61856
II	mean	351 ± 49	212	1588 ± 201	2.2 ± 0.3	71 ± 2	56 ± 4	12.7 ± 0.1	4 ± 1	13 ± 4	0.65 ± 0.08	24570 ± 251
	range	1702 - 1621	21 - 459	247 - 3972	0.4 - 8.9	51 - 93	28 - 114	10.2 - 14.1	0.3 - 33	0.7 - 134	0.09 - 2.66	20811 - 27153
I	mean range	73 ± 4 63 - 97	22.7 ± 0.4 21 - 24	304 ± 10 242- 347	0.45 ± 0.08 0.32 - 1.07	56.0 ± 0.6 53 - 58	28 ± 1 23 - 33	11.4 ± 0.2 10.8 - 12.1	1.2 ± 0.5 0.2 - 4.6		0.059 ± 0.005 0.040 - 0.087	

The calculated EF for each anthropogenic trace metal (Pb, Cu, Zn Cd, Ni, Cr, Co, Ag, Bi, Hg and Fe) is presented in Fig. 6. Unit V (uppermost sediments) was the least enriched metal interval, corresponding to the reference value (unit I). In unit II, the EFs were slightly higher for all metals, excluding Ag and Bi. Unit III was the most enriched interval for all metals, which is consistent with the results of the metal concentrations (Table 1, Fig. 6). Compared to other metals, Cr, Co, and Fe EFs increased most slightly later at 52 - 53 cm. Unit IV exhibited lower metal EFs than in unit III. Generally, the mean EFs values metals between units I, II and V did not vary considerably (Fig. 6).

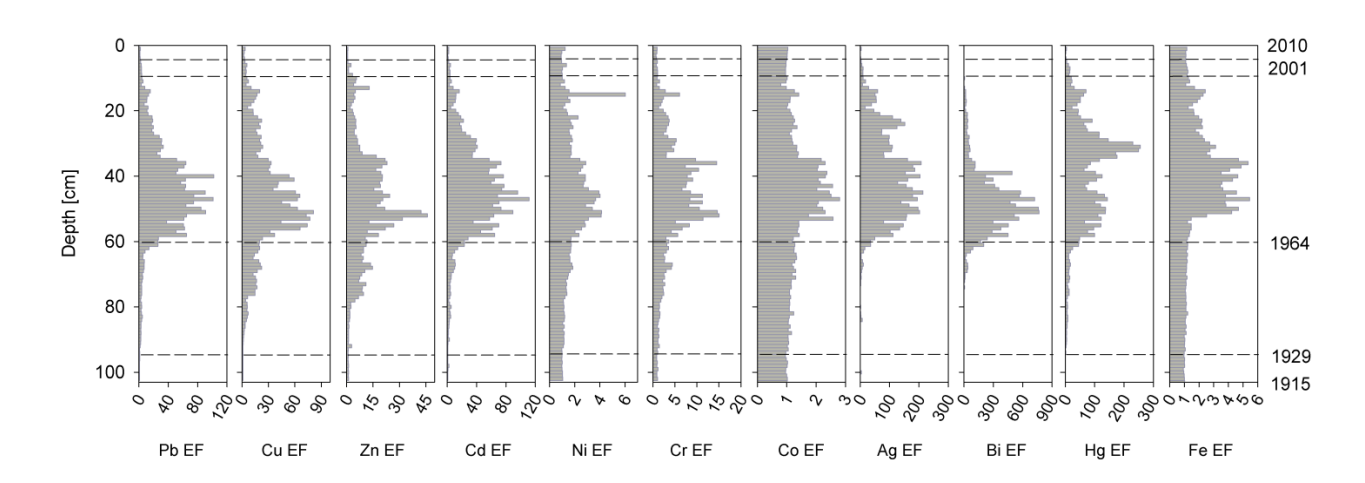


Figure 6. Enrichment factor (EF) profiles of anthropogenic elements. Horizontal short gray dashes represents the limits between stratigraphic units I to V from bottom to top.

4. Discussion

4.1. Physico-chemical parameters

Grain size profiles showed finer sediments in units I and II (Fig. 2a) corresponding to the uncontaminated sediments. From 1929 to 1934 (the base of unit II), the grain size was finer than all of unit I. In addition, the water and TOC contents decreased abruptly during these years, which coincided with the boundary between units I and II. The sudden decrease in these physico-chemical parameters therefore suggested a possible hiatus (at 90 - 94 cm), likely due to erosion due to underflows and mass movement processes, which are recorded in the distal basin (Kremer et al., 2015).

The WWTP contributed to the increase in sand-sized particles in Vidy Bay, with maximum sand values reported between 1964 and 2001 (units III and IV). However, in the measurements made using the Coulter LS100, it is not possible to distinguish between organic and inorganic coarse particles because both are classed as sand sized (Loizeau et al., 1994). Thus, it is likely that in unit III, the particles classified as sand sized, were a mixture of inorganic sand particles and organic matter. The coeval increase in TOC may confirm this assumption (Fig. 2a). However, coarse grains were observed in unit IV. The TOC and grain-size relationship was not present between

2001 and 2010 (unit IV). Therefore, we assume that the sandy silts deposited in unit IV were related to the WWTP outlet pipe relocation work.

4.2. Total organic carbon and mineral carbon

Maximum MinC concentrations characterized the base of the sediment core (unit I), reflecting endogenic calcite precipitation and detrital carbonates from the catchment basin. The TOC expelled by the WWTP gained importance over MinC starting in 1964 in the bay. The TOC amounts measured in recent sediments (units IV and V) were slightly above the initial values found in units I and II (higher MinC and lower TOC than unit III) as a result of the relocation of the WWTP outlet pipe.

4.3. Hydrogen Index, Oxygen Index and C/N ratio

Units I and II were characterized by high OI values and low HI values, indicating that sediments were dominated by allochthonous terrestrial organic matter (Ariztegui et al., 2001; Jaccard et al., 2009; Montero-Serrano et al., 2015; Steinmann et al., 2003). Such inverse HI and OI trends were also observed in the most recent sediments (units IV and V). However, in Vidy Bay and since 1964 (base of unit III), the inverse HI and OI tendencies have behaved similar to autochthonous (algal) material. However, it is not likely that this signal results from a sudden and massive increase in productivity due to the nutrient load but rather to the settling of organic-rich particles released by the WWTP. Similar HI and OI behavior in sludge deposit sediments has been observed in the Mediterranean Sea as a product of sewage discharges (Kruge et al., 2010). Unit V (Fig. 2a) showed the recovery of the sediment through increasing values of HI and decreasing values of OI toward values similar to those of natural sediments. However, the HI/OI values measured in this unit (Fig. 7) fall in-between the algal and terrestrial endmembers, suggesting higher productivity in the recent sediments than those deposited before 1964. The C/N ratio in unit III featured somewhat higher values than in units I, II and V (Fig. 2a), which would indicate increased terrestrial organic matter input, thus contradicting a priori the HI and OI results. However, as explained by Tyson (1995), the slightly more terrestrial appearance of the organic matter in unit III, as suggested by the C/N ratio, is due to the particular location of these sediments, i.e., close to the WWTP outlet pipe. Therefore, they are affected by degraded organic matter released by the sewage effluent.

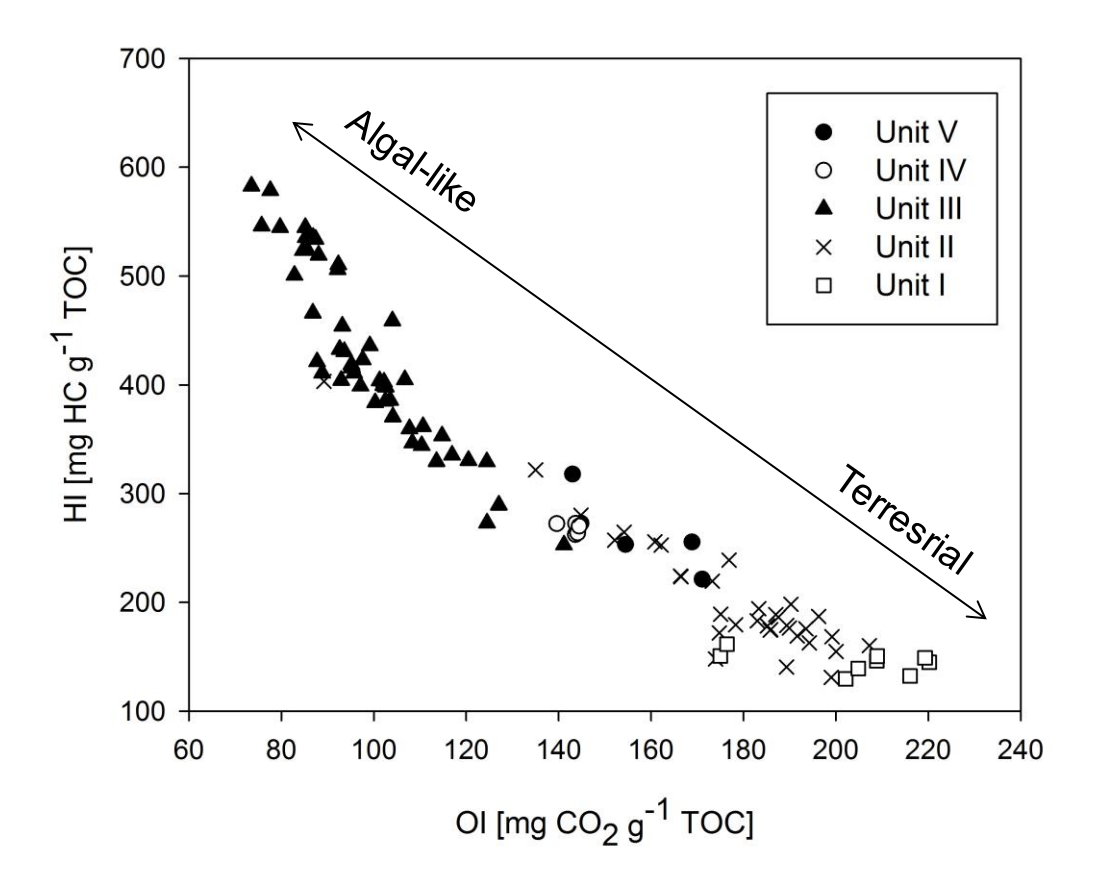


Figure 7. Hydrogen index (HI) versus oxygen index (OI) for all samples of EGD3. Double-headed arrows indicate the organic matter trends as discussed in the text.

4.4. Detrital composition of the sediment

The detrital elements showed, overall, a similar trend, with a large variability between 1915 and 1964 likely explained by flood-related runoff events in the watershed. These elements show a clear decrease since the WWTP implementation. The WWTP gathered up the urban runoff containing different substances and released them after treatment into the lake, likely changing the natural processes delivering sediment into the lake. Near 40 cm (1979), some sort of improvement in the WWTP likely helped return the natural values of Si, Al, K, and Rb to values similar to those before the

implementation of the WWTP (Fig. 4). Zr shows a distinct evolution from the rest of the clastic elements. A likely explanation is that this element is generally related to resistant minerals and increases in coarse-grained minerals (unit IV) (Corella et al., 2014; Cuven et al., 2010) likely deposited in Vidy Bay and during the WWTP outlet pipe relocation work. The Ca/Ti and Sr/Ti ratios do not exactly follow the same trend as the other elements because they are related to detrital carbonate transported to the lake by runoff processes and endogenic calcite precipitation.

4.5. Historical reconstruction of pollutants in Vidy Bay in the 20th century

The probable effect concentration (PEC) is consensus-based sediment quality guideline (SQG) that provides a reliable basis for assessing sediment quality conditions in freshwater ecosystems (MacDonald et al., 2000). These values provide a basis for predicting sediment toxicity. Prior to ca. 1930 (unit I), the sediments have the lowest concentrations of all the anthropogenic trace metals, which were always below the PEC values (Fig. 5). After this period, the sediments featured a slow increase in some trace metal concentrations (Pb, Cd, Cu, Zn and Hg), coinciding with intensified industrial activities. Following World War I, coal combustion and heavy metal ore smelting released particulate contamination into the atmosphere, and this contamination was subsequently deposited in bodies of freshwater. In particular, Cu and Zn experienced a significant increase in concentration starting in ca. 1946 (ca. 80 cm) and exceeded the PEC values (Fig. 5). In particular, increased Cu (Fig. 4) in could be linked to copper-based fungicides used **Swiss** vinevards (Daouk et al., 2015). The Pb, Cd, Cu, Zn and Hg concentrations increased significantly enhanced in 1964 due to the implementation of the WWTP in Vidy Bay (Fig. 5, Table 1). Most of the trace metal concentrations studied in the present work (for which a PEC value exists) exceeded the PEC threshold in unit III (Fig. 5). Although, Co concentrations did not appear to be much affected by the WWTP (Fig. 4), the EF calculated for this metal (Fig. 5) showed a clear contamination a few years after 1964.

The maximum values in this contaminated unit were (in mg kg⁻¹ dry weight) as follows: Pb 3,977; Cd 23, Cu 1,166; Zn 8,586; Hg 11, Ni 143, and Cr 265. To our knowledge, Vidy Bay is one of the few reported lacustrine sites where such a

contamination history is recorded in the sediment. To compare and discuss our results, we have chosen other water bodies polluted with trace toxic metals from sources other than municipal wastewater treatment plants. The Malter Reservoir, located close to a mining and industrial area in Germany, contains lower concentrations (in mg kg⁻¹) of Pb (740), Cu (240), and Zn (1,900) (Muller et al., 2000) than Vidy Bay. The mean EFs in sediments of Vidy Bay during the most contaminated period (Fig. 5) were close to those of Malter Reservoir for Co and Pb. In contrast, Cu was 3 to 4 times greater in Vidy than in this mining area, and Cd was lower than in Malter Reservoir (Muller et al., 2000). Compared to sediments that received urban effluents in Rhodes Harbour, Greece (Angelidis and Aloupi, 1995), the mean EFs of Cd, Cr, Cu, Fe, Pb and Zn in the Vidy Bay sediments deposited during the period when the WWTP effluent was directly influencing the sediments (unit III) (Fig. 6) are much higher than those found by Angelidis and Aloupi (1995). The maximum EF values (Fig. 6) were extremely high compared to other study areas, such as Koumoundourou Lake, Greece (Karageorgis et al., 2009). After reaching the maximum concentrations and EF values, the release of heavy metals and other compounds has progressively decreased from 35 - 37 cm (1982 - 1983) to the present. The general reduction of global atmospheric, industrial and domestic emissions of trace metals during the last decades is reflected by a drop in all the heavy metals shown in Fig. 5. In 2010, after the return to 1964 conditions resulting from the relocation of the WWTP outlet pipe in 2001, the Vidy Bay surface sediments exhibit lower amounts of metals than in the underlying unit III (e.g., Pb, 157 mg kg⁻¹; Cu, 76 mg kg⁻¹; Zn, 234 mg kg⁻¹ and Cd, 0.94 mg kg⁻¹). However, the concentrations in unit V were still higher than the reference values of the lake (Pb 30, Cu 30, Zn 60 and Cd 0.2 mg kg⁻¹; Arbouille et al. (1988)).

The Ag and Bi concentration and EF profiles (Figs. 5 and 6) are directly related to the WWTP effluent and unrelated to any atmospheric release by regional human activities at the beginning on the century. Therefore, their origin was not analogous. The Ag contamination in the Vidy Bay is related to waste produced by the Kodak S.A. photograph industry, established in Lausanne and connected to the WWTP in 1963. Although the EF in this period (Fig. 5) is similar to the Ag EF reported in Malter Reservoir sediments (Muller et al., 2000), the maximum Ag concentration measured in

Vidy Bay reached 126 mg kg⁻¹, almost 5 times larger than in Malter Reservoir (Muller et al., 2000). Kodak S.A. was expanded in 1986, which matched a second peak in Ag concentrations (104 mg kg⁻¹) located at 28 - 29 cm depth. Bi is a heavy metal with a provenance that remains unclear. Ferrari et al. (2000) and Karlsson et al. (2007) carried out studies on natural and anthropogenic atmospheric sources of Bi. This trace metal is found in WWTP sludge in different countries (Amneklev et al., 2015b; Fuerhacker et al., 2001). However, only a few studies have focused on Bi from sewage sludge in lakes. Bismuth is increasingly used as a substitute for Pb because Bi is generally considered a nontoxic heavy metal and therefore more frequently utilized. Household products, such as cosmetics and plastics, as well as industries and, to a lesser extent, hospitals are found to be the major contributors of Bi to WWTPs (Amneklev et al., 2015a; Amneklev et al., 2015b; Fuerhacker et al., 2001). Twelve municipalities with several industries related to the pharmaceutical industry, human health activities and chemical product manufacturing are connected to the Vidy WWTP. Thus, the high levels of Bi found in the Vidy Bay sediments coinciding with the implementation of the WWTP and the absence of this metal during the previous decades (Fig. 4) could be explained by the use of this element by the industries and domestic wastes of the Swiss municipalities connected to the WWTP. Indeed, Bi concentrations reached an extremely high value of 309 mg kg⁻¹ compared to the 37 mg kg⁻¹ present in the Malter Reservoir (Muller et al., 2000). Additionally, the Bi EF reached 768 in Vidy Bay, whereas the maximum value was approximately 100 in Malter Reservoir.

The decrease in trace metal concentrations from the late 1970s was likely due to the improvements in the efficiency of the WWTP, such as the introduction of a physic-chemical treatment that significantly increased the water treatment capacity (details in section 1.2. in this paper)

The effect of mercury emissions started to be evident in sediments dated to the 1920s (Fig. 4). Later on, since 1964, an important increase in Hg occurred in Vidy Bay. Local chemical and pharmaceutical industries developed products containing Hg (antifungal pesticides, antibacterial mercurochrome® and vaccines) (Ball et al., 2001;

Deflora et al., 1994; Mukherjee et al., 2004). These products were the main Hg sources to the WWTP, and Hg was subsequently released into the bay. However, contrary to the other heavy metals in this study, the maximum Hg concentration of 11 mg kg⁻¹ was observed between 28 and 35 cm, which correspond to the years 1982 and 1986. This value is the highest concentration of Hg ever found in Lake Geneva and is 300 times higher than the lake sediment background level (Arbouille et al., 1988). This Hg maximum did not correspond to any other measured heavy metal maximum (Fig. 4), implying that the WWTP outflow did not increase at that time. The lack of correlation with other metals suggests that there was some increase in the use or mercury wastes in some industries (or hospitals) during these years. This is of major concern because slope instabilities have already been recorded in the sediments of Lake Geneva (Kremer et al., 2014). In case of mass movements, the contaminated sediments could be resuspended, causing ecotoxicological damage to the lake ecosystem.

Fe and P concentrations reflected the water treatment history. The dephosphatation process was introduced in 1971 in the WWTP and involved adding FeCl₃ to precipitate phosphorous in the sludge and subsequently eliminating it from the sewage water. A clear increase in P and Fe values occurred in 1971, surely related to the beginning of the dephosphatation process (Fig. 5). This confirms that the addition of FeCl₃ since 1971 in the WWTP processes led to enrichments in P in the sewage sludge, which was subsequently released into the lake (see the concentrations in Table 1). An important decrease in both Fe and P was observed during the late 1970s, which was likely due to the use of new treatments and more efficient techniques in the WWTP. Fe and P are thus considered anthropogenic elements. The Fe geochemistry in Vidy Bay is mainly influenced by dissimilatory microbial iron oxide reducers that transform Fe(III) into Fe(II) (Percak-Dennett et al., 2013). The subsequent Fe(II)-rich sediments in presence of P involved precipitation of mineral phases, such as vivianite, or sorption of phosphates to ferrous hydroxides. The Fe(II)-P phases represented a significant portion of the reactive Fe in the Vidy Bay sediments. The PCA suggests that Bi, Cu, Zn, Co, Ni, Cr, Pb and Cd covaried in a very similar manner and exhibited a different behavior than Fe, Ag, Hg and P.

Finally, S is primarily bound to organic matter. Accordingly, S showed a slight increase from 1964 on; therefore, it is considered to be linked to anthropogenic inputs. Moreover, under anoxic conditions, S can form sulfidic compounds that act as fixative agents for chalcophile elements, such as Zn, Cd, Cu, Cr, Hg, Ag, Bi, and Fe (Goldschmidt, 1937).

5. Conclusions

Our multiproxy study of the sedimentary archives in Vidy Bay provides an opportunity to investigate the evolution of sediment contamination from pre-industrial times to the present, the environmental response to strong anthropogenic contamination and the timing and tempo of the recovery following the perturbation. The trace metal record (Pb, Cd, Cu, Zn and Hg) highlights the regional impact of industrial pollution starting in ca. 1930 and the high metal contamination starting in 1964 in the sediments surrounding the outlet pipe discharge. The parallel changes observed in grain size, TOC, MinC, HI and OI are in agreement with the trace metal results regarding the origin of the contamination. Some primarily detrital or authigenic elements, such as Si, Al, K, Rb, and to a lesser extent Zr and Sr, were also affected by the WWTP. The WWTP discharges modified the OM characteristics of the sediments, producing algallike characteristics (e.g., higher HI values). The particular conditions created by sewage water release entirely modified the environmental conditions of the affected area and therefore the geochemistry of sediments, making this sedimentological environment of special interest and incomparable to pristine lakes or lakes contaminated by different types of sources. The long-term geochemical evolution of both the clastic elements and trace metal pollution recorded in Vidy Bay exemplifies the need for paleolimnological studies to further understand the environmental consequences of human activities in lacustrine systems. This study helps to define target limnological conditions and management strategies in aquatic ecosystems and shows the need for high-resolution records and multiproxy studies to make correct assessments of pollution in lake systems.

Acknowledgements

The work was partially funded by the SNF research grant PDFMP2-123034. We thank Stéphanie Giradclos for the financial support for XRF analyses provided by the 'Elemo' project with contributions from the Swiss National Science Foundation (Research grants 200021-121666 and 200020-146889). We also thank Daniel Ariztegui for writing advice and result interpretation.

Supporting information

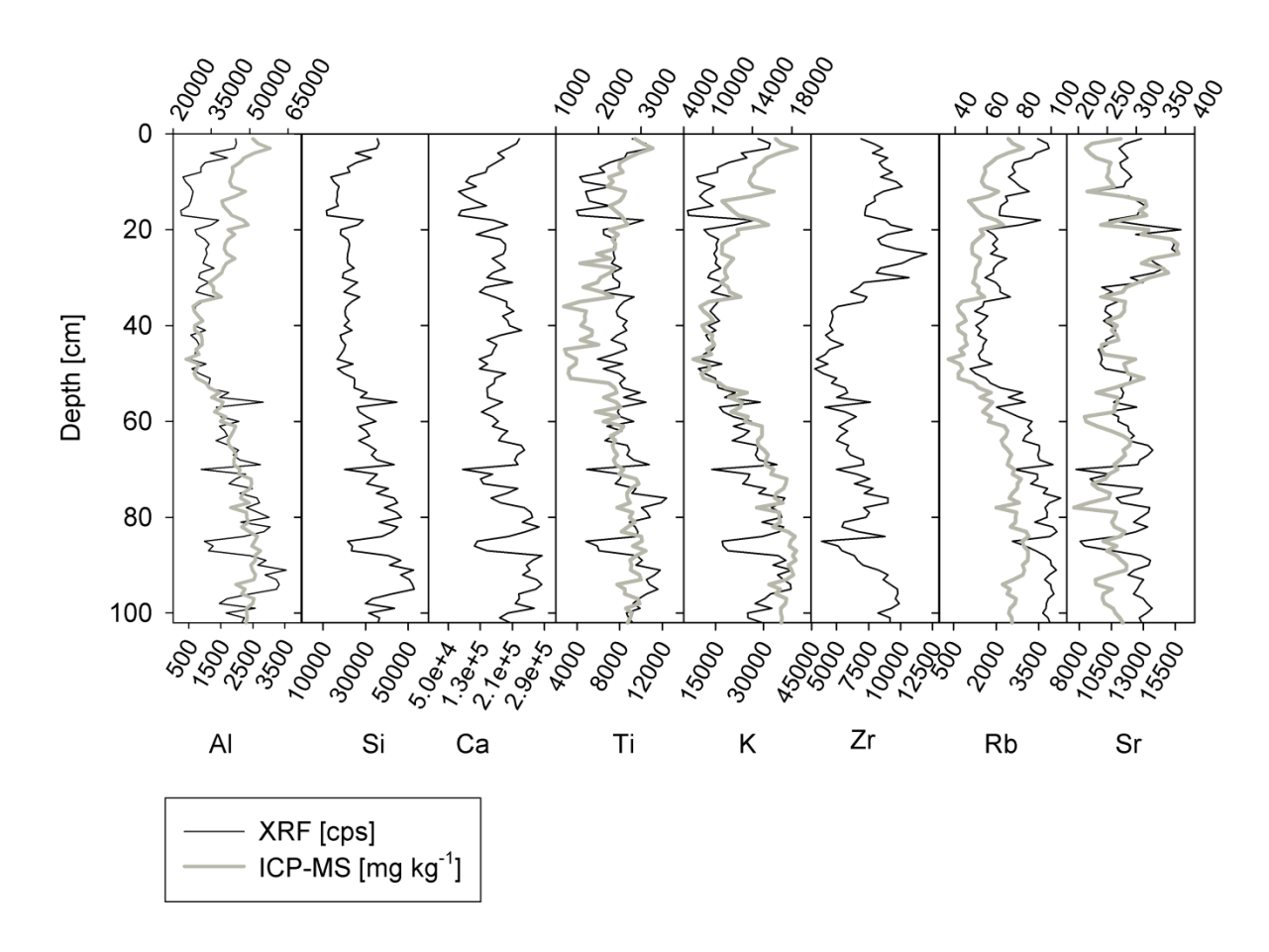


Figure S1. Geogenic element concentrations measured by XRF and ICP-MS.

References

- ALISSA, E. M. & FERNS, G. A. 2011. Heavy metal poisoning and cardiovascular disease. *J Toxicol*, 2011, 870125.
- AMAP/UNEP 2013. Technical Background Report for the Global Mercury Assessment 2013, Arctic Monitoringand Assessment Programme, Oslo, Norway/UNEP ChemicalsBranch, Geneva, Switzerland.
- AMNEKLEV, J., AUGUSTSSON, A., SÖRME, L. & BERGBÄCK, B. 2015a. Bismuth and Silver in Cosmetic Products: A Source of Environmental and Resource Concern? *Journal of Industrial Ecology*, 00.
- AMNEKLEV, J., SORME, L., AUGUSTSSON, A. & BERGBACK, B. 2015b. The Increase in Bismuth Consumption as Reflected in Sewage Sludge. *Water Air and Soil Pollution*, 226.
- ANGELIDIS, M. O. & ALOUPI, M. 1995. Metals in sediments of Rhodes Harbour, Greece. *Marine Pollution Bulletin*, 31, 273-276.
- APPLEBY, P. G. 2001. Chronostratigraphic Techniques in Recent Sediments. *In:* LAST, W. & SMOL, J. (eds.) *Tracking Environmental Change Using Lake Sediments*. Springer Netherlands.
- ARBOUILLE, D., HOWA, H., SPAN, D. & VERNET, J. P. 1988. Etude générale de la pollution par les métaux et repartition des nutriments dans les sédiments du Léman. *Commission internationale pour la protection des eaux du Léman*, Campagne 1988, 139-172.
- ARIZTEGUI, D., CHONDROGIANNI, C., LAMI, A., GUILIZZONI, P. & LAFARGUE, E. 2001. Lacustrine organic matter and the Holocene paleoenvironmental record of Lake Albano (central Italy). *Journal of Paleolimnology*, 26, 283-292.
- BALL, L. K., BALL, R. & PRATT, R. D. 2001. An assessment of thimerosal use in childhood vaccines. *Pediatrics*, 107, 1147-1154.
- BEHAR, F., BEAUMONT, V. & PENTEADO, H. L. D. 2001. Rock-Eval 6 technology: Performances and developments. *Oil & Gas Science and Technology-Revue D Ifp Energies Nouvelles*, 56, 111-134.
- CALMANO, W., HONG, J. & FORSTNER, U. 1993. Binding and Mobilization of Heavy-Metals in Contaminated Sediments Affected by Ph and Redox Potential. *Water Science and Technology*, 28, 223-235.
- CORELLA, J. P., BENITO, G., RODRIGUEZ-LLOVERAS, X., BRAUER, A. & VALERO-GARCES, B. L. 2014. Annually-resolved lake record of extreme hydrometeorological events since AD 1347 in NE Iberian Peninsula. *Quaternary Science Reviews*, 93, 77-90.
- CORELLA, J. P., EL AMRANI, A., SIGRO, J., MORELLON, M., RICO, E. & VALERO-GARCES, B. L. 2011a. Recent evolution of Lake Arreo, northern Spain: influences of land use change and climate. *Journal of Paleolimnology*, 46, 469-485.
- CORELLA, J. P., MORENO, A., MORELLON, M., RULL, V., GIRALT, S., RICO, M. T., PEREZ-SANZ, A. & VALERO-GARCES, B. L. 2011b. Climate and human impact on a meromictic lake during the last 6,000 years (Montcortes Lake, Central Pyrenees, Spain). *Journal of Paleolimnology*, 46, 351-367.
- CUVEN, S., FRANCUS, P. & LAMOUREUX, S. F. 2010. Estimation of grain size variability with micro X-ray fluorescence in laminated lacustrine sediments, Cape Bounty, Canadian High Arctic. *Journal of Paleolimnology*, 44, 803-817.
- CZEKALSKI, N., DIEZ, E. G. & BURGMANN, H. 2014. Wastewater as a point source of antibiotic-resistance genes in the sediment of a freshwater lake. *Isme Journal*, 8, 1381-1390.

- DAOUK, S., FREGE, C., BLANC, N., MOUNIER, S., REDON, R., MERDY, P., LUCAS, Y. & PFEIFER, H.-R. 2015. Fluorescence spectroscopy to study dissolved organic matter interactions with agrochemicals applied in Swiss vineyards. *Environmental Science and Pollution Research*, 22, 9284-9292.
- DEFLORA, S., BENNICELLI, C. & BAGNASCO, M. 1994. Genotoxicity of Mercury-Compounds a Review. *Mutation Research*, 317, 57-79.
- ESPITALIE, J., DEROO, G. & MARQUIS, F. 1985a. Rock-Eval Pyrolysis and Its Application .2. *Revue De L Institut Français Du Petrole*, 40, 755-784.
- ESPITALIE, J., DEROO, G. & MARQUIS, F. 1985b. Rock-Eval Pyrolysis and Its Applications. *Revue De L Institut Francais Du Petrole*, 40, 563-579.
- FERRARI, C. P., HONG, S., VAN DE VELDE, K., BOUTRON, C. F., RUDNIEV, S. N., BOLSHOV, M., CHISHOLM, W. & ROSMAN, K. J. R. 2000. Natural and anthropogenic bismuth in Central Greenland. *Atmospheric Environment*, 34, 941-948.
- FORSTNER, U. 1982. Accumulative Phases for Heavy-Metals in Limnic Sediments. *Hydrobiologia*, 91-2, 269-284.
- FUERHACKER, M., SCHARF, S., PICHLER, W., ERTL, T. & HABERL, R. 2001. Sources and behaviour of bismuth active substances (BiAS) in a municipal sewage treatment plant. *Science of the Total Environment*, 277, 95-100.
- GASCON DIEZ, E., BRAVO, A. G., PORTA, N. A., MASSON, M., GRAHAM, N. D., STOLL, S., AKHTMAN, Y., AMOUROUX, D. & LOIZEAU, J. L. 2014. Influence of a wastewater treatment plant on mercury contamination and sediment characteristics in Vidy Bay (Lake Geneva, Switzerland). *Aquatic Sciences*, 76, S21-S32.
- GIRALT, S., MORENO, A., BAO, R., SAEZ, A., PREGO, R., VALERO-GARCES, B. L., PUEYO, J. J., GONZALEZ-SAMPERIZ, P. & TABERNER, C. 2008. A statistical approach to disentangle environmental forcings in a lacustrine record: the Lago Chungara case (Chilean Altiplano). *Journal of Paleolimnology*, 40, 195-215.
- GOLDSCHMIDT, V. M. 1937. The principles of distribution of chemical elements in minerals and rocks. The seventh Hugo Muller Lecture, delivered before the Chemical Society on March 17th, 1937. *Journal of the Chemical Society*, 655-673.
- HANKANSON, L. & JANSSON, M. 1983. Principles of lake sedimentology. *Springer-Verlag, Berlin Heidelberg*, 316.
- HENNEKAM, R. & DE LANGE, G. 2012. X-ray fluorescence core scanning of wet marine sediments: methods to improve quality and reproducibility of high-resolution paleoenvironmental records. *Limnology and Oceanography-Methods*, 10, 991-1003.
- HU, H. 2000. Exposure to metals. *Prim Care*, 27, 983-96.
- IBRAHIM, D., FROBERG, B., WOLF, A. & RUSYNIAK, D. E. 2006. Heavy metal poisoning: clinical presentations and pathophysiology. *Clin Lab Med*, 26, 67-97, viii.
- JACCARD, T., ARIZTEGUI, D. & WILKINSON, K. J. 2009. Assessing past changes in bioavailable zinc from a terrestrial (Zn/Si)(opal) record. *Chemical Geology*, 258, 362-367.
- KARAGEORGIS, A. P., KATSANEVAKIS, S. & KABERI, H. 2009. Use of Enrichment Factors for the Assessment of Heavy Metal Contamination in the Sediments of Koumoundourou Lake, Greece. *Water Air and Soil Pollution*, 204, 243-258.
- KARLSSON, S., DUKER, A. & GRAHN, E. 2007. Sediment chronologies of As, Bi, and Ga in Sweden impact of industrialisation. *Journal of Environmental Science and Health Part a-Toxic/Hazardous Substances & Environmental Engineering*, 42, 155-164.
- KERSTEN, M. & SMEDES, F. 2002. Normalization procedures for sediment contaminants in spatial and temporal trend monitoring. *Journal of Environmental Monitoring*, 4, 109-115.

- KREMER, K., CORELLA, J. P., HILBE, M., MARILLIER, F., DUPUY, D., ZENHAUSERN, G. & GIRARDCLOS, S. 2015. Changes in distal sedimentation regime of the Rhone delta system controlled by subaquatic channels (Lake Geneva, Switzerland/France). *Marine Geology*, 370, 125-135.
- KREMER, K., MARILLIER, F., HILBE, M., SIMPSON, G., DUPUY, D., YRRO, B. J. F., RACHOUD-SCHNEIDER, A. M., CORBOUD, P., BELLWALD, B., WILDI, W. & GIRARDCLOS, S. 2014. Lake dwellers occupation gap in Lake Geneva (France-Switzerland) possibly explained by an earthquake-mass movement-tsunami event during Early Bronze Age. *Earth and Planetary Science Letters*, 385, 28-39.
- KRUGE, M. A., PERMANYER, A., SERRA, J. & YU, D. 2010. Geochemical investigation of an offshore sewage sludge deposit, Barcelona, Catalonia, Spain. *Journal of Analytical and Applied Pyrolysis*, 89, 204-217.
- LANG, C. 1985. Eutrophication of Lake Geneva indicated by the oligochaete communities of the profundal. *Hydrobiologia*, 126, 237-243.
- LAWRENCE, A. L. & MASON, R. P. 2001. Factors controlling the bioaccumulation of mercury and methylmercury by the estuarine amphipod Leptocheirus plumulosus. *Environmental Pollution*, 111, 217-231.
- LOIZEAU, J.-L., PARDOS, M., MONNA, F., PEYTREMANN, C., GLASS-HALLER, L. & DOMINIK, J. 2004. The impact of a sewage treatment plant's effluent on sediment quality in a small bay in Lake Geneva (Switzerland–France). Part 2: Temporal evolution of heavy metals. *Lakes & Reservoirs*, 9, 53-63.
- LOIZEAU, J. L., ARBOUILLE, D., SANTIAGO, S. & VERNET, J. P. 1994. Evaluation of a Wide-Range Laser Diffraction Grain-Size Analyzer for Use with Sediments. *Sedimentology*, 41, 353-361.
- LOIZEAU, J. L. & DOMINIK, J. 2005. The history of eutrophication and restoration of Lake Geneva. *Terre et Environnement*, 50, 43–56.
- LOIZEAU, J. L., ROZE, S., PEYTREMANN, C., MONNA, F. & DOMINIK, J. 2003. Mapping sediment accumulation rate by using volume magnetic susceptibility core correlation in a contaminated bay (Lake Geneva, Switzerland). *Eclogae Geologicae Helvetiae*, 96, S73-S79.
- MACDONALD, D. D., INGERSOLL, C. G. & BERGER, T. A. 2000. Development and evaluation of consensus-based sediment quality guidelines for freshwater ecosystems. *Archives of Environmental Contamination and Toxicology*, 39, 20-31.
- MARGOT, J., KIENLE, C., MAGNET, A., WEIL, M., ROSSI, L., DE ALENCASTRO, L. F., ABEGGLEN, C., THONNEY, D., CHEVRE, N., SCHARER, M. & BARRY, D. A. 2013. Treatment of micropollutants in municipal wastewater: Ozone or powdered activated carbon? *Science of the Total Environment*, 461, 480-498.
- MASSON, M. & TERCIER-WAEBER, M. L. 2014. Trace metal speciation at the sediment-water interface of Vidy Bay: influence of contrasting sediment characteristics. *Aquatic Sciences*, 76, S47-S58.
- MONNA, F., DOMINIK, J., LOIZEAU, J. L., PARDOS, M. & ARPAGAUS, P. 1999. Origin and evolution of Pb in sediments of Lake Geneva (Switzerland-France). Establishing a stable Pb record. *Environmental Science & Technology*, 33, 2850-2857.
- MONOD, R. 1983. Evolution physico-chimique des eaux du Léman. Commission internationale pour la protection des eaux du Léman, Campagne 1983, 208.
- MONTERO-SERRANO, J. C., FOELLMI, K. B., ADATTE, T., SPANGENBERG, J. E., TRIBOVILLARD, N., FANTASIA, A. & SUAN, G. 2015. Continental weathering and redox conditions during the early Toarcian Oceanic Anoxic Event in the northwestern Tethys: Insight from the Posidonia Shale section in the Swiss Jura Mountains. *Palaeogeography Palaeoclimatology Palaeoecology*, 429, 83-99.

- MUKHERJEE, A. B., ZEVENHOVEN, R., BRODERSEN, J., HYLANDER, L. D. & BHATTACHARYA, P. 2004. Mercury in waste in the European Union: sources, disposal methods and risks. *Resources Conservation and Recycling*, 42, 155-182.
- MULLER, J., RUPPERT, H., MURAMATSU, Y. & SCHNEIDER, J. 2000. Reservoir sediments a witness of mining and industrial development (Malter Reservoir, eastern Erzgebirge, Germany). *Environmental Geology*, 39, 1341-1351.
- NRIAGU, J. O. 1996. A history of global metal pollution. Science, 272, 223-224.
- PERCAK-DENNETT, E. M., LOIZEAU, J. L., BEARD, B. L., JOHNSON, C. M. & RODEN, E. E. 2013. Iron isotope geochemistry of biogenic magnetite-bearing sediments from the Bay of Vidy, Lake Geneva. *Chemical Geology*, 360, 32-40.
- PRÉAVIS N° 2010/65, D. D. 2010. Modification de la Convention intercommunale relative à l'exploitation de la station d'épuration des eaux usées et de traitement des boues de l'agglomération lausannoise STEP de Vîdy. *Préavis, rapport-préavis*, 6.
- REIMANN, C. & DE CARITAT, P. 2000. Intrinsic flaws of element enrichment factors (EFs) in environmental geochemistry. *Environmental Science & Technology*, 34, 5084-5091.
- REIMANN, C. & DE CARITAT, P. 2005. Distinguishing between natural and anthropogenic sources for elements in the environment: regional geochemical surveys versus enrichment factors. *Science of the Total Environment*, 337, 91-107.
- REYNOLDSON, T. B. 1987. Interactions between Sediment Contaminants and Benthic Organisms. *Hydrobiologia*, 149, 53-66.
- ROOS-BARRACLOUGH, F., GIVELET, N., MARTINEZ-CORTIZAS, A., GOODSITE, M. E., BIESTER, H. & SHOTYK, W. 2002. An analytical protocol for the determination of total mercury concentrations in solid peat samples. *Science of the Total Environment*, 292, 129-139.
- SAUVAIN, L., BUECHE, M., JUNIER, T., MASSON, M., WUNDERLIN, T., KOHLER-MILLERET, R., DIEZ, E. G., LOIZEAU, J. L., TERCIER-WAEBER, M. L. & JUNIER, P. 2014. Bacterial communities in trace metal contaminated lake sediments are dominated by endospore-forming bacteria. *Aquatic Sciences*, 76, S33-S46.
- SHOLKOVITZ, E. R. & PRICE, N. B. 1980. Major-Element Chemistry of Suspended Matter in the Amazon Estuary. *Geochimica Et Cosmochimica Acta*, 44, 163-171.
- STEINMANN, P., ADATTE, T. & LAMBERT, P. 2003. Recent changes in sedimentary organic matter from Lake Neuchatel (Switzerland) as traced by Rock-Eval pyrolysis. *Eclogae Geologicae Helvetiae*, 96, S109-S116.
- SZAKOVA, I., KOLIHOVA, D., MIHOLOVA, D. & MADER, P. 2004. Single-purpose atomic absorption spectrometer AMA-254 for mercury determination and its performance in analysis of agricultural and environmental materials. *Chemical Papers-Chemicke Zvesti*, 58, 311-315.
- THEVENON, F., GRAHAM, N. D., CHIARADIA, M., ARPAGAUS, P., WILDI, W. & POTE, J. 2011. Local to regional scale industrial heavy metal pollution recorded in sediments of large freshwater lakes in central Europe (lakes Geneva and Lucerne) over the last centuries. *Science of the Total Environment*, 412, 239-247.
- THEVENON, F. & POTE, J. 2012. Water Pollution History of Switzerland Recorded by Sediments of the Large and Deep Perialpine Lakes Lucerne and Geneva. *Water Air and Soil Pollution*, 223, 6157-6169.
- TJALLINGII, R., ROHL, U., KOLLING, M. & BICKERT, T. 2007. Influence of the water content on X-ray fluorescence core-scanning measurements in soft marine sediments. *Geochemistry Geophysics Geosystems*, 8.
- TRIBOVILLARD, N., ALGEO, T. J., LYONS, T. & RIBOULLEAU, A. 2006. Trace metals as paleoredox and paleoproductivity proxies: An update. *Chemical Geology*, 232, 12-32.

- TYSON, R. V. 1995. Bulk geochemical characterization and classification of organic matter: carbon:nitrogen ratios and lignin-derived phenols. *In:* SPRINGER (ed.) *Sedimentary Organic Matter.* London: Chapman & Hall.
- VESELY, J. 2000. The history of metal pollution recorded in the sediments of Bohemian Forest lakes: Since the Bronze Age to the present. *Silva Gabreta*, vol. 4, p. 147—166.
- WANG, Q. R., KIM, D., DIONYSIOU, D. D., SORIAL, G. A. & TIMBERLAKE, D. 2004. Sources and remediation for mercury contamination in aquatic systems a literature review. *Environmental Pollution*, 131, 323-336.

CHAPTER III

Mercury contamination in sediments

This chapter investigates the influence of the wastewater treatment plant effluent of Vidy Bay on surface sediments, based on mercury concentrations, color, texture and structure. The established types of sediments in this study were correlated to the distance of the outlet pipe and to the mercury species. This study provides an overview of the current spatial influence of wastewater discharges and potential contamination exchanges between the pore water and the water column.

Influence of a WasteWater Treatment Plant on mercury contamination and sediment characteristics in Vidy Bay (Lake Geneva, Switzerland)

Elena Gascon Diez¹, Andrea Garcia Bravo², Natacha à Porta¹, Matthieu Masson³, Neil D. Graham¹, Serge Stoll¹, Yosef Akhtman⁴, David Amouroux⁵, Jean-Luc Loizeau¹

An article of similar form has been published. Refer to:

Gascon Diez, E., Garcia Bravo, A., A Porta, N., Masson, M., Graham, N., Stoll, S., Loizeau, J-L. (2013). Influence of a wastewater treatment plant on mercury contamination and sediment characteristics in Vidy Bay (Lake Geneva, Switzerland). *Aquatic Sciences*, doi:10.1007/s00027-013-0325-4

¹ Institut F.-A. Forel, Earth and Environmental Sciences Section, Faculty of Sciences, Route de Suisse 10, 1290 Versoix, Switzerland and Institute for Environmental Sciences, University of Geneva, 1211 Geneva, Switzerland

² Limnology Department, Evolutionary Biology Centre, EBC. Norbyvägen 18D 75236, Uppsala, Sweden

³ Department of Inorganic and Analytical Chemistry, Faculty of Sciences, University of Geneva, Sciences II, 30 Quai E-Ansermet, 1211 Geneva, Switzerland

⁴ Ecole Polytechnique Fédérale de Lausanne EPFL ENAC IIE TOPO, Station 18, CH-1015 Lausanne Switzerland

⁵ Laboratoire de Chimie Analytique Bio-Inorganique et Environnement, IPREM UMR 5254 CNRS Université de Pau et des Pays de l'Adour, Hélioparc , 64053 Pau, France

Abstract

Previous direct observations of the sediment surface in Vidy Bay, Lake Geneva (Switzerland), revealed a range of sediment characteristics in terms of colour, texture and morphology. Dives with the MIR submersibles during the éLEMO project permitted the exploration of a large portion of Vidy Bay. It is the most contaminated part of Lake Geneva, due to inputs of treated and untreated waters from a large wastewater treatment plant (WWTP). To evaluate the influence of WWTP effluent on mercury contamination and sediment characteristics, 14 sediment cores were retrieved in the vicinity of the wastewater treatment plant effluent. Total mercury concentrations in sediments ranged between 0.32 and 10.1 mg/kg. Inorganic mercury and monomethylmercury concentrations in overlying and pore waters were also measured. The total partition coefficients of mercury (logK_d) ranged from 3.6 to 5.8. The monomethylmercury concentration in pore waters of surface sediments was a large proportion of the total mercury concentration ($44 \pm 25 \%$). A Spearman test showed a negative correlation between the distance to the wastewater treatment plant outlet and the concentrations of total mercury in sediments and pore waters. Visual observations from the submersible allowed recognizing six different types of sediment. The areal distribution of these different sediment types clearly showed the influence of the wastewater treatment plant outlet on the sediment surface patterns. However, no relationship with mercury concentrations could be established.

Keywords: methylmercury, lake sediment, wastewater treatment plant, pore water

1. Introduction

Mercury (Hg) is a global pollutant and its toxicity depends on the distribution of its various forms (Langer et al. 2001). Monomethylmercury (MMHg) is one of the most hazardous Hg species since it bioaccumulates in organisms and biomagnifies along the food chain (Watras and Bloom 1992; Mason et al. 1995; Cossa et al. 2012) and it is a neurotoxin to humans and wildlife (WHO/IPCS 1990; Clarkson 1993; Harada 1995; Scheulhammer et al. 2007; Blank et al. 2013).

The main sources of Hg in lakes are watershed runoff and atmospheric deposits (Fitzgerald et al. 1991). Hg in superficial waters can be either dissolved or adsorbed onto suspended particles and organic matter (OM) in the water column. Hg is exchanged between aquatic compartments through various physicochemical processes such as diffusion, sedimentation, erosion, dissolution and bacterial transformation. Therefore, Hg in the solid phase, having reached the sediments, can be buried, resuspended, released or even methylated, making sediments a sink and a source of Hg (Blasco et al. 2000; Bale 2000). Methylation occurs primarily, but not exclusively, in anoxic waters and sediments (DeLaune et al. 2004). It is carried out by some species of bacteria belonging to the groups of sulphate- (SRB) and iron-reducing bacteria (IRB) (Compeau and Bartha 1985; Gilmour and Henry 1991; Gilmour et al. 1992; Pak and Bartha 1998; Kerin et al. 2006; Fleming et al. 2006; Hamelin et al. 2011; Parks et al. 2013). Geochemical parameters such as Eh, pH, nutrient availability, and temperature as well as the concentration of inorganic and organic complexing agents will influence the fate of the particulate Hg in aquatic systems (Ullrich et al. 2001).

Lake Geneva (Switzerland – France) is the largest freshwater lake in Western Europe with a total volume of 89 km³. Since the implementation of a WasteWater Treatment Plant (WWTP) in Lausanne in 1964, its effluents have affected the sediments in Vidy Bay. Among other pollutants, high concentrations of OM, total mercury (THg), bacteria and trace metals have been recorded (Loizeau et al. 2004; Pardos et al. 2004; Pote et al. 2008). Dephosphorization treatment, based on the addition of iron chloride in the WWTP, induced the release of iron into the bay. Hg²⁺ and MMHg have a high tendency to form complexes, in particular with soft ligands such as sulphur and iron

(Ullrich et al. 2001). In anoxic conditions, oxyhydroxides dissolve and release any associated Hg. The dissolution of iron colloids, or the presence of electron-acceptors for metal-reducing bacteria, may stimulate the release of Hg from the solid phase and, consequently, enhance Hg methylation (Fleming et al. 2006).

As anthropogenic Hg in aquatic environments is of major concern, we focus on a specific area of approximately 1 km² in Vidy Bay, which has already been proven to be the most contaminated area of the lake (e.g. Pote et al. 2008). Previous direct observations in the Bay using a submarine pointed out the presence of heterogeneous surface sediments, characterized by marked differences in sediment colour and texture; particularly, white, black, and greenish or brownish surface sediment had been observed (J.-L. Loizeau, personal communication). Some of the observed physical differences are related to the presence of a bacterial mat and likely to redox conditions; i.e., white coatings are probably due to the presence of *Beggiatoa*, a genus of white, filamentous proteobacteria (Sauvain et al. 2013, this issue). The aim of this research is to determine if, besides the influence of the distance from the Hg source, there is any large-scale influence of the various sediment types (reflecting both sedimentological and biogeochemical processes) on THg concentrations in sediments, and THg and MMHg contents in pore waters.

2. Methods

2.1. Direct sediment observation

In the frame of the éLEMO project (Wüest et al, this issue), six dives (June 20 and 21; July 19, 21, and 22; and August 16, 2011) were performed in Vidy Bay using the MIR scientific sumersibles. These dives, covering a total length of 16.6 km (Fig. 1), were performed close to the lake sediments in order to directly observe sediment structures, textures and colours, and to collect sediment cores. Video recordings were made to document sediment surface characteristics. These videos, in addition to dive logs, served as a basis to establish a detailed map of the sediment structures present in the Bay. Correspondence of video with positionning was based on the time given by GPS. Submarine trajectories and core positions (Table 1) were calculated based on the GPS

position of the floating platform, triangulation of the submersibles, and interpolation of missing data (Akhtman et al. 2012). Additional images were also obtained using a mini video camera attached to a corer deployed from the La Licorne research vessel.

Table 1. Sediment core locations and corresponding sediment type

Core	WGS84 Coordinates		SWISS C	oordinates	Distance to	Depth	Sediment
number	Latitude	Longitude	N	E	WWTP outlet		type
	(Deg decim)	(Deg decim)	(m)	(m)	(m)	(m)	
1	46.50856	6.58275	151165	534309	526	48	3
2	46.50853	6.58274	151161	534308	529	49	3
3	46.50842	6.58674	151146	534615	403	51	5
4	46.51111	6.58481	151447	534470	226	45	5
5	46.51114	6.58479	151450	534468	226	45	5
6	46.51024	6.58528	151349	534505	258	53	5
7	46.51002	6.58563	151325	534532	262	52	5
8	46.50888	6.58689	151197	534627	351	54	6
9	46.50905	6.58367	151219	534380	438	69	3
10	46.50873	6.58497	151183	534479	411	43	5
11	46.50710	6.58653	151004	534598	543	68	2
12	46.50876	6.58670	151184	534612	366	60	6
13	46.51040	6.58508	151368	534490	255	50	5
14	46.51047	6.58548	151375	534521	228	50	5
WWTP outlet	46.51572	6.58822	151956	534738	0	35	5

Six types of sediment surfaces based on colour, texture, and structure (Figs. 1 and 2) were distinguished. They are described following their occurrence from the deep basin towards the lakeshore and WWTP outlet as following:

Type 1 is characterized by enigmatic, yet well developed cushion and trench structures (Fig. 2a). Cushions are generaly 40 - 60 cm in diameter, surrounded by 10 to 20 cm wide depressions. The vertical amplitude of the structures is about 10 to 20 cm. The sediment surface was beige and composed by clayey silts. It was observed in the deepest part of the bay, and covers a large surface area extending beyond the present survey. These structures have been previously described (Vernet 1966; Sturm et al. 1984; Dominik et al. 1992) and no core was retreived in this sediment type.

Type 2 corresponds to a fine-grained, flat, beige sediment surface, crossed by long shallow trenches (Fig. 2b). It was observed at the rim of the cushion-trench structures. It covers small surface areas in the Bay (Fig. 1). Core #11 was retreived from this sediment type;

Type 3 is charaterized by flat lake bottom covered by a beige sediments with no significant variation either in structure or colour. It was observed on slopes, between 30 m and 100 m depth (Fig. 2c). Cores #1, 2, and 9 were collected in this sediment type

Type 4 resembles type 3, but is punctuated with small holes, 10 cm in diameter and few centimeters deep (Fig. 2d). The bottom of the depression may be black. This sediment type was observed in the vincinity of the WWTP outlet. No core was retreived in this sediment type.

Type 5 is charaterized by a heterogeneous assemblage of sediment colour on relatively flat sediment surface, resembling a camouflage pattern. Sediment colours vary between beige, black, and white (Fig. 2e). Individual surface colour areas range from square decimetres to metres. This sediment type was essentially observed at the outlet of the WWTP, and covers an area of approximately 0.25 km². Most cores (#3 to #7, #10, #13, #14) were collected in this sediment type in different colour zones.

Type 6 corresponds to a very small area in the Bay, a few hundreds of m². It is distinct because the sediments were almost entirely greyish-brown to black and covered by

litter (including q-tips, cigarette butts, and sanitary towels, Fig. 2f). This type was observed 300 m downslope of the WWTP effluent within the type 5 sediment area. Cores #8 and #12 were collected in this sediment type.

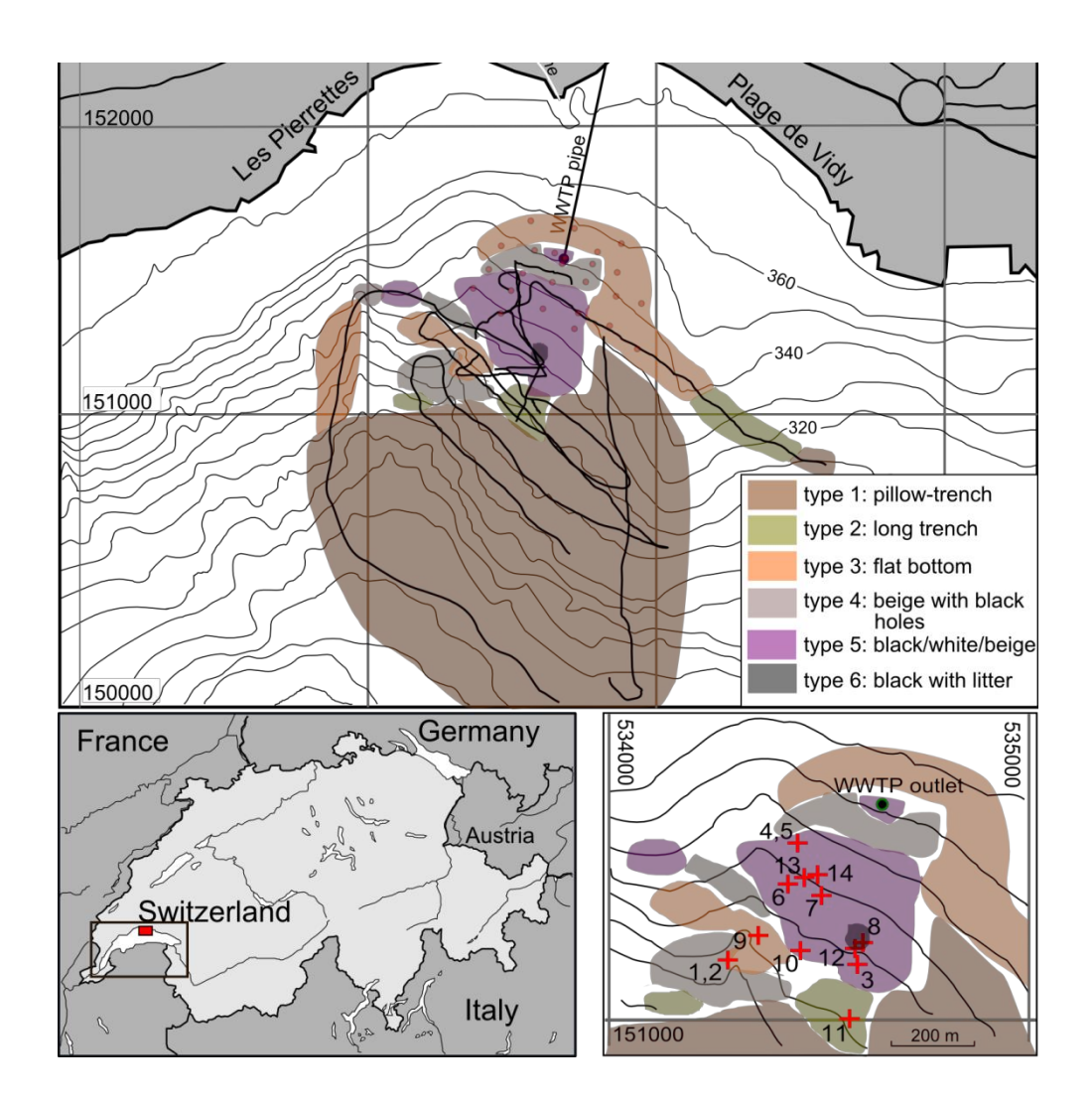


Figure 1. Map of Vidy Bay and sediment type distribution. Bold lines represent routes of the submarine; small red circles are punctual observations with a submerged camera. Insets: left; situation of Lake Geneva on the Switzerland-France border. The red square indicates the location of Vidy Bay; right, close view of the sediment core locations (red crosses).

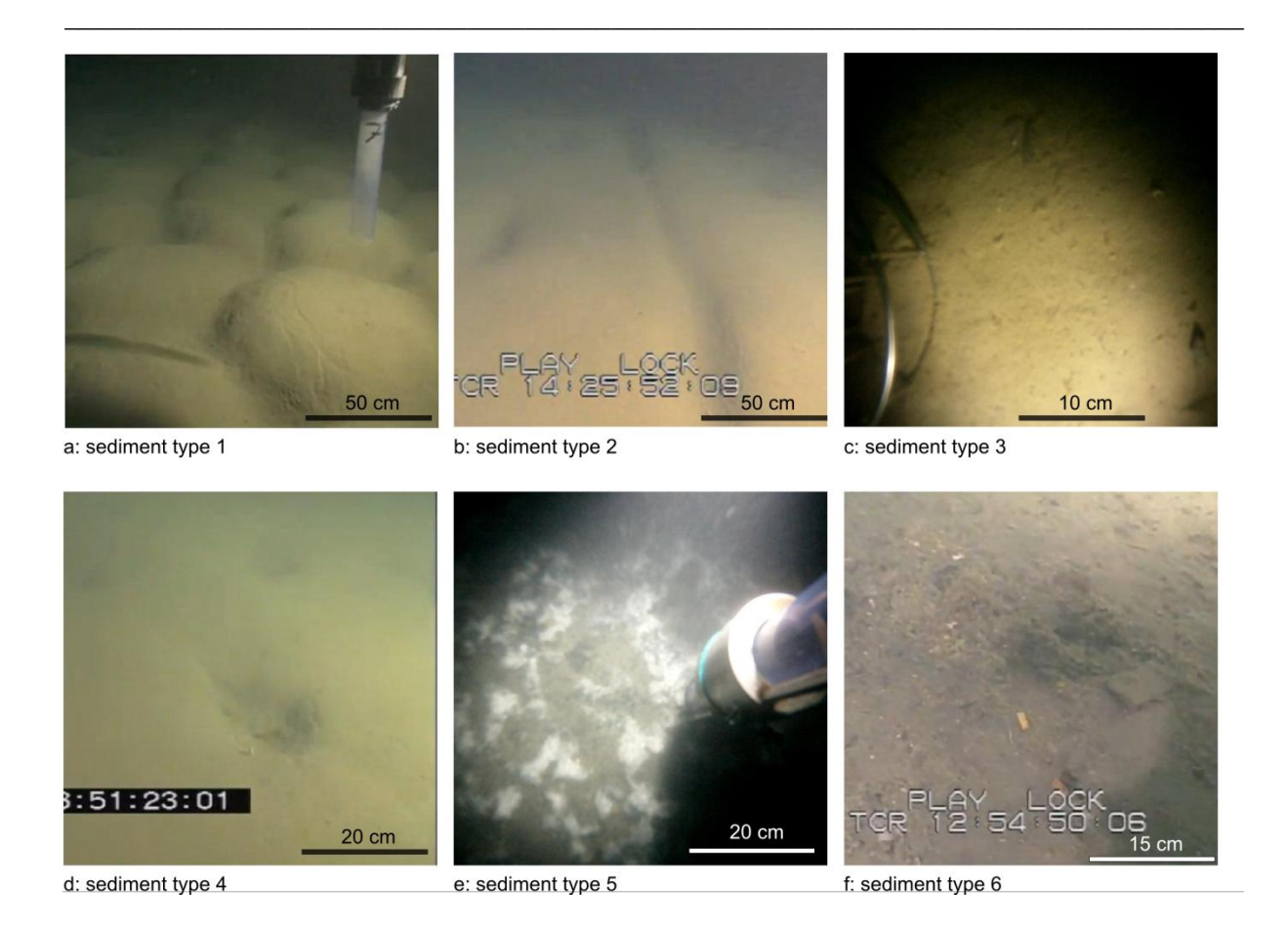


Figure 2. Photos of the different types of sediments surfaces. Type 1 - trenches and cushions; Type 2 - long trenches; Type 3 - flat beige sediment; Type 4 - Flat beige surface with holes; Type 5 - Black/white/beige sediment; Type 6 - flat with debris (cigarette butts, paper, sanitary towels, etc.). Pictures were taken from the MIR submarines, with the exception of types 3 and 5, which were taken from a camera attached to sampling device.

2.2. Core sampling and sediment processing

A total of 14 cores, using a specially designed push corer (Girardclos et al. 2012), were retrieved in the different zones of the Bay defined by visual observations. Sediment cores were transported to a nearby laboratory where they were placed in a glove-tent under an N_2 -atmosphere. The overlying water was extracted with syringes and a subsample was stored in clean bottles (see procedure below). The remainder was filtered through 0.45 μ m Sterivex syringe filters and stored in 250 ml teflon bottles at

4 °C. Both filtered and unfiltered water samples were acidified with suprapur HCl (1 % v/v). Sediments were extruded and sliced at 0 - 1.5 cm, 1.5 - 3 cm, and 3 - 6 cm intervals. Each sediment layer was transferred to a teflon centrifugation tube and centrifuged at 3500 rpm for 40 minutes to extract the pore water. The centrifuge tubes were placed back into the glove-tent under N₂-atmosphere where the supernant water was filtered with 0.45 μm Sterivex syringe filters, and stored in 30ml teflon flasks inside two polyethylene bags. The cleaning procedure for the teflon bottles and vessels used to store water and analyse mercury species was carried-out in series of three baths: 1) a soap Extran® MA 03 bath for 1 hour under sonification and then rinsed with MilliQ water; 2) two-hour sonification in a 10 % nitric acid bath, conducted a second time after changing the acid and rinsing with MilliQ water; and 3) two-hour sonification in a 10 % HCl bath and MilliQ water rinse.

2.3. Sedimentological and chemical analyses

Sediment grain-size distribution was determined on wet sediments using a laser diffraction Coulter LS-100 analyser, following the procedure described by Loizeau et al. (1994). Sediments were freeze-dried in a CHRIST BETA 1-8K freeze-drying unit (-54 °C, 6 Pa) for a minimum of 48 h. The organic matter content in sediments (OM_{sed}) was measured by Loss On Ignition (LOI); samples were heated to 550 °C for 1 hour in a muffle furnace (Nabertherm – LE14/11). Sulphate concentration in pore water was measured by Ionic Chromatography (Dionex ICS-3000) with a IonPac®AS19 (4.250 mm) column. Iron concentration in pore water was measured by FG-AAS (Varian, AA240FS). The accuracy was within 8% of certified values of the reference material (SLRS-4) and the analytical error was less than 5%.

Total mercury in dry sediment (THg_{sed}) was analysed by Cold Vapor Atomic Absorption Spectrophotometry (CV-AAS) using an automatic mercury analyser, Altec Model AMA 254 (Száková et al. 2004), following the procedure described by Roos-Barraclough et al. (2002) and Schafer et al. (2006). All analyses were run in triplicate. The detection limit and working range were 0.01 ng and 0.05 - 600 ng, respectively. Concentrations obtained for repeated analyses of the certified reference material never

exceeded the specified range given for MESS-3 reference material (National Research Council Canada).

MMHg and IHg (inorganic mercury) in overlying and pore waters (MMHgow, MMHgpw and IHgow, IHgpw, respectively) were analysed by species-specific isotopic dilution and capillary gas chromatography (Focus GC, ThermoFinnigan) coupled to an ICP-MS (X7 II, ThermoElectron) to correct for species inter-conversion (Monperrus et al. 2005). Total mercury concentrations in overlying and pore waters (THgow, THgpw) were obtained by adding MMHgpw and IHgpw concentrations. MMHg concentrations in sediment were not measured because Bravo et al. (2011) had shown a positive correlation with THg concentration. Thus, the MMHg concentration in the sediments sampled would follow the same trends as exhibited by THg.

2.4. Statistical analyses

As data were not normally distributed, a Spearman test was used to evaluate correlations between the distance to the wastewater outlet and the Hg forms and OM concentrations. The Spearman rank correlation coefficient r_s was computed into a p-value to determine if the variables were significantly correlated (Siegel 1956). The level of significance was set to 0.05. Statistical analyses were performed with R 2.14.1 software. As sediment types 2 and 3, as well as 5 and 6, were solely discriminated by their morphology, cores retrieved in these sediment types were grouped as type 2 - 3 and 5 - 6 for the statistical analysis.

The distances between the WWTP outlet and the cores were significantly different between types 2 - 3 and 5 - 6. Therefore, when the correlation between the distance to the outlet and the measured variable was statistically significant, it was not possible to separate the effects of distance to the WWTP outlet from the effect of sediment type. In turn, the Mann-Whitney-Wilcoxon test was used to assess the influence of sediment type on the measured variable when the correlation to distance was not significant.

3. Results and discussion

3.1. Surface sediment analyses

The 14 cores were mainly collected on the downward slope from the WWTP outlet (Fig. 1, inset). Distances of coring sites to the WWTP outlet ranged from 226 to 543 m (Table 1). Surface sediments were sandy silt containing a relatively large proportion of organic matter (9 to 16 %) related to the WWTP effluent. The mean grain size was $68 \pm 22 \,\mu m$.

The concentrations of sulphate (SO_4^{-2}) and dissolved iron (Fe) in pore and overlying waters (Table 2) gave indications on the redox conditions of the water samples. Concentrations of SO_4^{-2} in overlying water varied between 45 and 56 mg/L, which corresponded to the concentrations observed in Lake Geneva water column (Zahner 1984). In pore waters, SO_4^{-2} concentrations were much less and varied between not detectable to 5.6 mg/L. A gradual decrease in concentration between the upper layer (0-1.5 cm) and the deepest layer was observed. Although layers 0-1.5 cm were more concentrated in SO_4^{-2} than deeper layers, they were considered as anoxic since these concentrations were approximately 10 times lower than those recorded in the overlying waters. Additionally, dissolved Fe concentrations (Table 2) corroborated the sulphate results with generally low concentrations (between 7 and 21 μ g/L) in overlying (oxygenated) waters and increased Fe contents with depth in anoxic pore waters (between 26 and 6990 μ g/L).

Based on sulphate and Fe measurements, surface layers of all sediment cores showed anoxic conditions. Nevertheless, a brownish surface layer was observed. This colour layer reflects the presence of iron oxides and characterizes sediment of types 2 and 3 (core #11 and #9, respectively). Reduced dissolved Fe likely reaches the surface of the sediments and in contact with the oxygenated overlying water might be oxidized. A thin layer of iron (few mm) oxides would explain the brownish colour.

Table 2. Mercury species, sulphate and iron concentrations in lake sediments, pore water, and overlying water samples. F: filtered, NF: non-filtered, n.d.: not detected. MMHg/THg represents ratios in pore waters and overlying waters. The uncertainty of the OM is 5%. Uncertainties are given at one-sigma standard deviation.

Core umber	Sample layers	THg _{Sed} (mg/kg)	$\begin{array}{c} \text{MMHg}_{\text{OW or PW}} \\ \text{(ng/L)} \end{array}$	$\begin{array}{c} IHg_{OW \ or \ PW} \\ (ng/L) \end{array}$	THg _{OW or PW} (ng/L)	$logK_dTHg$	MMHg/THg (%)	OM (%)	SO ₄ -2 (mg/L)	Fe (µg/L)
1	Overlying water F	-	0.05 ± 0.01	0.44 ± 0.01	0.49 ± 0.01	-	10.0	-	-	-
1	Overlying water NF	-	0.19 ± 0.01	1.29 ± 0.01	1.48 ± 0.01	-	12.7	-	-	-
1	0-1.5cm	0.57 ± 0.03	5.7 ± 0.5	6.1 ± 0.1	11.8 ± 0.5	4.69	48.5	9.3	-	-
1	1.5-3cm	0.6 ± 0.1	-	1.3 ± 0.2	1.3 ± 0.2	5.64	-	9.4	-	-
1	3-6cm	0.66 ± 0.01	0.78 ± 0.00	0.68 ± 0.04	1.46 ± 0.04	5.65	53.4	9.1	-	-
2	Overlying water F	-	0.05 ± 0.01	0.87 ± 0.01	0.92 ± 0.01	-	5.8	-	-	-
2	Overlying water NF	-	0.81 ± 0.01	54 ± 2	55 ± 2	-	1.5	-	-	-
2	0-1.5cm	0.7 ± 0.2	0.32 ± 0.04	3.2 ± 0.1	3.5 ± 0.1	5.31	9.2	9.6	-	_
2	1.5-3cm	1.9 ± 0.1	2.0 ± 0.2	79 ± 2	81 ± 2	4.36	2.4	11.9	-	-
2	3-6cm	4.4 ± 0.3	0.64 ± 0.07	14.2 ± 0.2	14.9 ± 0.3	5.47	4.3	17.0	-	-
3	Overlying water F	-	0.06 ± 0.01	0.34 ± 0.03	0.40 ± 0.03	_	15.0	_	-	-
3	Overlying water NF	-	0.14 ± 0.02	1.6 ± 0.1	1.7 ± 0.1	-	8.3	-	-	-
3	0-1.5cm	1.2 ± 0.2	1.1 ± 0.1	2.0 ± 0.1	3.1 ± 0.2	5.60	35.0	16.1	_	_
3	1.5-3cm	1.0 ± 0.1	0.47 ± 0.05	1.4 ± 0.1	1.9 ± 0.1	5.74	25.5	13.7	-	-
3	3-6cm	1.0 ± 0.1	0.26 ± 0.04	1.32 ± 0.00	1.6 ± 0.0	5.80	16.7	11.3	-	-
4	Overlying water F	-	0.12 ± 0.02	0.78 ± 0.04	0.90 ± 0.05	-	13.1	_	47.31	9.24
4	Overlying water NF	-	1.2 ± 0.9	36 ± 2	37 ± 2	-	3.3	-	-	-
4	0-1.5cm	1.4 ± 0.2	3.4 ± 0.3	8.7 ± 0.2	12.1 ± 0.3	5.07	28.2	12.4	0.24	25.6
4	1.5-3cm	0.8 ± 0.1	1.0 ± 0.1	11.7 ± 0.6	12.7 ± 0.6	4.78	7.7	10.3	0.93	2150
4	3-6cm	1.4 ± 0.4	0.8 ± 0.1	41 ± 1	42 ± 1	4.53	1.8	9.8	2.80	6990
5	Overlying water F	-	0.06 ± 0.01	0.85 ± 0.09	0.9 ± 0.1	-	7.0	-	47.86	10.2
5	Overlying water NF	-	0.88 ± 0.09	30 ± 2	30 ± 2	-	2.9	-	-	-
5	0-1.5cm	1.3 ± 0.4	11.1 ± 0.5	3.3 ± 0.4	14.4 ± 0.7	4.96	77.1	14.5	0.31	542
5	1.5-3cm	1.00 ± 0.00	1.5 ± 0.2	3.0 ± 0.2	4.5 ± 0.2	5.34	32.7	11.7	0.25	436
5	3-6cm	1.0 ± 0.2	0.28 ± 0.04	2.9 ± 0.3	3.2 ± 0.3	5.47	8.9	10.3	0.03	1150
6	Overlying water F	-	0.07 ± 0.01	0.80 ± 0.01	0.87 ± 0.01	-	7.6	-	47.32	12.3
6	Overlying water NF	-	0.52 ± 0.04	8.6 ± 0.5	9.1 ± 0.5	-	5.7	-	-	-
6	0-1.5cm	1.61 ± 0.02	1.6 ± 0.3	5.2 ± 0.3	6.8 ± 0.4	5.37	23.3	10.8	2.96	176
6	1.5-3cm	1.3 ± 0.6	6 ± 2	8.3 ± 0.5	14 ± 2	4.97	42.4	12.3	0.38	224
6	3-6cm	1.3 ± 0.3	1.1 ± 0.2	6.5 ± 0.3	7.7 ± 0.3	5.24	14.7	10.9	0.39	2360
7	Overlying water F	-	0.5 ± 0.1	2.54 ± 0.04	3.0 ± 0.1	-	15.5	-	44.88	21.2
7	Overlying water NF	-	3.7 ± 0.2	218 ± 17	222 ± 17	-	1.7	-	-	-
7	0-1.5cm	5.2 ± 0.3	22 ± 3	276 ± 49	298 ± 76	4.23	8.9	-	5.15	252
7	1.5-3cm	10 ± 1	9 ± 1	719 ± 234	728 ± 234	4.14	1.2	-	0.49	621
7	3-6cm	9 ± 1	13 ± 3	-	-	3.58	-	-	-	732

Table 2. (continued)

Core	Sample layers	THg _{Sed} (mg/kg)	MMHg _{OW or PW} (ng/L)	$\begin{array}{c} IHg_{OW \ or \ PW} \\ (ng/L) \end{array}$	THg _{OW or PW} (ng/L)	logK _d THg	MMHg/THg (%)	OM (%)	SO ₄ -2 (mg/L)	Fe (µg/L)
8	Overlying water F Overlying water NF	-	0.12 ± 0.05 0.42 ± 0.02	0.52 ± 0.02 3.7 ± 0.1	0.6 ± 0.1 4.2 ± 0.1	- -	18.9 10.1	-	47.69 -	10.8
8	0-1.5cm	0.6 ± 0.2	3.2 ± 0.7	3.6 ± 0.2	6.7 ± 0.8	4.94	47.2	10.6	5.15	62.5
8	1.5-3cm	0.50 ± 0.09	1.4 ± 0.7	3.6 ± 0.1	5.0 ± 0.7	5.00	27.7	9.6	0.49	211
8	3-6cm	0.36 ± 0.08	0.43 ± 0.06	4.2 ± 0.1	4.6 ± 0.1	4.90	9.2	8.6	0.09	635
9 9	Overlying water F Overlying water NF	- -	0.44 ± 0.01	- 24.9 ± 0.5	- 25.4 ± 0.5	-	- 1.7	- -	56.70	11.1
9	0-1.5cm	0.7 ± 0.1	2.8 ± 0.4	1.5 ± 0.1	4.3 ± 0.4	5.23	64.8	10.7	_	266
9	1.5-3cm	0.7 ± 0.1 1.0 ± 0.3	1.3 ± 0.1	3.9 ± 0.3	5.2 ± 0.3	5.28	25.7	10.7	-	443
9	3-6cm	1.3 ± 0.3	-	-	-	-	-	9.5	-	644
10	Overlying water F	-	0.07 ± 0.01	0.45 ± 0.04	0.52 ± 0.04	_	13.1	_	53.04	7.01
10	Overlying water NF	-	0.25 ± 0.03	23 ± 1	23 ± 1	-	1.1	-	-	-
10	0-1.5cm	0.8 ± 0.2	2.4 ± 0.3	0.98 ± 0.07	3.3 ± 0.3	5.35	70.6	9.9	2.94	174
10	1.5-3cm	0.57 ± 0.06	1.6 ± 0.4	3.9 ± 0.2	5.6 ± 0.5	5.01	29.4	10.0	0.82	206
10	3-6cm	0.62 ± 0.08	1.4 ± 0.8	6 ± 3	7 ± 3	4.96	19.7	10.1	n.d.	916
11	Overlying water F	_	0.03 ± 0.00	0.39 ± 0.01	0.42 ± 0.01	_	7.6	_	56.64	7.38
11	Overlying water NF	-	0.41 ± 0.06	7.3 ± 0.1	7.7 ± 0.1	-	5.3	-	-	-
11	0-1.5cm	0.38 ± 0.03	1.7 ± 0.2	1.2 ± 0.1	2.9 ± 0.2	5.12	59.2	9.2	4.02	532
11	1.5-3cm	0.32 ± 0.01	1.1 ± 0.2	3.6 ± 0.2	4.6 ± 0.3	4.84	22.6	8.4	0.14	1040
11	3-6cm	0.4 ± 0.1	0.9 ± 0.1	14.5 ± 0.2	15.3 ± 0.3	4.35	5.7	8.0	0.22	1510
12	Overlying water F	-	-	-	-	_	-	-	-	-
12	Overlying water NF	-	0.5 ± 0.1	2.1 ± 0.2	2.5 ± 0.2	-	17.8	-	-	-
12	0-3cm	0.7 ± 0.2	5.5 ± 0.5	10.6 ± 0.2	16.1 ± 0.5	4.65	34.1	8.9	-	-
12	3-6cm	0.5 ± 0.1	1.5 ± 0.4	6.5 ± 0.4	8.1 ± 0.6	4.81	19.1	9.0	-	-
13	Overlying water F	_	_	_	_	_	-	_	_	_
13	Overlying water NF	-	1.7 ± 0.3	3.4 ± 0.2	5.2 ± 0.4	-	33.7	-	-	-
13	0-1.5cm	1.5 ± 0.5	13 ± 2	11.8 ± 0.2	25 ± 2	4.78	53.2	14.3	-	-
	1.5-3cm	1.5 ± 0.2	5.1 ± 0.6	11.0 ± 0.7	16.1 ± 0.9	4.96	31.5	13.3	-	-
13	3-6cm	1.6 ± 0.2	0.83 ± 0.04	45.9 ± 0.4	46.7 ± 0.4	4.53	1.8	9.4		-
14	Overlying water F	-	0.20 ± 0.02	0.43 ± 0.01	0.63 ± 0.02	-	32.0		-	-
14	Overlying water NF	-	0.79 ± 0.06	1.19 ± 0.02	2.0 ± 0.1	-	39.9	-	-	-
14	0-1.5cm	1.20 ± 0.01	6.9 ± 0.5	5.1 ± 0.2	12.0 ± 0.5	5.00	57.7	14.0	-	-
14	1.5-3cm	0.92 ± 0.04	0.61 ± 0.07	4.01 ± 0.04	4.6 ± 0.1	5.30	13.1	10.6	-	-
14	3-6cm	1.2 ± 0.2	0.61 ± 0.01	32.9 ± 0.4	33.5 ± 0.4	4.58	1.8	9.4	-	-

3.2. THg_{sed}: an indicator of the contamination from the WWTP

THg_{sed} concentrations in the 14 sediment cores ranged between 0.32 and 10 mg/kg (Table 2). The highest THg_{sed} concentrations were found in sediment core #7 (Fig. 1). The maximum value of THg was about 330 times higher than the natural background level of Lake Geneva (0.03 mg/kg, Vernet and Viel 1984). THg_{sed} concentrations in this sediment core increased with depth (Table 2). This sediment core was also found to be highly concentrated in particulate Cd, Pb and Cu (Masson and Tercier-Waeber 2013, this issue); and to be significantly different in terms of abundance and type of bacteria (Sauvain et al. 2013, this issue). The heterogeneous partition of contaminants in Vidy Bay sediments might result from the wandering of the plume released by the WWTP outlet and subsequent settling of contaminated particles. Although THgsed concentrations in core #2 were lower than those found in core #7, they were also relatively high in the third layer (4.4 mg/kg, Table 2). Due to these high values, cores #2 and #7 were considered as outliers and not taken into account in further statistical calculations. The dispersion of THg_{sed} in the upper layer (0-1.5 cm) is shown in figure 3. Most concentrations measured in the Bay exceeded the Threshold Effect Concentration (TEC) of 0.18 mg/kg (MacDonald et al. 2000). Additionally, 9 of them exceeded, or were at the limit of, the Probable Effect Concentration (PEC) of 1.06 mg/kg. These THg concentrations in Vidy Bay sediments correspond to those reported by Pote et al. (2008). No significant correlation was found between sediment type and the Hg concentration in the sediments. Nevertheless, the range of THg_{sed} concentrations in sediment cores grouped, considering the distance to the WWTP effluent (Fig. 3) showed that type 2 - 3 (distant to the WWTP effluent) presented lower THg concentrations than type 5 - 6 (closest to the WWTP effluent).

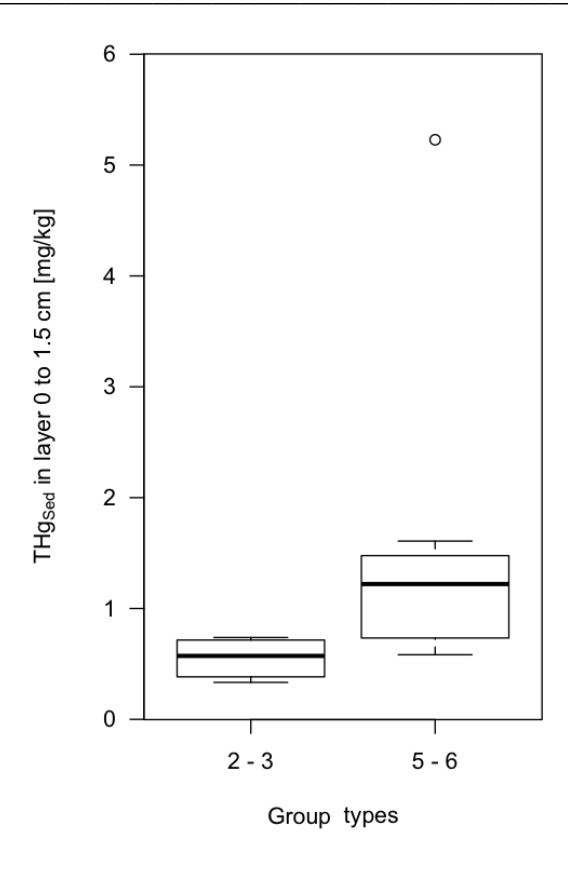


Figure 3. Concentration ranges of THg in surface sediments by sediment types (all cores included). The thick line inside the box is the median, the box indicates the upper and lower quartiles, the dashed whisker lines give the range of extreme values to a maximum of 1.5 times the interquartile range. Outliers are indicated with circles.

3.3. Hg speciation in pore water

Pore water in core #7 was found to be highly concentrated in THg_{PW} (from 298 to 728 ng/L), followed by core #2 (from 3.5 to 81 ng/L). In the other sediment cores, THg_{PW} concentrations were lower and ranged between 1.3 and 46.7 ng/L (Table 2). The THg partition coefficient, $logK_d$ (in L/kg), is defined in this study as the ratio between THg concentrations measured in sediment (THg_{sed}) and in pore water (THg_{PW}) (Turner et al. 2004). The $logK_d$ values ranged between 3.6 and 5.8. Similar results have been found in Lake Superior and Lake Michigan sediments ($logK_d = 4.8 \pm 0.1$ and $logK_d = 5.7$, respectively; Rolfhus et al. 2003; Hurley et al. 1996). The highest MMHg_{PW} concentrations have been found in core #7, ranging between 9 and 22 ng/L. These

concentrations were high as compared to the other 13 sediment cores; MMHg_{PW} concentrations ranged from 0.32 to 11.1 ng/L. The average MMHg_{PW} concentration in all sediments cores, except core #7, was 4.5 ± 4.1 ng/L in the 0 - 1.5 cm layer, 2.6 ± 2.1 ng/L in the 1.5 - 3 cm layer and 7.9 ± 4.0 ng/L in the 3 - 6 cm layer.

The MMHg_{PW}/THg_{PW} ratio was found to be depth dependant and was 0.44 ± 0.25 in the 0 - 1.5 cm layer. This result is similar to that found in other contaminated lacustrine bays, such as Lavaca Bay (Texas) with a MMHg_{PW}/THg_{PW} ratio of 0.41 ± 0.33 (Bloom et al. 1999). In other areas affected by atmospheric Hg deposition, as in small lakes in Ontario, Canada, MMHg_{PW}/THg_{PW} ratio ranged between 0.01 and 0.76 (He et al. 2007). A large proportion of the MMHg found in Vidy Bay decreased with sediment depth, with 22 ± 14 % in the 1.5 - 3 cm layer and 13 ± 13 % in the 3 - 6 cm layer.

The percentage of MMHg has often been used as a proxy of Hg methylation activity in sediments (cf. Drott et al. 2008). In the present study, since the MMHg_{PW}/THg_{PW} ratio was generally higher in the 0 - 1.5 cm layer than in deeper layers, the main production of MMHg likely occurs in the surface of sediments. Sulphate (up to 5 mg/L) and iron concentrations (Table 2) measured in sediment pore water of Vidy Bay indicates the availability of acceptor electron to the main Hg methylators, the sulphate-reducing and iron-reducing bacteria.

3.4. Hg speciation in overlying waters

THg concentrations in overlying waters for filtered (3.0 \pm 0.1 ng/L) and non-filtered overlying water (222 \pm 17 ng/L) in core #7 followed the same trend as the parameters measured in the pore water. In core #2, only the non-filtered overlying water is high in THgow at 55 \pm 2 ng/L. Without taking these outliers into account, THgow concentration ranged between 0.40 and 0.92 ng/L in filtered overlying water; and between 1.48 and 37 ng/L in non-filtered overlying water.

The highest MMHgow concentrations were found in core #7 in filtered and non-filtered overlying waters (0.5 \pm 0.1 ng/L and 3.7 \pm 0.2 ng/L, respectively) as compared to the other 13 sediment cores, where MMHgow concentrations ranged

between 0.03 and 0.20 ng/L for filtered overlying waters, and between 0.14 and 1.7 ng/L for non-filtered overlying waters. In any case, MMHg concentrations found in Vidy Bay lake bottom waters exceed the value of 0.05 ng/L found in the centre of Lake Geneva (Bravo, 2010).

MMHg concentrations measured in overlying waters were between 10 and 100 times lower than those measured in pore waters, indicating a probable diffusion of MMHg from the sediments to the water column, and showing that methylation takes place preferentially in the surface sediments as observed in many studies (cf. Ullrich et al. 2001). However, no correlation was found between MMHg_{PW} (layer 0 - 1.5 cm) and MMHg_{OW} ($r_s = 0.042$).

3.5. Influence of sediment types on Hg forms

For layer 0 - 1.5 cm and all layers combined, a Spearman test showed a significant negative correlation between distance to the WWTP outlet and the following parameters: THg_{Sed} , THg_{PW} , filtered THg_{OW} and non-filtered MMHgow concentrations (p-values < 0.05, Table 3).

Table 3. Correlation p-values between the measured parameters (in sediments, pore water, and the overlying water) with distance to the WWTP outlet

Parameters	Spearman p-values		Parameters	Spearmai	n p-values
in sediments	Layer 0 - 1.5 cm	All layers combined	in overlying waters	Overlying water Non Filtered	Overlying water Filtered
THg _{sed}	0.01*	0.01*			
OM	0.04*	0.01*			
$\mathrm{MMHg}_{\mathrm{PW}}$	0.12	0.93	$\mathrm{MMHg}_{\mathrm{OW}}$	0.01*	0.08
$\mathrm{THg}_{\mathrm{PW}}$	0.02*	0.01*	THg_{OW}	0.27	0.01*
$\mathrm{MMHg_{PW}}$ / $\mathrm{THg_{PW}}$	0.49	0.12	MMHg _{OW} / THg _{OW}	0.59	0.64
logK _d THg	0.67	0.35			

^{*} indicates a p<0.05

Because the sediment types were also dependant on distance from the WWTP outlet (Fig. 1), it was not possible to evaluate whether there was a statistically significant difference of these parameters between sediment types.

Table 4. Independence Mann-Whitney-Wilcoxon test for non-distance correlated variables (Table 3) and the groups of sediment type, p-value threshold = 0.05

Ī	Parameters	Mann-Whitney	-Wilcoxon p-values	Parameters	Mann-Whitney-Wilcoxon p-v		
	in sediments	Layer All layers		in overlying waters	Overlying water	Overlying water	
		0 - 1.5 cm	combined		Non Filtered	Filtered	
Ī	$\mathrm{MMHg}_{\mathrm{PW}}$	0.73	0.97	MMHg _{OW}		0.06	
	$logK_dTHg$	1.00	0.95	THg_{OW}	0.86		
	$MMHg_{PW}$ / THg_{PW}	0.37	0.22	MMHg _{OW} / THg _{OW}	0.60	0.33	

On the other hand, logK_d, MMHg_{PW}, MMHg_{PW}/THg_{PW} ratios, non-filtered THg_{OW} and filtered MMHg_{OW} concentrations were not correlated to distance from the WWTP outlet (p-values > 0.05, Table 3). Therefore a Mann-Whitney-Wilcoxon test was performed to assess the differences between sediment types for these parameters. All p-values were found to be greater than 0.05 (Table 4), which suggests that there was difference between sediment statistical type and $log K_d$ $MMHg_{PW}$, MMHg_{PW}/THg_{PW} ratio, non-filtered THg_{OW} and filtered MMHg_{OW} concentrations. Therefore, at the studied scale, it appeared that the strong differences in sediment surfaces were essentially due to redox variations at the sediment surface and the presence or absence of a bacterial mat (Sauvain et al. 2013, this issue). These differences seemed to have no direct effect on mercury transformation processes in the sediment. The survey performed in the present study could not assess the impact of the noticeably altered sediments (sediment type 5: 0.25 km², in the vicinity of the WWTP) on mercury fate. However, a large variation in the concentration of mercury forms, uncorrelated to distance to the main source, still were observed. For instance, MMHg_{PW} concentrations ranged between 0.26 and 27.2 ng/L in core samples. These variations should be related to local heterogeneities of biogeochemical processes at the scale of centimetres to metres.

4. Summary

THg_{PW} concentrations were found to be high in the whole Bay with concentrations increasing as sampling sites approached the main source. This correlation between distance and THg_{PW} concentration confirms the WWTP as a source of Hg contamination within the Bay. MMHg_{PW} concentrations and their fraction on THg_{PW} were not directly influenced by the WWTP effluent; this indicated that biogeochemical processes, not visually apparent from the sediment types, dominated MMHg formation in pore waters. MMHg_{PW} concentrations and the MMHg_{PW}/THg_{PW} ratios were higher in the top sediment layer, indicating a higher methylation rate in these sediments. The integration of physicochemical parameters and bacteria biodiversity analysis on these superficial sediments would be of great interest to understand the source of increased MMHg_{PW}, as compared to sediment depth, to sediment type, and to other aquatic environments.

Acknowledgments

This publication is part of the international, interdisciplinary research project ELEMO (http://www.elemo.ch) to investigate the deep-waters of Lake Geneva using two Russian MIR submarines. Funding for this study was provided by the *Fondation pour l'Etude des Eaux du Léman* (FEEL). Additional funding for the work described in this paper was provided by Swiss National Science Foundation SNSF PDFMP2 123034 and 123048 (LÉMAN-21). We are grateful for the support.

We thank the Russian MIR crew members (www.elemo.ch/mir-team) for their excellent performance and the SAGRAVE team who provided and operated the platform from which the dives were carried out. We also thank Ulrich Lemmin and Jean-Denis Bourquin for project coordination. The service of Mikhail Kranoperov (Russian Honorary Consulate) as liaison is greatly appreciated. Philippe Arpagaus piloted the "La Licorne" scientific vessel for supplementary sampling. Marylou Tercier-Waeber for helping in supplementary sampling and writing advises. The manuscript greatly benefits from comments of two anonymous reviewers and Alfred Wüest.

References

- Akhtman Y, Martelletti L, Greanjean O, Lemmin U (2012) Collaborative Web-GIS platform for systematic exploration of Lake Geneva. In: Proceedings of the XXII Congress of the International Society for Photogrammetry and Remote Sensing, vol. XXXIX-B4, num. IV/1, p. 1-6, 25 August 1 September 2012, Melbourne, Australia
- Bale AE (2000) Modeling aquatic mercury fate in Clear Lake, Calif. J Environ Eng 126:153-163
- Blank N, Hudson AG, Vonlanthen P, Seehausen O, Hammerschmidt CR, Senn DB (2013) Speciation leads to divergent methylmercury accumulation in sympatric whitefish. Aquat Sci 75:261-273
- Blasco J, Saenz V, Gomez-Parra A (2000) Heavy metal fluxes at the sediment-water interface of three coastal ecosystems from south-west of the Iberian Peninsula. Sci Total Environ 247:189-199
- Bloom NS, Gill GA, Cappellino S, Dobbs C, Mcshea L, Driscoll C, Mason R, Rudd J (1999) Speciation and cycling of mercury in Lavaca Bay, Texas, sediments. Environ Sci Technol 33:7-13
- Bravo AG (2010) Mercury methylation and trophic transfer in contaminated freshwater systems. Dissertation, Université de Geneve
- Bravo AG, Bouchet S, Amouroux D, Pote J, Dominik J (2011) Distribution of mercury and organic matter in particle-size classes in sediments contaminated by a waste water treatment plant: Vidy Bay, Lake Geneva, Switzerland. J Environ Monitor 13:974-982
- Clarkson TW (1993) Mercury Major Issues in Environmental-Health. Environ Health Perspect 100:31-38
- Compeau GC, Bartha R (1985) Sulfate-reducing bacteria Principal methylators of mercury in anoxic estuarine sediment. Appl Environ Microbiol 50:498-502
- Cossa D, Harmelin-Vivien M, Mellon-Duval C, Loizeau V, Averty B, Crochet S, Chou L, Cadiou JF (2012) Influences of bioavailability, trophic position, and growth on methylmercury in hakes (Merluccius merluccius) from northwestern Mediterranean and northeastern Atlantic. Environ Sci Technol 46:4885-4893
- DeLaune RD, Jugsujinda A, Devai I, Patrick WH (2004) Relationship of sediment redox conditions to methyl mercury in surface sediment of Louisiana Lakes. J Environ Sci Health A Tox Hazard Subst Environ Eng 39:1925-33
- Dominik J, Loizeau JL, Span D (1992) Radioisotopic evidence of perturbations of recent sedimentary record in lakes: a word of caution for climate studies. Clim Dynam 6:145-152
- Drott A, Lambertsson L, Björn E, and Skyllberg U. (2008) Do potential methylation rates reflect accumulated methyl mercury in contaminated sediments? Environ Sci Technol 42:153-158
- Fitzgerald WF, Mason RP, Vandal GM (1991) Atmospheric cycling and air-water exchange of mercury over midcontinental lacustrine regions. Water Air Soil Poll 56:745-767
- Fleming EJ, Mack EE, Green PG, Nelson DC (2006) Mercury methylation from unexpected sources: Molybdate-inhibited freshwater sediments and an iron-reducing bacterium. Appl Environ Microb 72:457-464
- Gilmour C, Henry, E (1991) Mercury methylation in aquatic systems affected by acid deposition. Environ Pollut 71:131-169
- Gilmour C, Henry E, and Mitchell R (1992) Sulfate stimulation of mercury methylation in freshwater sediments. Environ Sci Technol 26:2281–2287
- Girardclos S, Hilbe M, Corella JP, Loizeau JL, Kremer K, DelSontro T, Arantegui A, Moscariello A, Arlaud F, Akhtman Y, Anselmetti F, Lemmin U (2012) Searching the

- Rhone delta channel in Lake Geneva since François-Alphonse Forel. Arch Sci 65:103-118
- Hamelin S, Amyot M, Barkay T, Wang YP, Planas D (2011) Methanogens: Principal methylators of mercury in lake periphyton. Environ Sci Technol 45:7693-7700
- Harada M (1995) Minamata disease methylmercury poisoning in Japan caused by environmental-pollution. Crit Rev Toxicol 25:1-24
- He TR, Lu J, Yang F, Feng XB (2007) Horizontal and vertical variability of mercury species in pore water and sediments in small lakes in Ontario. Sci Total Environ 386:53-64
- Hurley JP, Shafer MM, Cowell SE, Overdier JT, Hughes PE, Armstrong DE (1996) Trace metal assessment of Lake Michigan tributaries using low-level techniques. Environ Sci Technol 30:2093-2098
- Kerin EJ, Gilmour C, Roden E, Suzuki MT, Coates JD, Mason RP (2006) Mercury methylation by dissimilatory iron-reducing bacteria. Appl Environ Microb 72:7919-7921
- Langer CS, Fitzgerald WF, Visscher PT, Vandal GM (2001) Biogeochemical cycling of methylmercury at Barn Island Salt Marsh, Stonington, CT, USA. Wetl Ecol Manag 9:295–310
- Loizeau JL, Arbouille D, Santiago S, Vernet JP (1994) Evaluation of a wide-range laser diffraction grain-size analyzer for use with sediments. Sedimentology, 41:353-361
- Loizeau JL, Pardos M, Monna F, Peytremann C, Haller L, Dominik J (2004) The impact of a sewage treatment plant's effluent on sediment quality in a small bay in Lake Geneva (Switzerland-France). Part 2. Temporal evolution of heavy metals. Lakes & Reservoirs: Res Manag 9:53-63
- MacDonald DD, Ingersoll CG, Berger TA (2000) Development and evaluation of consensusbased sediment quality guidelines for freshwater ecosystems. Arch Environ Con Tox 39:20-31
- Mason RP, Reinfelder JR, Morel FMM (1995) Bioaccumulation of mercury and methylmercury. Water Air Soil Poll 80:915-921
- Masson M, Tercier-Waeber ML (2013) Trace metal speciation at the sediment-water interface of the Vidy Bay: Influence of contrasting sediment characteristics. Aquat Sci this issue
- Monperrus M, Tessier E, Veschambre S, Amouroux D, Donard O (2005) Simultaneous speciation of mercury and butyltin compounds in natural waters and snow by propylation and species-specific isotope dilution mass spectrometry analysis. Anal Bioanal Chem 381:854-862
- Pak K and Bartha R (1998) Mercury methylation and demethylation in anoxic lake sediments and by strictly anaerobic bacteria. Appl Environ Microb 64:1013-1017
- Pardos M, Benninghoff C, De Alencastro LF, Wildi W (2004) The impact of a sewage treatment plant's effluent on sediment quality in a small bay in Lake Geneva (Switzerland–France). Part 1: Spatial distribution of contaminants and the potential for biological impacts. Lakes Reserv.: Res. Manage 9:41–52
- Parks JM, Johs A, Podar M, Bridou R, Hurt RA, Smith SD, Tomanicek SJ, Qian Y, Brown SD, Brandt CC, Palumbo AV, Smith JC, Wall JD, Elias DA, Liang L (2013) The genetic basis for bacterial mercury methylation. Science 339:1332-1335
- Pote J, Haller L, Loizeau JL, Bravo AG, Sastre V, Wildi W (2008) Effects of a sewage treatment plant outlet pipe extension on the distribution of contaminants in the sediments of the Bay of Vidy, Lake Geneva, Switzerland. Bioresour Technol 99:7122-7131
- Rolfhus KR, Sakamoto HE, Cleckner LB, Stoor RW, Babiarz CL, Back RC, Manolopoulos H, Hurley JP (2003) Distribution and fluxes of total and methylmercury in Lake Superior. Environ Sci Technol 37:865-872

- Roos-Barraclough F, Givelet N, Martinez-Cortizas A, Goodsite ME, Biester H, Shotyk W (2002) An analytical protocol for the determination of total mercury concentrations in solid peat samples. Sci Total Environ 292:129-139
- Sauvain L, Bueche M, Junier T, Masson M, Wunderlin T, Kohler-Milleret R, Gascon Diez E, Loizeau JL, Tercier-Waeber ML, Junier P (2013) Bacterial communities in trace metal contaminated lake sediments are dominated by endospore-forming bacteria. Aquat Sci this issue
- Schafer J, Blanc G, Audry S, Cossa D, Bossy C (2006) Mercury in the Lot-Garonne River system (France): Sources, fluxes and anthropogenic component. Appl Geochem 21:515-527
- Scheulhammer AM, Meyer MW, Sandheinrich MB, Murray MW (2007) Effects of environmental methylmercury on the health of wild birds, mammals, and fish. Ambio 36:12-18
- Siegel S (1956) Nonparametric statistics for the behavioral sciences. Kosaido Printing Co. LTD, Tokyo
- Sturm M, Zwissig A, Piccard J (1984) Bio-erosive humpack-structures an example of sediment/water interface alteration in Lake Geneva. 3rd Inter Symposium Interaction between Sediments and Water, CEP Consultants: 126
- Száková J, Kolihová D, Miholová D, Mader P (2004) Single-purpose atomic absorption spectrometer AMA-254 for mercury determination and its performance in analysis of agricultural and environmental materials. Chem Pap 58:311-315
- Turner A, Millward GE, Le Roux SM (2004) Significance of oxides and particulate organic matter in controlling trace metal partitioning in a contaminated estuary. Mar Chem 88:179-192
- Ullrich SM, Tanton TW, Abdrashitova SA (2001) Mercury in the aquatic environment: A review of factors affecting methylation. Crit Rev Env Sci Tec 31: 241-293
- Vernet JP (1966) Prise de vue sous-lacustres dans le Léman lors de plongées du mésoscaphe "Auguste-Picard". Bull Soc Vaudoise Sci Nat 69:287-292
- Vernet JP, Viel M (1984) Métaux lourds dans les sédiments lacustres. In: Commission Internationale pour la Protection des Eaux du Léman contre la Pollution (ed) Synthèse des travaux 1957-1982, Lausanne, pp. 227-238
- Wüest A, Anselmetti FS, Arey JS, Ibelings BW, Loizeau JL, Vennemann T, Lemmin U (2013) Into the abyss of Lake Geneva Interdisciplinary field investigations using the MIR submersibles. Aquat Sci this issue
- Watras CJ, Bloom NS (1992) Mercury and methylmercury in individual zooplankton implications for bioaccumulation. Limnol Oceanogr 37:1313-1318
- WHO/IPCS (1990) Methylmercury. Geneva, World Health Organization, International Programme on Chemical Safety. Environ Health Criteria 101 WHO Library Cataloguing in Publication Data
- Zahner P (1984) Sulfates. In: Commission Internationale pour la Protection des Eaux du Léman contre la Pollution (ed) Synthèse des travaux 1957-1982, Lausanne, pp. 193-198

CHAPTER IV

Mercury distribution from the shore to the deep waters

This chapter presents the mercury transport throughout the study of fluxes. The dynamics here provide a better understanding on vertical and horizontal mercury dispersion as a particle-bound contaminant. The sedimentation pathway determines particle transfer from the shallow to the deep waters in a large lake of Western Europe.

Spatial distribution and fluxes of total and methylmercury in settling particles and sediments from the shore to the deep waters of Lake Geneva, Switzerland.

Elena Gascón Díez ¹ , Neil D. Graham ¹ and Jean-Luc Loizeau ¹	
¹ Institut FA. Forel and the Institute for Environmental Sciences, University of Ge Boulevard Carl-Vogt 66, 1211 Geneva, Switzerland	eneva,

Abstract

Mercury is a well-known particle-bound pollutant which is of great concern in the Vidy Bay and surrounding area of Lake Geneva due to the input of wastewaters from a municipal wastewater treatment plant. To better understand the sources and dynamics of mercury in and around Vidy Bay, total mercury and methylmercury concentrations and fluxes were studied in surface sediments and settling particles. Two-tiered sediment traps were deployed at two sites of Lake Geneva, and were sampled on a monthly basis for almost two years to estimate total mercury settling fluxes, and the influence of the lateral sedimentation component in moving from the shallow to deeper lake. Combined results of concentrations and fluxes showed that (i) the Vidy Bay catchment area, likely combined with the effluent of the wastewater treatment plant, provides particle-bound mercury and other sediment components such as organic matter to the bay; (ii) resuspension and/or lateral advection has been observed in the bottom tier of the sediment traps (5 m above the lakebed); (iii) although the most distal sampling site (~ 3 km from the shoreline) showed a decrease of total mercury fluxes, sediment accumulation rates and organic matter fluxes suggested that this area is still affected by the coastal boundary, as compared to sites in the center of the lake. Regarding methylmercury results, higher concentrations and fluxes were observed in settling particles than in sediments, suggesting that Hg-methylation processes were preferentially occurring within the water column.

Keywords

Mercury fluxes, mercury transport, settling particles, methylmercury

1. Introduction

Mercury (Hg) in the atmosphere is largely found as elemental mercury. Due to the relative insolubility of gaseous Hg, this trace metal is of easy transport through the atmosphere and it is subject to dry and wet deposition in the aquatic systems (Mason et al., 1994). Once in the water column, Hg adsorbs primarily onto particulate organic matter (OM) and inorganic suspended particles in the water column and eventually settles to the sediment surface after aggregation and coagulation sedimentation processes. Therefore sediments are the principal reservoir of Hg in aquatic systems (Benoit et al., 1998; Wang et al., 1998). Methylmercuy (MeHg) is a neurotoxin and one of most hazardous forms of Hg. It accumulates in aquatic organisms and bioamplifies through the food chain. MeHg is a threat for the human health since the uptake of MeHg by the population is via fish comsumption. MeHg results from the biotransformation of inorganic mercury in suboxic sediments by specific anaerobic micoorganisms, including sulfate-reducing bacteria (SRB), iron-reducing bacteria (IRB) and methanogens (Compeau and Bartha, 1984; Korthals and Winfrey, 1987; Parks et al., 2013; Gilmour et al., 2013; Podar et al., 2015). In turn, sediments can be a significant source of Hg to the water column depending on the biogeochemical and transport processes taking place in both sediments and waters. (Gagnon et al., 1997; Rigaud et al., 2013). Although many studies on trace metals have focused on mercury fluxes at the sediment-water interface over short periods of time (e.g. Bloom et al., 1999; Rolfhus et al., 2003; Mason et al., 2006; Feyte et al., 2012), less attention has been paid to particle-bound Hg settling fluxes and the effects of resuspension on the fate of mercury over longer periods of time. It has been shown that sediment resuspension plays a role in Hg methylation and in MeHg transfer from sediments to organisms in shallow aquatic systems (Kim et al., 2006). However, resuspension is not restricted to shallow waters and can occur when current induced bottom shear stress exceeds the cohesive, electro-static, force between surface sediments (Taylor and Birch, 2000). In some cases depending on the lake hydrodynamics, resuspended material can constitute the dominant source of input for particle fluxes (Evans, 1994). Resuspension of sediments is an important process enabling the redistribution of particulate material and associated contaminants. Particles are the principal vector for

trace metal transport; hence, it is of major concern to understand the particle dynamics to assess contaminant dispersal and fate. Monthly fluxes of Hg bound to settling particles were recorded in sediment traps in Lake Geneva. Together with sedimentological parameters (grain size, organic matter and carbonate content), they were used to assess the dispersion of particle-bound pollutants and to quantify the relative importance of transport processes such as direct settling and resuspension/lateral advection.

Study site

Lake Geneva is a warm monomictic peri-alpine lake located on the border between Switzerland and France (Fig. 1). It has a surface area of 580 km², a maximal depth of 309 m, and a volume of ~89 km³. The main tributary to the lake is the Rhône River (70%) with a mean input of 185 m³/s, and particle concentrations ranging from 20 to 2,000 mg/L in the winter and summer, respectively (Dominik et al., 1987). The study was carried out in and around Vidy Bay, which is the most contaminated part of Lake Geneva. Vidy Bay receives some urban runoff trough the Chamberonne River, and minor inputs are transported by the Venoge River that also flows to the west in the vicinity of the bay. Vidy Bay is also affected by treated and untreated (overflows) domestic and industrial wastewaters released by the wastewater treatment plant (WWTP) of the city of Lausanne (e.g. Pardos et al, 2004; Poté et al. 2008; Thevenon et al., 2011). The WWTP discharges between 1 and 3 m³/s, reaching as much as ~7 m³/s when intense precipitation occurs (Razmi et al., 2013). In 2011, the mean total mercury (THg) concentration in WWTP sludges collected at the Vidy Bay WWTP was 3.8 μg/g (Burnier et al., 2011).

2. Materials and methods

2.1. Sediment and settling particles sampling

Sediment traps were deployed on a monthly basis between December 2009 and September 2011 from the Institut F.-A. Forel research vessel, "La Licorne". The traps were deployed at two locations, NG2 (6° 35' 0'' E, 46° 30' 6'' N; Swiss coordinates: 534350 E, 150400 N) at 138 m depth, and NG3 (6° 34' 46'' E, 46° 29' 40'' N; Swiss coordinates: 534050 E, 149600 N) at 192 m depth (Fig. 1). Sediment traps consisted of a weight, an acoustic release, two tiers of sediment trap tubes and buoys (Fig. 1). Each tier of sediment traps consisted of a frame holding six 80 x 11 cm Plexiglas tubes, resulting in a total surface area of 520 cm². One tier was placed at 5 m above the sediment surface while the other was placed 75 m below the lake surface.

Surface sediments below the traps were sampled at the same time and on the same frequency as the sediment traps using two Mortimer-Jenkin-type gravity corers attached together in parallel. The top 1 cm centimeter of sediment was subsampled by extrusion.

Additionally, surface sediments (~ 1 cm depth) were collected using a Van Veen grab sampler at 15 additional sites (numbered EG1 - EG15) along a transect extending from Vidy Bay towards the deeper adjacent main basin (Fig. 3).

A 60-cm long sediment core was also retrieved at NG2 on May 14th 2014, using a UWITEC gravity corer. This core was used to date sediments and determine recent sediment accumulation rates.

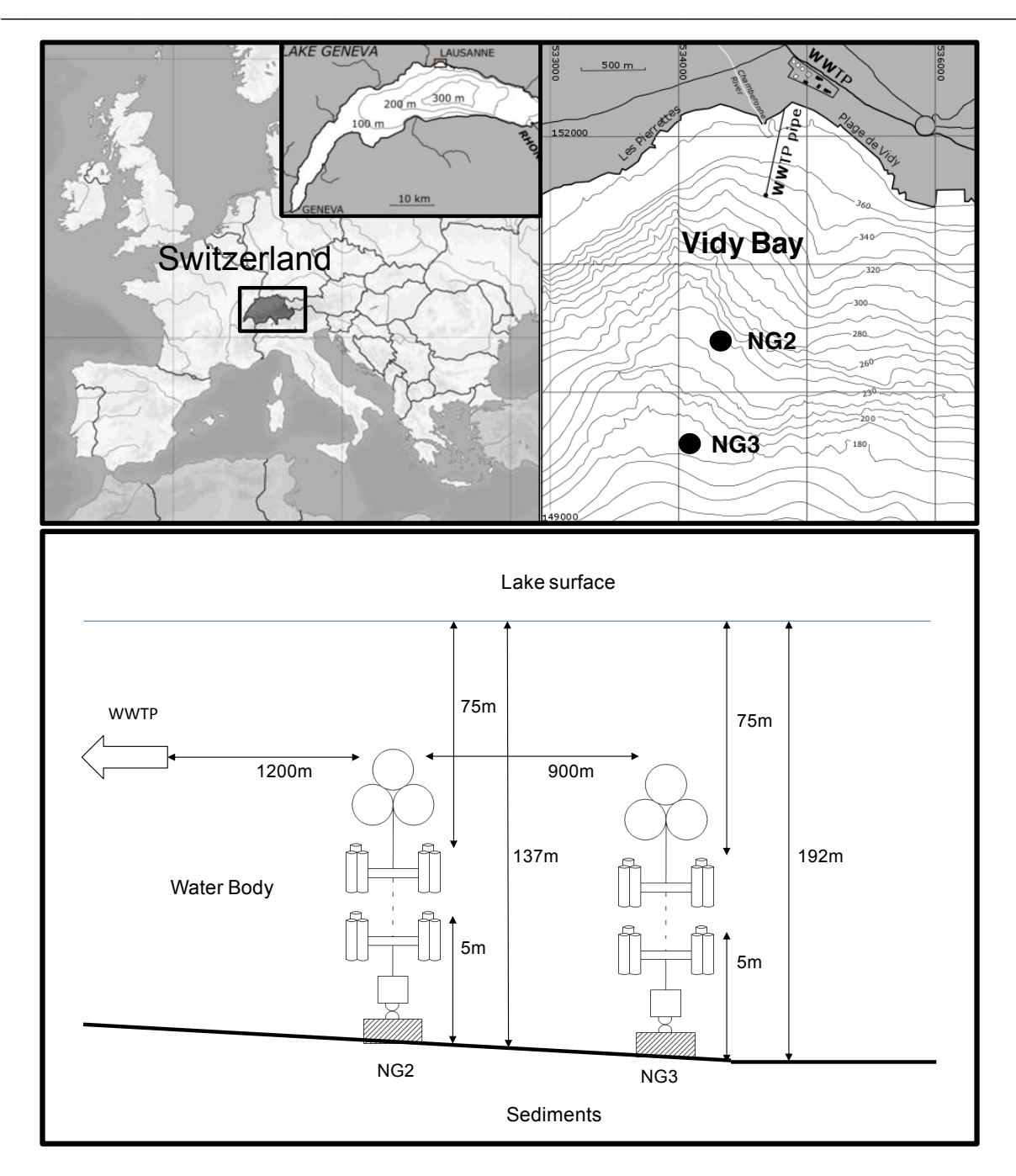


Figure 1. Top: Map of the study area and location of sampling stations close to Vidy Bay as related to Lake Geneva in Switzerland. Isolines corresponded to the lake altitude, lake level at 372 m a.s.l. Bottom: Scheme of the chain of traps deployed at NG1 and NG2 (not to scale).

2.2. Geochemical analyses

Sediment grain-size distribution was determined on wet sediments using a laser diffraction analyser (Coulter LS-100, Beckman-Coulter, USA), following the procedure described by Loizeau et al. (1994).

Samples were freeze-dried in a CHRIST BETA 1-8 K freeze-drying unit (-54 °C, 6 Pa) for a minimum of 48 h. OM and carbonate (CaCO₃) contents in sediments were estimated by Loss on Ignition. Samples were heated to 550 °C for 30 minutes to estimate the OM mass loss and then heated to 1,000 °C for another 30 minutes to estimate the CaCO₃ content (Dean, 1974). The CaCO₃ content was calculated by multiplying the mass loss at 1,000 °C by 2.2742, the molar mass ratio of calcite to carbon dioxide.

Total mercury (THg) in dry sediment was analysed by Cold Vapor Atomic Absorption Spectrophotometry (CV-AAS) using an automatic mercury analyser, AMA-254 (Altec, ČR), following the procedure described by Roos-Barraclough et al. (2002). All analyses were conducted in triplicate. The detection limit and working range were 0.01 ng and 0.05 - 600 ng, respectively. Concentrations obtained for repeated analyses of the certified reference material never exceeded the specified acceptance range given for the MESS-3 reference material (National Research Council of Canada).

MeHg in solid matrix was extracted using a HNO₃ leaching/CH₂Cl₂ extraction method (Liu et al., 2012), followed by ethylation onto Tenax® traps. GC separation (Bloom, 1989) and Cold Vapor Atomic Fluorescence Spectrometry (CV-AFS) detection were run using a Model III CVAFS Detector (Brooks Rand®, USA). Recovery of extractions and analyses of the certified reference material (ERM®-CC580) were consistently above 85%.

2.3. Sediment dating and mercury flux in sediments at NG2

To determine long term mercury fluxes to the sediments, a 60-cm long sediment core was retrieved and split in two halves. Water content and porosity were measured following the method of Håkanson and Jansson (1983). Depth scale was converted to

mass scale in order to compute sediment accumulation rates (SAR), in g/cm² y. SAR were calculated by dividing the mass of sediments accumulated between two time markers by the surface area of the sediment core and by the elapsed time between the time markers. Four time markers were used: (i & ii) occurrences of ¹³⁷Cs fallout peaks in 1954 and 1964 from atmospheric nuclear weapon testing; (iii) ¹³⁷Cs fallout peak from the 1986 Chernobyl accident; and (iv) the surface sediment in 2014. ¹³⁷Cs and ⁷Be activities were measured in freeze-dried and homogenized sediment samples using an HPGe gamma spectrometer (Ortec EG&G).

Overall THg and MeHg fluxes to the surface sediments for the period from December 2009 to September 2011 were calculated by multiplying the SAR to the first cm of the sediment core (see above in this section) by the overall THg or MeHg average concentration of the surface sediments for this period. Units are expressed in $\mu g/m^2$ d and ng/m^2 d for THg and MeHg, respectively.

SAR in sediment traps were calculated by Graham (2015) are presented in Supporting Information (SI, Table 1).

2.4. Statistical analyses

Normality was tested using the Shapiro-Wilk test. THg and MeHg concentration datasets did not follow a normal distribution in top and bottom combined sediment traps. Therfore, median values were used to compare groups, and Kruskal-Wallis one-way analysis of variance on ranks test was performed in order to compare THg concentration and fluxes in combined top and bottom sediment trapas in autumn, summer, spring and winter. Overall the significance level was set to 0.05. All the statistical analyses were performed with SigmaPlot 11.0 software

3. Results

3.1. Grain-size distribution evolution

Temporal and spatial variations in mean grain size of settling particles are presented in figure 2. Trends were similar at both NG2 and NG3, with lower overall values in 2010 than in 2011. Moreover, minimum values were found in both top and bottom traps, from the summer to autumn of 2010. These values correspond to relatively high OM and CaCO₃ fluxes determined in the same samples by Graham (2015). In contrast, 2011 presented its highest values during summer-autumn at both sites, with the lowest values present in winter, mainly at NG2.

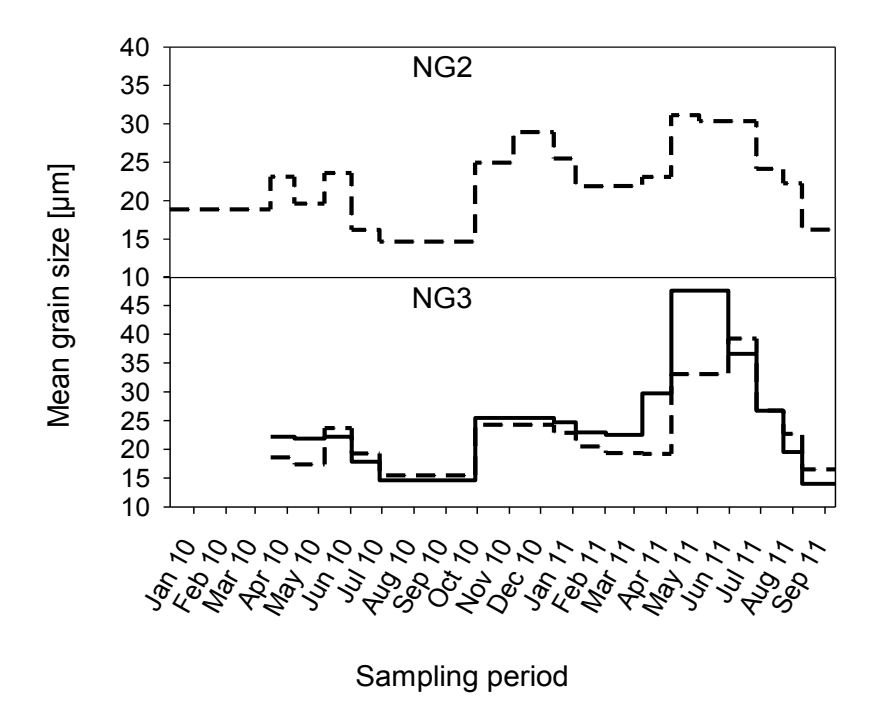


Figure 2. Mean grain size distribution of settling particles at NG2 and NG3. Solid line: top sediment trap. Dashed line: bottom sediment trap.

3.2. THg concentrations and fluxes

THg concentrations were measured in the surface sediments of fifteen sites in and around Vidy Bay (Fig. 3). Ten of these sites were placed on a north-south transect passing through the WWTP outlet pipe, which is located between EG1 and EG2. EG1, upslope of the outlet pipe, had the lowest concentration of THg ($0.039 \pm 0.001 \,\mu\text{g/g}$) whereas EG2, located approximately 20 m in front of the outlet pipe, registered the maximal concentration of $1.33 \pm 0.03 \,\mu\text{g/g}$. Moving along the transect from EG2 to EG10, including NG2 and NG3, concentrations fell to $0.22 \,\mu\text{g/g}$. The remaining sites on either side of the transect, EG11 to EG15, ranged from 0.55 ± 0.08 to $0.173 \pm 0.003 \,\mu\text{g/g}$ as a function of the distance to the outlet pipe and/or the shore.

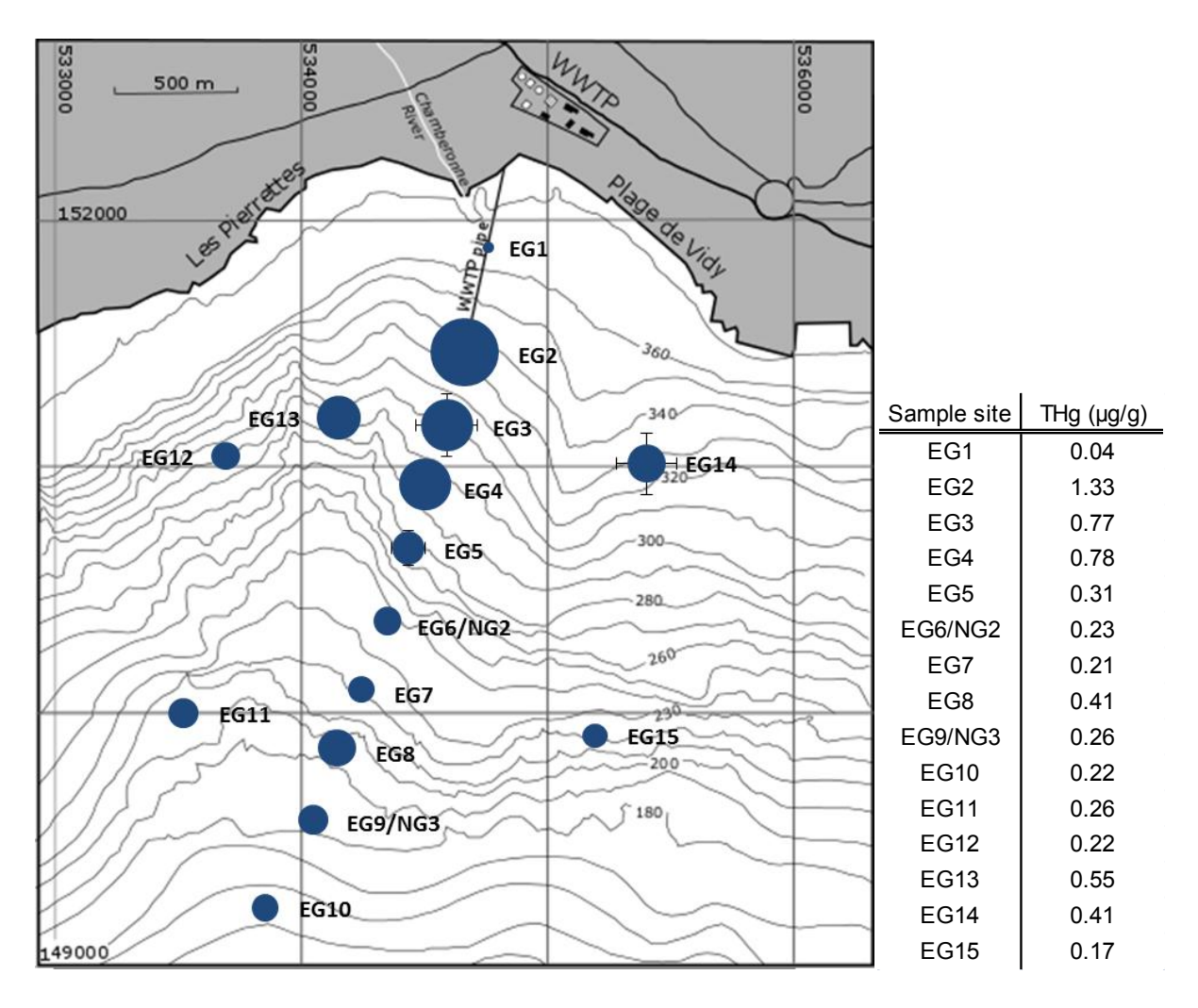


Figure 3. Spatial variability of THg in surface sediment concentration in Vidy Bay and surrounding area. Surface area of circle is proportional to THg content.

Median THg concentrations measured in settling particles at NG2 and NG3 were 0.154 µg/g and 0.097 µg/g, respectively. THg concentrations measured on particles recovered in the top and bottom sediments traps ranged between 0.073 \pm 0.001 and 0.27 \pm 0.01 µg/g at NG2, and between 0.038 \pm 0.001 and 0.21 \pm 0.01 µg/g at NG3; both sites followed similar seasonal patterns (Fig. 4). The highest THg concentrations were found in autumn-winter and the lowest contents in summer-autumn. Spring was considered as a transition period with intermediate values. Although seasonal variations followed the same trend at both locations, settling particles presented significantly higher THg concentrations at both depths of NG2 as compared to NG3. Particularly in autumn-winter THg concentrations in settling particles at NG2 were above the average concentration measured in sediments, whereas at NG3, THg concentrations were always lower in settling particles than in the average concentration of sediments.

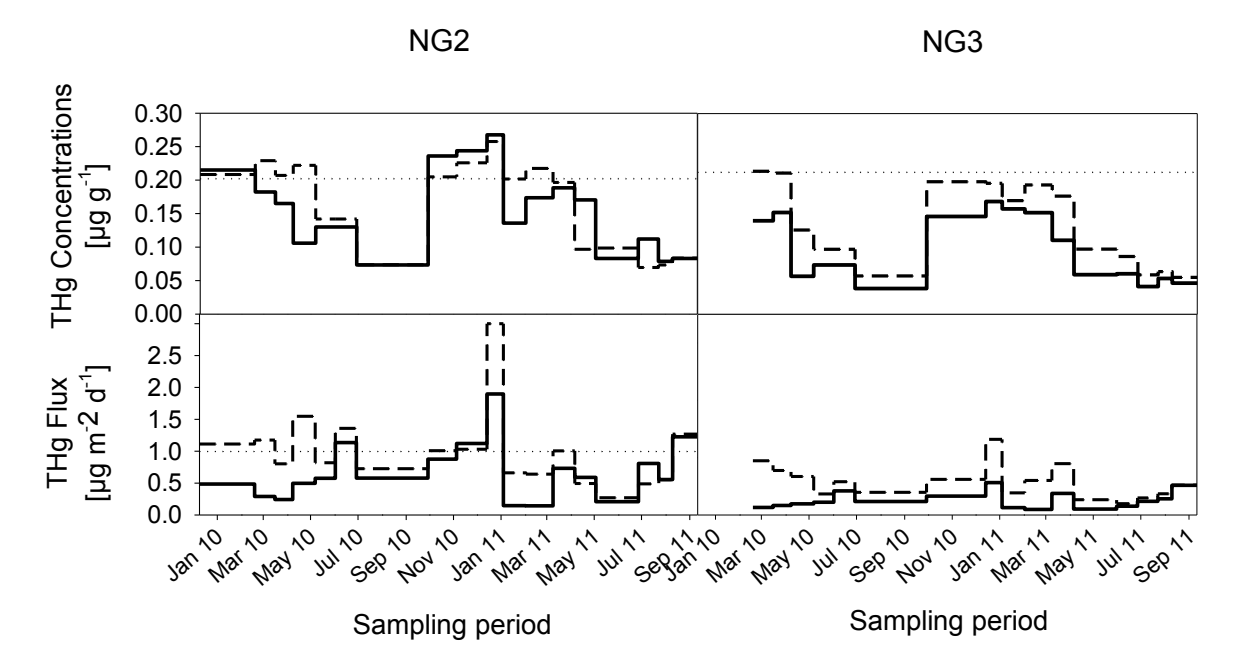


Figure 4. THg concentrations and fluxes in settling particles and sediments at NG2 and NG3. Solid line: top sediment trap. Dashed line: bottom sediment trap. Dotted line: mean THg concentration or flux in surface sediments during the entire period of sampling.

To further understand the THg dynamics, THg fluxes were calculated for the top and bottom sediment traps of both NG2 and NG3 (Fig. 4). THg fluxes ranged between 0.144 \pm 0.002 and 1.6 \pm 0.3 $\mu g/m^2$ d at NG2, and between 0.10 \pm 0.05 and 0.89 \pm 0.03 $\mu g/m^2$ d at NG3. Overall, at both sites, THg fluxes were greater in the bottom trap than in the top trap (Fig. 4). Seasonal variability of THg fluxes was less pronounced than Hg concentration variability. The flux ranges did not include values obtained in December 2010 which were atypically high for the bottom trap of both sites, particularly at NG2 (3.00 \pm 0.03 $\mu g/m^2$ d at NG2 and 1.31 \pm 0.06 $\mu g/m^2$ d at NG3). These peaks were due to an abnormally elevated input of settling particles in December 2010 which is more characteristic of mild temperature periods (Graham, 2015) (see discussion). THg flux was also estimated in the surface sediments from the long-term sediment accumulation rate at NG2. SAR from the 60-cm sediment core at the during the period between December 2009 and September 2011 was 0.18 g/cm² y and the mean THg concentration was 0.20 \pm 0.03 g/cm², resulting a mean THg flux of 1.0 g/cm² for that period.

3.3. MeHg concentrations and fluxes

MeHg concentrations at NG2 ranged from 0.41 ± 0.04 ng/g to 11.38 ± 0.02 ng/g with a median concentration of 2.55 ng/g, and between 0.39 ± 0.02 ng/g and 13.47 ± 0.02 ng/g at NG3 with a median concentration of 2.17 ng/g (Fig. 5). The seasonal evolution of MeHg concentrations in settling particles at NG2 showed that in 2010, the highest concentrations were found during winter in the bottom trap. Contrary to THg concentrations, MeHg content in the summer-autumn of 2010 and 2011 were elevated and generally greater in the top trap, although, the maximal concentration at this site was measured in October 2010. Overall, at NG2, MeHg concentrations were above the average concentration in sediments (Fig. 5). NG3 showed lower concentrations in autumn-spring and the highest concentrations in summer and autumn. During the latter period, MeHg concentrations in sediments traps were notably higher than the MeHg mean concentration in the surface sediments (1-2 ng/g), especially the concentrations in the bottom trap which were almost continuously greater than those of the top trap.

Fluxes were calculated to better understand the seasonal behavior of MeHg in settling particles. MeHg fluxes varied between 0.44 ± 0.02 and 68.4 ± 0.6 ng/m² d at NG2, between 0.68 ± 0.02 and 58.5 ± 0.5 ng/m² d at NG3, and median values were 9.81 and 10.7 ng/m² d respectively. As shown in Fig. 5, trends of MeHg fluxes at both sites were similar to concentration trends, that is, greater fluxes of MeHg in the summer and autumn as compared to the winter and spring. Similarly to THg fluxes in sediments, MeHg fluxes were estimated in sediments from the SAR corresponding to 2009 to 2011 (0.18 g/cm² y) and the mean MeHg (0.9 \pm 0.4 ng/g). MeHg fluxes to the sediment traps of NG2 were significantly above the mean MeHg flux at the surface sediments (4.44 ng/m² d). Finally, likewise to the MeHg concentrations, the fluxes of MeHg measured in the bottom trap, especially at NG3, are greater than those measured in the top trap.

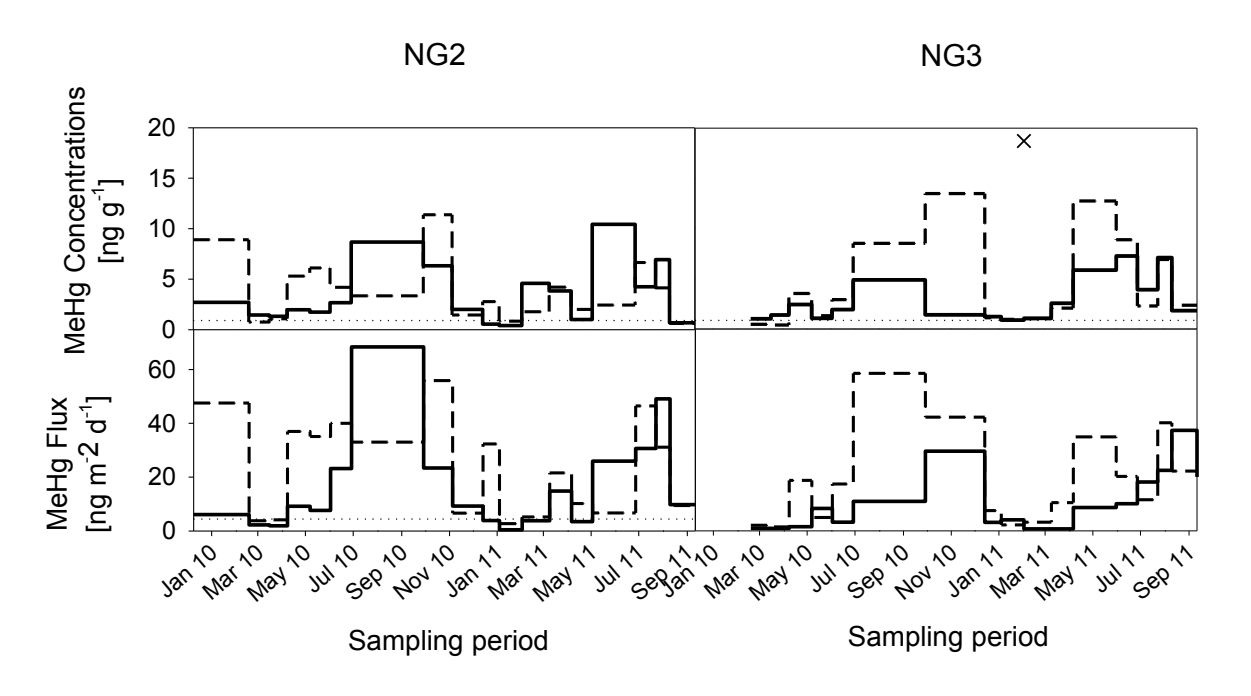


Figure 5. MeHg concentrations and fluxes in settling particles at NG2 and NG3. Solid line: top sediment trap. Dashed line: bottom sediment trap. Dotted line: mean MeHg concentration or flux in surface sediments during the sampling periods.

4. Discussion

4.1. Grain-size distribution

The finer mean grain sizes were found during the summer of 2010 and September 2011 at NG2 and NG3 (Fig. 2), corresponding to the highest fluxes of OM and CaCO₃ for the same sites and periods measured by Graham (2015), shown in Table S1. This suggests that the composition of settling particles during these periods was mainly formed by aggregation of endogenic CaCO₃ crystals and fine particulate OM. Coarser mean particle diameters were found in winter 2010/11 and early summer 2011 at NG2, whereas at NG3, coarse mean particle diameters appeared only in early summer 2011 and were more abundant in the bottom trap. These differences in grain size showed that NG2 more often recorded the presence of coarse-grained particles. Thus, NG2 being 1 km closer to the shore and the WWTP effluent, may be subject to variations in load of coarse silt and large organic particles that have less of an influence at NG3. To further understand the origin of these coarser means of the particle distributions, we compared the periods in which they were measured in the sediment traps with the rises of the Rhone River (the most important tributary to Lake Geneva) and the Venoge River, the most important local river to Vidy Bay. However, no temporal concordance was found between the appearance of the coarse particles at NG2 and NG3, and the seasonal swelling of rivers and increased rainfall (Fig. S1). Therefore, the origin of coarse particles, predominantly at NG2, could be related to the proximity to the shore, which drains coarse material.

4.2. The fate of THg

Many sampling sites are required to assess THg distribution in Vidy Bay due to the high heterogeneity of THg concentrations (Poté et al., 2008; Gascon Diez et al., 2014) in lake surface sediments (Fig. 3). EG1 was the closest point to the shore and showed the lowest concentration measured in the bay (0.039 μ g/g). The low concentrations found at EG1 could be explained by the presence of coarse-grained particles discharged by the Chamberonne River that are not favorable to THg adsorption. Indeed, Hg sorption depends on the physico-chemial characteristics of sediments such

as the mineral composition, the electrostatic forces and the surface area per unit of weight. Therefore, Hg adsorbs more easily to the 0-200 μ m sediment fraction (Bengtsson and Picado, 2008). EG2, at about 20 m distance from the outlet pipe, showed to be the most affected site in the bay with the highest values (Fig. 3). Concentrations decreased from EG2 towards the main basin, reaching a concentration plateau (~ 0.2 μ g/g) between EG7 to EG10, where concentrations were similar to those previously recorded for the center of the lake (0.17 μ g/g). This suggests that the effect of the WWTP diminishes with distance, which is in agreement with previous studies (Bravo et al., 2011; Gascon Diez et al., 2014; Poté et al., 2008).

Concentration data alone was not enough to fully understand the dynamics of THg associated with particles since variations in SAR modified the particulate THg signal, as an example, when SAR increase, THg concentration decreases. As shown in Fig. 4, fluxes of THg in settling particles showed a smaller variability than the corresponding concentrations implying that concentrations of THg were strongly influenced by the seasonal trends of sedimentation rates. Statistical analyses support this assumption: whereas the difference between the median values among the THg fluxes on the different seasons were not significant (p-value > 0.05), the difference among the THg concentrations between winter and summer were significant (p-value < 0.05), at both sites, NG2 and NG3. On the other hand, THg flux data at both sites showed that the deposition of THg was greater in the bottom traps than in the top traps, pointing to the likely influence of lateral advection of particles and/or sediment resuspensions at 5 m above the sediment surface. THg fluxes were slightly greater at NG2 than at NG3, and as NG2 is about one km closer to shore, lateral advections at this site could be due to resuspension from the shallower areas where the sediments are slightly charged with THg from the WWTP. In turn, NG3, with lower THg fluxes, would likely not be affected by inputs from the coastal zone. Previous studies at these sites (Graham, 2015) showed similar trends for SAR, OM and CaCO₃ fluxes (Table 1).

Table 1. Comparative table of SAR, OM, and CaCO₃ fluxes per sampling site and year. Data from Dominik et al. (1993) and Graham (2015). Sampling depth are represented by (a) 59 m (b) 75 m (c) 299 m (d) 132 m and (e) 192 m

SAR [g/m² d]	SHL2 - 1986	SHL2 - 1987	SHL2 - 1991	NG2 - 2010	NG3 - 2010	NG2 - 2011	NG3 - 2011
Top trap	2.40 ^a	2.22 ^a	2.02 ^a	4.93 ^b	3.64 ^b	4.43 ^b	3.48 ^b
Bottom trap	2.68 ^c	2.90 ^c	2.21 ^c	6.97 ^d	5.05 ^e	5.38 ^d	4.10 ^e
OM [g/m ² d]	SHL2 - 1986	SHL2 - 1987	SHL2 - 1991	NG2 - 2010	NG3 - 2010	NG2 - 2011	NG3 - 2011
Top trap	0.13 ^a	0.11 ^a	0.11 ^a	0.43 ^a	0.30 ^b	0.38 ^b	0.33 ^b
Bottom trap	0.17 ^c	0.15 ^c	0.12 ^c	0.64 ^d	0.39 ^e	0.44 ^d	0.36 ^e
CaCO ₃ [g/m ² d]	SHL2 - 1986	SHL2 - 1987	SHL2 - 1991	NG2 - 2010	NG3 - 2010	NG2 - 2011	NG3 - 2011
Top trap	1.03 ^a	1.00 ^a	0.81 ^a	1.26 ^b	0.98 ^b	1.40 ^b	1.23 ^b
Bottom trap	1.07 ^c	1.21 ^c	0.63 ^c	1.74 ^d	1.35 ^e	1.63 ^d	1.43 ^e

Comparing this data with previously published results for the center of the lake (Dominik et al., 1993), it is noted that the SAR and OM fluxes at NG2 were greater than at NG3 (as was also the case for the THg fluxes) suggesting that particles coming from the coastal zone or WWTP also contained greater concentrations of OM which decreased with distance from the shore as these resuspensions settled out of the water column. The differences in CaCO₃ fluxes between NG2, NG3, and the center of the lake were not as marked as for SAR, OM and THg fluxes, suggesting that endogenic CaCO₃ is a significant source of calcite in the lake (Gascon Diez et al., under review; chapter V of this thesis). Thus, production and settling of endogenic CaCO₃ crystals, which is linked to the seasonal variation (Dominik et al., 1993) and are likely responsible of the low concentrations of THg, through signal dilution, found in sediment traps. In any case, SAR, OM and CaCO₃ fluxes at both sites were greater in the bottom traps than in the top traps, and also greater at NG2 than NG3, reinforcing the interpretation and effect of lateral advections and/or resuspension to the THg fluxes discussed above. In turn, THg concentrations in sediments were expected to be greater at NG2 than at NG3, instead, surface sediments at both sites presented close average value. Overall, THg concentrations and fluxes in settling particles and sediments at NG2 were similar; however, THg concentrations in settling particles were lower than concentration in sediments at NG3 (THg fluxes in sediments were not measured at this site). The question of why the concentrations of THg in sediments are higher than in settling particles at NG3 remains unanswered and more data, from a longer sampling period or measuring THg fluxes to sediment surface at NG3, is needed.

Finally, the maximum SAR, OM, CaCO₃ and THg fluxes measured in December 2010 were likely due to intense rainfalls between October 2010 and January 2011 which entailed a huge rise in the discharge of the Venoge River (Fig. S1) sweeping along with it detrital material, organic matter and particulate mercury. This event could be responsible of the high fluxes measured in both sites.

Another important input of inorganic Hg is aquatic system is the atmosphere. Although, atmospheric depositional fluxes were not directly determined in this study, Hammerschmidt and Fitzgerald, 2005 estimated the atmospheric deposition in Hg contaminated areas to be around 3.5 μ g/m² y (Lake County, North America). Considering this value, the atmospheric deposition could account for approximately 2% at NG2 and 3.5% at NG3 to the THg fluxes. However, more measurements in this direction would be needed to fully understand the Hg dynamics in Lake Geneva.

4.3. The fate of MeHg

Anoxic conditions prevailed in subsurface sediments while particles settled through oxic waters (dissolved oxygen ~ 7 mg/L, Gascon Diez et al., under review; Savoye et al., 2015), thus, higher concentrations of MeHg were expected in the sediments as opposed to in settling particles. However, MeHg concentrations in settling particles largely exceeded the concentrations found in sediments (Fig. 5) and contrary to THg, the largest MeHg concentrations were found during the summer. This temporal trend in the MeHg concentrations was similar to MeHg flux trends. In addition, contrary to THg fluxes, MeHg fluxes did not show significant differences with relation to the distance from shore. We suggest that in the case of MeHg, the high content of fresh planktonic OM promoted the activity of the heterotrophic bacteria involved in Hg-methylation processes (Heimburger et al., 2010; Schartup et al., 2015), Thus, the MeHg found in settling particles would likely be related to internal production rather

than the effect of the WWTP effluent. In addition, it is known that a high percentage of the THg in fish is under MeHg form (e.g. Bravo et al., 2010), and previous studies in Lake Geneva demonstrated that no significant difference in concentration of THg exists between fish in Vidy Bay and fish collected from the water column ~ 10 km to the west (à Porta, 2013) of the bay. This suggests that the concentration of biolabile MeHg is similar in the water body.

Although some authors suggest that Hg-methylation may occur in settling particles in the water column (Eckley and Hintelmann, 2006; Monperrus et al., 2007), it remains unexplained in the present study, how anaerobic bacteria are able to methylate mercury in particles settling under oxic conditions. We suggest that an anoxic microenvironment with fresh organic matter would be formed inside the settling particles; however, further investigations are being carried out in line with these results (Gascon Diez et al., under review).

5. Summary

THg dispersion pathway from the shoreline to deeper waters of the lake showed a decrease of particle-bound THg following this direction. However, the comparison of SAR, OM and CaCO₃ between the sites NG2, NG3 and SHL2 (the center of the lake), indicated that, although THg fluxes at NG3 were lower than at NG2, NG3 was still affected by the inputs from the shallow lake zones. On the other hand, THg fluxes were observed to be overall higher in the bottom trap than in the top trap, indicating sediment suspension or lateral THg fluxes more important at the bottom of the lake.

MeHg concentrations and fluxes were highly variable and did not follow the same trend as THg. Significantly higher MeHg concentrations and fluxes were found in settling particles than in sediments, suggesting an internal Hg-methylation process within the sediment traps and/or the settling particles.

Acknowledgements

We thank Philippe Arpagaus helping during the samplings, "La Direction générale de l'environnement DGE – Inspection de la pêche" and "Canton de Vaud" for allowing us to deploy the sediment traps in Lake Geneva. The work was partially funded by SNF research grant PDFMP2-123034

Supporting information

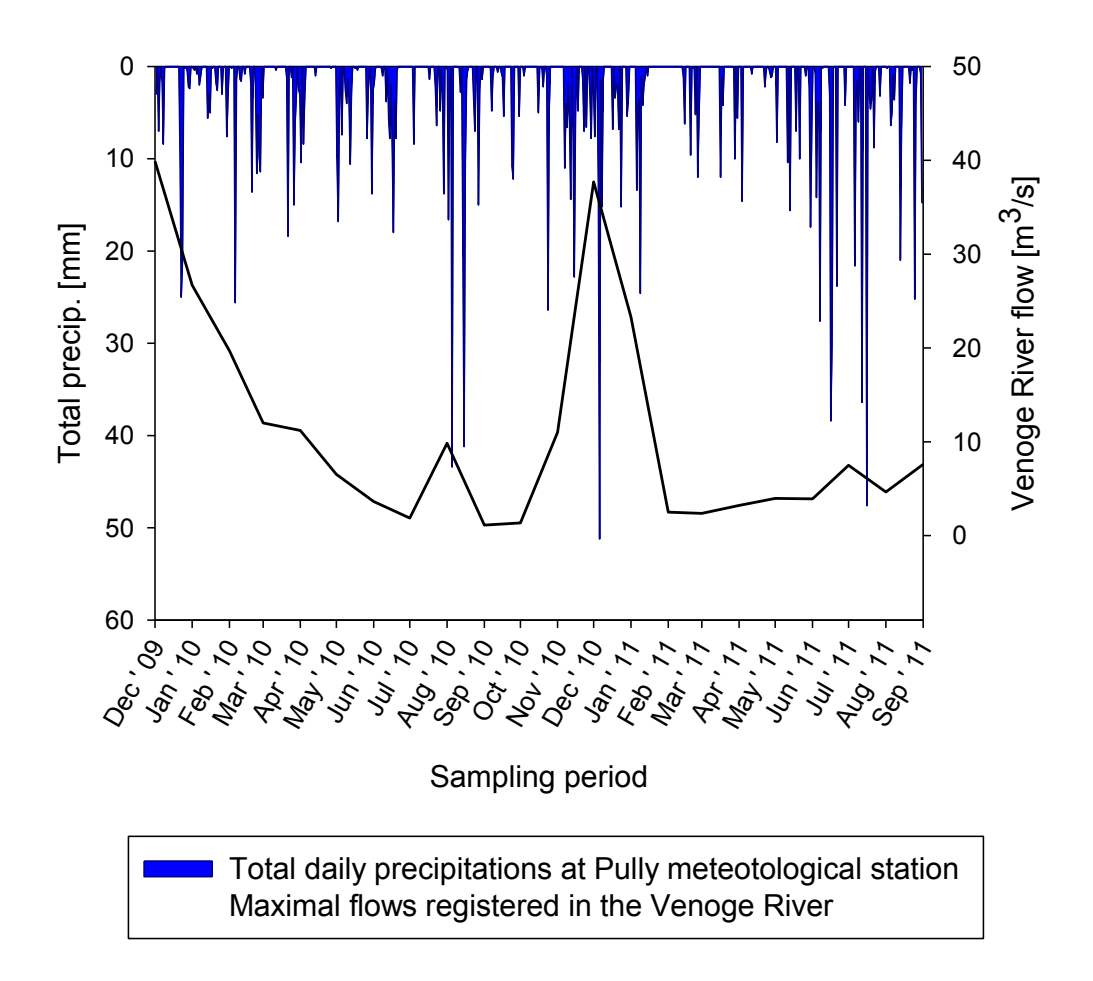


Figure S1. Total daily precipitation measured at the Pully weather station, coupled with flow data of the Venoge River that runs into Lake Geneva in the vicinity of Vidy Bay. Data collected from http://www.agrometeo.ch/fr/meteorology/datas and http://www.hydrodaten.admin.ch/fr/2432.html

Table S1. Sampling dates, SAR, OM and CaCO₃ data collected at NG2 and NG3 (Graham, 2015).

				NG2 Top	Trap					NG2 Botto	m Trap		
Date in	Date out	SAR [g/m² d]	1 δ	OM [%]	1 δ	CaCO ₃ [%]	1 δ	SAR [g/m² d]	1 δ	OM [%]	1 δ	CaCO ₃ [%]	1 δ
13/11/2009	09/12/2009	7.80	0.03	14.1	0.1	23.5	0.2	8.29	0.03	11.73	0.07	24.4	0.2
09/12/2009	18/02/2010	2.249	0.003	9.66	0.05	24.3	0.1	5.338	0.007	8.86	0.04	25.09	0.09
18/02/2010	16/03/2010	1.588	0.005	8.04	0.09	25.9	0.2	5.13	0.02	6.90	0.07	27.1	0.2
16/03/2010	08/04/2010	1.458	0.005	11.3	0.2	22.5	0.4	3.86	0.01	9.5	0.1	22.6	0.3
08/04/2010	07/05/2010	4.67	0.01	12.3	0.2	43.4	0.3	6.96	0.02	11.0	0.1	33.9	0.3
07/05/2010	02/06/2010	4.42	0.01	9.61	0.06	25.3	0.1	5.75	0.02	9.24	0.07	31.4	0.2
02/06/2010	29/06/2010	8.73	0.03	6.09	0.05	17.2	0.1	9.55	0.03	7.00	0.04	17.10	0.09
29/06/2010	20/09/2010	7.887	0.008	6.66	0.03	27.32	0.07	9.84	0.01	9.18	0.03	25.54	0.06
29/09/2010	05/11/2010	3.700	0.009	10.53	0.06	19.8	0.1	4.91	0.01	9.49	0.05	19.6	0.1
05/11/2010	10/12/2010	4.60	0.01	9.83	0.05	25.4	0.1	4.56	0.01	9.13	0.06	25.0	0.1
14/12/2010	04/01/2011	7.09	0.03	9.02	0.09	27.6	0.2	11.64	0.05	8.38	0.07	25.8	0.2
04/01/2011	02/02/2011	1.080	0.003	14.1	0.1	23.3	0.2	3.271	0.009	8.66	0.09	23.2	0.2
02/02/2011	09/03/2011	0.829	0.002	13.1	0.1	17.1	0.2	2.936	0.007	7.74	0.06	22.6	0.1
09/03/2011	06/04/2011	3.88	0.01	10.1	0.2	36.7	0.4	5.11	0.02	7.5	0.1	22.6	0.3
06/04/2011	03/05/2011	3.46	0.01	8.05	0.08	65.8	0.2	5.11	0.02	7.61	0.09	56.8	0.2
03/05/2011	27/06/2011	2.488	0.004	11.3	0.1	22.0	0.2	2.740	0.004	11.4	0.1	24.0	0.2
27/06/2011	23/07/2011	7.21	0.02	7.74	0.07	38.2	0.2	6.98	0.02	8.07	0.07	37.8	0.2
23/07/2011	10/08/2011	7.08	0.04	8.65	0.07	38.3	0.2	7.52	0.04	9.29	0.07	36.6	0.2
10/08/2011	11/09/2011	14.75	0.04	7.43	0.07	31.6	0.2	15.18	0.04	7.53	0.08	35.1	0.2
11/09/2011	15/11/2011	2.252	0.006	6.31	0.04	14.46	0.09	2.458	0.007	5.02	0.04	13.85	0.09
Date in	Date out	SAR	1 δ	NG3 Top	o Trap 1 δ	CaCO ₃	1 δ	SAR	1 δ	NG3 Botto	om Trap 1 δ	CaCO ₃	1 δ
		[g/m ² d]		[%]		[%]		[g/m ² d]		[%]		[%]	
18/02/2010	16/03/2010	0.934	0.003	9.2	0.1	21.2	0.2	4.415	0.003	6.23	0.06	27.2	0.2
16/03/2010	08/04/2010	1.090	0.004	12.6	0.2	18.4	0.5	3.672	0.004	9.0	0.1	21.7	0.3
08/04/2010	07/05/2010	3.417	0.003	12.5	0.2	47.5	0.4	5.323	0.003	10.7	0.1	32.5	0.3
07/05/2010	02/06/2010	3.008	0.003	10.62	0.08	25.8	0.2	3.768	0.003	9.57	0.07	36.1	0.2
02/06/2010	29/06/2010	5.712	0.003	6.87	0.06	15.7	0.1	5.973	0.003	7.71	0.06	16.7	0.1
29/06/2010	20/09/2010	6.062	0.001	6.45	0.03	29.17	0.06	6.874	0.001	6.39	0.03	29.30	0.07
29/09/2010	10/12/2010	2.250	0.001	9.57	0.06	21.5	0.1	3.138	0.001	8.72	0.05	22.7	0.1
14/12/2010	04/01/2011	3.350	0.004	9.7	0.1	26.2	0.3	6.748	0.004	8.41	0.09	24.01	0.2
04/01/2011	02/02/2011	0.813	0.003	12.2	0.2	20.5	0.4	2.273	0.003	8.94	0.09	22.5	0.2
02/02/2011	09/03/2011	0.636	0.002	10.27	0.09	19.0	0.2	3.117	0.002	7.10	0.07	22.0	0.2
09/03/2011	06/04/2011	3.400	0.003	9	2	27	4	5.068	0.003	6.2	0.2	20.0	0.4
06/04/2011	31/05/2011	1.716	0.002	13.1	0.1	43.0	0.3	2.741	0.002	9.31	0.07	43.4	0.2
31/05/2011	27/06/2011	2.501	0.003	12.16	0.09	22.3	0.2	2.282	0.003	11.76	0.09	26.6	0.2
27/06/2011	23/07/2011	5.765	0.003	7.92	0.07	41.8	0.2	5.067	0.003	8.33	0.08	39.1	0.2
23/07/2011	10/08/2011	5.265	0.005	9.58	0.08	41.6	0.2	5.804	0.005	10.01	0.08	36.9	0.2
10/08/2011	11/09/2011	11.100	0.003	7.62	0.07	39.1	0.2	9.428	0.003	8.13	0.08	47.5	0.2

3.467

0.002

10.07

0.2

11/09/2011

15/11/2011

2.980

0.002

11.13

0.18

References

- à Porta, N. 2013. Contamination en mercure des poissons du Léman selon le site de pêche. Masters thesis no. 097, University of Geneva.
- Bengtsson, G., Picado, F., 2008. Mercury sorption to sediments: Dependence on grain size, dissolved organic carbon, and suspended bacteria. Chemosphere. 73, 526-531.
- Benoit, J.M., Gilmour, C.C., Mason, R.P., Riedel, G.S., Riedel, G.F., 1998. Behavior of mercury in the Patuxent River estuary. Biogeochemistry, 40, 249-265.
- Blasco, J., Saenz, V., Gomez-Parra, A., 2000. Heavy metal fluxes at the sediment-water interface of three coastal ecosystems from south-west of the Iberian Peninsula. Sci. Total Environ. 247, 189-199.
- Bloom, N., 1989. Determination of Picogram Levels of Methylmercury by Aqueous Phase Ethylation, Followed by Cryogenic Gas-Chromatography with Cold Vapor Atomic Fluorescence Detection. Can. J. Fish. Aquat Sci. 46, 1131-1140.
- Bloom, N.S., Gill, G.A., Cappellino, S., Dobbs, C., Mcshea, L., Driscoll, C., Mason, R., Rudd, J., 1999. Speciation and cycling of mercury in Lavaca Bay, Texas, sediments. Environ. Sci. Technol. 33, 7-13.
- Boening, D.W., 2000. Ecological effects, transport, and fate of mercury: a general review. Chemosphere. 40, 1335-1351.
- Bravo, A.G., Loizeau, J.L., Bouchet, S., Richard, A., Rubin, J.F., Ungureanu, V.G., Amouroux, D., Dominik, J., 2010. Mercury human exposure through fish consumption in a reservoir contaminated by a chlor-alkali plant: Babeni reservoir (Romania). Environ. Sci. Pollut. R. 17, 1422-1432.
- Bravo, A.G., Bouchet, S., Amouroux, D., Pote, J., Dominik, J., 2011. Distribution of mercury and organic matter in particle-size classes in sediments contaminated by a waste water treatment plant: Vidy Bay, Lake Geneva, Switzerland. *J.* Environ. Monitor. 13, 974-982.
- Burnier, G., Jaquerod, C.A., Poget, E., Vioget, P., 2011. Bilans 2011 de l'épuration vaudoise. Rapport du service des eaux, sols et assaisnissement, Etat de Vaud, 27 pp.
- Compeau, G., Bartha, R., 1984. Methylation and Demethylation of Mercury under Controlled Redox, Ph, and Salinity Conditions. Appl. Environ. Microb. 48, 1203-1207.
- Dean, W.E., 1974. Determination of carbonate and organic matter in calcareous sediments and sedimentary rocks by loss on ignition; comparison with other methods. J. Sediment. Res. 44, 242–248.
- Dominik, J., Burrus, D., Vernet, J.P., 1987. Transport of the Environmental Radionuclides in an Alpine Watershed. Earth. Planet. Sc. Lett. 84, 165-180.
- Dominik, J., Dulinski, M., Span, D., Hofmann, A., Faverger, P.Y., Vernet, J.P., 1993. Transfert de matière et de radio-isotopes entre l'eau et les sédiments dans le Léman. Commission international pour la protection des eaux du Léman contre la pollution.
- Eckley, C.S., Hintelmann, H., 2006. Determination of mercury methylation potentials in the water column of lakes across Canada. Sci. Total Environ. 368, 111-125.
- Evans, R.D., 1994. Empirical-Evidence of the Importance of Sediment Resuspension in Lakes. Hydrobiologia. 284, 5-12.
- Feyte, S., Gobeil, C., Tessier, A., Cossa, D., 2012. Mercury dynamics in lake sediments. Geochim. Cosmochim. Ac. 82, 92-112.
- Gagnon, C., Pelletier, E., Mucci, A., 1997. Behaviour of anthropogenic mercury in coastal marine sediments. Mar. Chem. 59, 159-176.
- Gandais, V., 1989. Origines et variations spatio-temporelles des flux de matière particulaire au centre du Léman. Ph.D. thesis. University of Geneva

- Gascon Diez, E., Bravo, A.G., Porta, N.A., Masson, M., Graham, N.D., Stoll, S., Akhtman, Y., Amouroux, D., Loizeau, J.L., 2014. Influence of a wastewater treatment plant on mercury contamination and sediment characteristics in Vidy Bay (Lake Geneva, Switzerland). Aquat. Sci. 76, S21-S32.
- Gascon Diez, E., Loizeau, J.L., Cosio, C., Bouchet, S., Adatte, T., Amouroux, D., Bravo, A. G. Role of settling particles on mercury methylation in the oxic water column of freshwater systems. *Under review in Environmental Sciences and Technology*.
- Gilmour, C.C., Podar, M., Bullock, A.L., Graham, A.M., Brown, S.D., Somenahally, A.C., Johs, A., Hurt, R.A., Bailey, K.L., Elias, D.A., 2013. Mercury Methylation by Novel Microorganisms from New Environments. Environ. Sci. Technol. 47, 11810-11820.
- Graham, N.D., 2015. The fate of sediment-bound contaminants: a case study of Vidy Bay (Lake Geneva, Switzerland). Ph.D. thesis no. 4760, University of Geneva.
- Hammerschmidt, C.R., Fitzgerald, W.F. 2005., Methylmercury in mosquitoes related to atmospheric mercury deposition and contamination. Environ. Sci. Technol. 39, 3034-3039.
- Hånkanson, L., Jansson, M., 1983. Principles of lake sedimentology. Springer-Verlag, Berlin.
 Heimburger, L.E., Cossa, D., Marty, J.C., Migon, C., Averty, B., Dufour, A., Ras, J., 2010.
 Methyl mercury distributions in relation to the presence of nano- and picophytoplankton in an oceanic water column (Ligurian Sea, North-western Mediterranean). Geochim. Cosmochim. Ac. 74, 5549-5559.
- Kim, E.H., Mason, R.P., Porter, E.T., Soulen, H.L., 2006. The impact of resuspension on sediment mercury dynamics, and methylmercury production and fate: A mesocosm study. Mar. Chem. 102, 300-315.
- Korthals, E.T., Winfrey, M.R., 1987. Seasonal and Spatial Variations in Mercury Methylation and Demethylation in an Oligotrophic Lake. Appl. Environ. Microb. 53, 2397-2404.
- Liu, B., Yan, H.Y., Wang, C.P., Li, Q. H., Guedron, S., Spangenberg, J.E., Feng, X.B., Dominik, J., 2012. Insights into low fish mercury bioaccumulation in a mercury-contaminated reservoir, Guizhou, China. Environ. Pollut. 160, 109-117.
- Loizeau, J.L., Arbouille, D., Santiago, S., Vernet, J.P., 1994. Evaluation of a Wide-Range Laser Diffraction Grain-Size Analyzer for Use with Sediments. Sedimentology. 41, 353-361.
- Loizeau, J.L., Roze, S., Peytremann, C., Monna, F., Dominik, J., 2003. Mapping sediment accumulation rate by using volume magnetic susceptibility core correlation in a contaminated bay (Lake Geneva, Switzerland). Eclogae. Geol. Helv. 96, S73-S79.
- Macdonald, D.D., Ingersoll, C.G., Berger, T.A., 2000. Development and evaluation of consensus-based sediment quality guidelines for freshwater ecosystems. Arch. Environ. Con. Tox. 39, 20-31.
- Mason, R.P., Fitzgerald, W.F., Morel F. M., 1994. The biogeochemical cycling of elemental mercury anthropogenic influences. Geochim. Cosmochim. Ac. 58 (15), 3191-3198
- Mason, R.P., Kim, E.H., Cornwell, J., Heyes, D., 2006. An examination of the factors influencing the flux of mercury, methylmercury and other constituents from estuarine sediment. Mar. Chem. 102, 96-110.
- Monperrus, M., Tessier, E., Amouroux, D., Leynaert, A., Huonnic, P., Donard, O.F.X., 2007. Mercury methylation, demethylation and reduction rates in coastal and marine surface waters of the Mediterranean Sea. Mar. Chem. 107, 49-63.
- Owens, E.M., Bookman, R., Effler, S.W., Driscoll, C.T., Matthews, D.A., Effler, A.J.P. 2009. Resuspension of Mercury-Contaminated Sediments from an In-Lake Industrial Waste Deposit. J. Environ. Eng-Asce. 135, 526-534.
- Pardos, M., Benninghoff, C., De Alencastro, L.F., Wildi, W., 2004. The impact of a sewage treatment plant's effluent on sediment quality in a small bay in Lake Geneva

- (Switzerland–France). Part 1: Spatial distribution of contaminants and the potential for biological impacts. Lakes Reserv. Res. Manag. 9, 41–52.
- Parks, J.M., Johs, A., Podar, M., Bridou, R., Hurt, R.A., Smith, S.D., Tomanicek, S.J., Qian, Y., Brown, S.D., Brandt, C.C., Palumbo, A.V., Smith, J.C., Wall, J.D., Elias, D.A., Liang, L.Y., 2013. The Genetic Basis for Bacterial Mercury Methylation. Science. 339, 1332-1335.
- Podar, M., Gilmour, C.C., Brandt, C.C., Soren, A., Brown, S.D., Crable, B.R., Palumbo, A.V., Somenahally, A.C., Elias, D.A., 2015. Global prevalence and distribution of genes and microorganisms involved in mercury methylation. Sci. Adv. 1.
- Pote, J., Haller, L., Loizeau, J.L., Bravo, A.G, Sastre, V., Wildi, W., 2008. Effects of a sewage treatment plant outlet pipe extension on the distribution of contaminants in the sediments of the Bay of Vidy, Lake Geneva, Switzerland. Bioresource Technol. 99, 7122–7131. doi:10.1016/j.biortech.2007.12.075
- Razmi, A.M., Barry D. A., Bakhtyar, R., Le Dantec, N., Dastgheib, A., Lemin, U., Wüest, A., 2013. Current variability in a wide and open lacustrine embayment in Lake Geneva (Switzerland). J. Great. Lakes. Res. 39, 455-465.
- Rigaud, S., Radakovitch, O., Couture, R.M., Deflandre, B., Cossa, D., Garnier, C., Garnier, J.M., 2013. Mobility and fluxes of trace elements and nutrients at the sediment-water interface of a lagoon under contrasting water column oxygenation conditions. Appl. Geochem. 31, 35-51.
- Rolfhus, K.R., Sakamoto, H.E., Cleckner, L.B., Stoor, R.W., Babiarz, C.L., Back, R.C., Manolopoulos, H., Hurley, J.P., 2003. Distribution and fluxes of total and methylmercury in Lake Superior. Environ. Sci. Technol. 37, 865-872.
- Roos-Barraclough, F., Givelet, N., Martinez-Cortizas, A., Goodsite, M. E., Biester, H., Shotyk, W., 2002. An analytical protocol for the determination of total mercury concentrations in solid peat samples. Sci. Total Environ. 292, 129-139.
- Savoye, L., Quetin, P.,Klein A., 2015. Physico-chemical changes in the waters of Lake Geneva. Meteorological datas. Contributions from the tributaries of Lake Geneva and from the Rhone below Geneva. Rapport Commission international pour la protection des eaux du Léman contre pollution Campagne 2014,19-67.
- Schartup, A.T., Ndu, U., Balcom, P.H., Mason, R.P. & Sunderland, E.M. 2015. Contrasting Effects of Marine and Terrestrially Derived Dissolved Organic Matter on Mercury Speciation and Bioavailability in Seawater. Environ. Sci. Technol. 49, 5965-5972.
- Taylor, S.E., Birch, G.F., 2000. Contaminant dynamics in offchannel embayments of Port Jackson, New South Wales. A. G. S. O. 5-6, 233-237.
- Thevenon, F., Graham, N.D., Chiaradia, M., Arpagaus, P., Wildi, W., Pote, J., 2011. Local to regional scale industrial heavy metal pollution recorded in sediments of large freshwater lakes in central Europe (lakes Geneva and Lucerne) over the last centuries. Sci. Total Environ. 412, 239-247
- Wang, W.X., Stupakoff, I., Gagnon, C., Fisher, N.S., 1998. Bioavailability of inorganic and methylmercury to a marine deposit feeding polychaete. Environ. Sci. Technol. 32, 2564-2571.

CHAPTER V

Mercury methylation in settling particles

This chapter investigates the importance of settling particles to mercury speciation. Constraining the biochemical processes occurring within the particles is crucial for the understanding of the general mercury cycle, and in particular it allows a better definition of the pathways of particle-bound organomercurials.

Role of settling particles on mercury methylation in the oxic water column of freshwater systems

Elena Gascón Díez¹, Jean-Luc Loizeau¹, Claudia Cosio¹, Sylvain Bouchet², Thierry Adatte³, David Amouroux² and Andrea G. Bravo⁴

An article of similar form to this chapter in under review to *Environmental sciences* and technology for publishing

¹ Department F.-A. Forel for environmental and water sciences, University of Geneva, Boulevard Carl-Vogt 66, 1211

² Laboratoire de Chimie Analytique Bio-Inorganique et Environnement, Institut des Sciences Analytiques et de Physico-Chimie pour l'Environnement et les Matériaux, UMR 5254 CNRS, Université de Pau et des Pays de l'Adour, Hélioparc, 64053 Pau, France

³ Institute of Earth Sciences (ISTE), University of Lausanne, 1015 Lausanne, Switzerland

⁴ Limnology Department, Evolutionary Biology Centre, EBC, Norbyvägen 18D, 75236 Uppsala Sweden

Abstract

As the methylation of inorganic mercury (Hg^{II}) to neurotoxic methylmercury (MeHg) has been attributed to the activity of anaerobic bacteria, the formation of MeHg in the oxic water column of marine ecosystems has puzzled scientists over the past years. Here we show for the first time that MeHg can be produced in particles sinking through oxygenated water column of lakes. Total mercury (THg) and MeHg concentrations were measured in settling particles and in surface sediments of the largest freshwater lake in Western Europe (Lake Geneva). Whilst THg concentration differences between sediments and settling particles were not significant, MeHg concentrations were up to ten-fold greater in settling particles. MeHg demethylation rate constants (k_d) were of similar magnitude in both compartments. In contrast, Hg methylation rate constants (k_m) were one order of magnitude greater in settling particles. The net potential for MeHg formation, assessed by the ratio between the two rate constants $(k_m k_d^{-1})$, was therefore up to ten times higher in settling particles, denoting that in-situ transformations likely contributed to the high MeHg concentration found in settling particles. Hg methylation was inhibited (~80 %) in settling particles amended with molybdate, demonstrating the prominent role of biological sulfate-reduction in the process.

Keywords: methylmecury, mercury methylation, water column, sediments, settling particles.

1. Introduction

Anthropogenic activities such as artisanal gold mining, waste disposal, metal and cement industries, and the burning of fossil-fuel fired power plants have greatly increased mercury (Hg) dispersion and concentration in aquatic systems worldwide¹. Understanding the biological formation of the neurotoxic methylmercury (MeHg) in aquatic ecosystems is critical because MeHg is bio-accumulated and biomagnified in food webs, eventually affecting wildlife and human health². It has been reported that methylation of inorganic-Hg (IHg) into MeHg mainly occurs at oxygen water columns³ and/or sediments⁴⁻⁶ and is carried out by specific strains of a large set of potential methylators such as sulfate-reducing bacteria (SRB), iron-reducing bacteria (FeRB), and methanogens^{7,8}. As Hg-methylation is mainly carried out by anaerobic microorganisms, it has been assumed for a long time that compared to sediments MeHg formation in oxic environments, such as water columns, was negligible due to the presence of oxygen and the lower concentrations of bacteria and nutrients^{5,9}. Consequently Hg-methylation in pelagic freshwater systems remains largely less explored than in sediments. In marine environments however, Hg-methylation was recently reported to occur in the sub-oxic 10,11 and even in the oxic layer of the water column¹²⁻¹⁶. MeHg was hypothesized to be formed by microbes associated with sinking particulate organic matter (OM)¹²⁻¹⁸, but it remains unclear whether these organisms are aerobic or anaerobic. Indeed, the genes responsible for Hg-methylation (hgcAB) were rarely found in oxygenated layers of the open ocean¹⁹, suggesting that an unidentified metabolic pathway could be responsible for MeHg production in this environment. In fresh water ecosystems, MeHg formation has been extensively investigated in sediments^{6,20-24} and biofilms²⁵⁻³⁰ but rarely in the hypolimnetic waters^{3,31}. MeHg formed in hypolimnetic waters compartment may actually represent a significant source of MeHg to the food chain when the volume of such water is larger than the volume of surface sediments³. Recent studies suggest that atmospheric Hg can be methylated³² and even accumulated in food chains³³ within 24 hours after its deposition. Assuming that recently deposited Hg should theoretically reach anoxic waters or sediments to be methylated, there is still no experimental explanation for such rapid MeHg formation in aquatic ecosystems. Indeed, the fastest in situ MeHg production, assessed by the addition of Hg-spikes on a lake ecosystem, was detected in anoxic bottom waters only after 72 hours³⁴. We have thus hypothesized that rapid methylation³² of recently deposited Hg could only be explained if Hg methylation processes occur in the water column, in particular in settling particulate OM, even under oxic prevailing conditions. This can be of major concern in deep lakes and oceans where MeHg generated in the water column may be rapidly available to enter the aquatic food web because it does not need to diffuse out from the sediments^{3,35}. As different concentrations of MeHg have been reported in water column of lakes with identical inputs of IHg³⁶, this study aims to provide an improved understanding of the drivers and sources controlling MeHg levels in aquatic systems.

Here we measured Total-Hg (THg) and MeHg concentrations in settling particles and sediments of the largest freshwater lake in Western Europe (Lake Geneva) for two years and performed experimental studies to determine the rates, mechanisms, and factors controlling the MeHg concentrations found in its oxic water column. This study shows for the first time that IHg can be methylated in settling particles of oxic lake waters and suggest that SRB or organisms related to them such as syntrophs³⁷ are involved in the process.

2. Materials and methods

2.1. Study site and sampling strategy

Lake Geneva has an area of 580.1 km², a maximum depth of 309 m and a volume of 89 km³. It is a oxic monomictic lake with infrequent complete turnover³8 From December 2009 to September 2011, sediments and settling particles were collected in Lake Geneva on a monthly basis at the sampling site NG2 (6° 35′ 0′′ E, 46° 30′ 6′′ N; Swiss coordinates (m): 534350 E, 150400 N). This site has been previously described by Graham³9 and detailed maps are presented in the supporting information (Figure S1). Briefly, NG2 is located at 138 m depth and 1,100 m from an outlet pipe discharging in Vidy Bay both treated and untreated sewage water of a wastewater treatment plant (WWTP) located near the city of Lausanne²0,40-43.

To collect the settling particles, we used a sediment trap system formed by a weight, an acoustic release, a sediment trap frame composed of six 80-cm-long Plexiglas tubes of 11 cm internal diameter placed 5 m above the sediment (actual sampling depth: 132 m), and maintained by buoys⁴⁴ (Figure S1). Sediments underneath the traps were recovered at the date of the sediment traps exchange, using two Mortimer gravity corers attached together from which the first centimetre was subsequently subsampled³⁹. Furthermore, surface sediments (~ 1 cm depth) were collected during the summer 2010 using a Van Veen grab sampler at 15 additional sites (numbered EG1 - EG15) along a transect extending from Vidy Bay towards the main deep basin (Figure S2). An aliquot of the WWTP sewage sludge was also sampled for subsequent Hg analyses.

2.2. Hg-methylation and demethylation rate constants in sediments and settling particles

Sediment traps were placed back at NG2, on May 15th and were changed on June 10th, July 14th and finally removed on August 14th, 2014. Hg-methylation rates were determined in the upper first cm of sediments, where the highest MeHg concentrations were previously observed⁴³, and in settling particles. At 132 m depth in Lake Geneva, dissolved oxygen was ≥ 7 mg 1^{-1} , temperature 5.5 °C, conductivity $\sim 300 \text{ }\mu\text{S }\text{ }\text{cm}^{-1}$ and pH ~ 8 (Figure S3)⁴⁵. A volume of 32 ml of sediments was collected from the top of a sediment core and was dispensed into a 40 ml vial (head-space glass vials with PTFE caps) and were amended with 55 µl of 10 mg l⁻¹ of ¹⁹⁹HgCl₂ and 80 μl of 0.4 mg l⁻¹ of ²⁰¹MeHgCl and shaken, creating a sort of slurry. Similarly, 32 ml of settling particles with their overlying water were placed into a 40 ml vial, amended and shaken. To better constrain the role of anaerobic sulphate-reduction on the Hg-methylation, we also amended sediments and settling particles with molybdate (Na₂MoO₄; 2.4 mM final concentration), a specific inhibitor of the sulphate reducing metabolism²⁴. Immediately after the Hg tracers' amendment (t₀), one sub-sample was centrifuged at 3500 rpm for 25 minutes to extract the pore water, and the supernatant water was filtered with 0.45 µm Sterivex syringe filters and stored in 15 ml PP flasks at -20 °C for subsequent anion measurements. Three

remaining sediment sub-samples were frozen and freeze-dried. Thus, three control-replicate (no $Na_2MoO_4^{2-}$ addition) and three molybdate-replicate (with $Na_2MoO_4^{2-}$) slurries were incubated close to lake temperature (4 °C) in the dark. After 48h (t_f), we collected the pore water as described for t₀ and we used the remaining sediment for further determination of potential Hg-methylation. All sample manipulations were done under a N_2 -atmosphere.

2.3. Laboratory analyses

2.3.1. THg and MeHg concentrations in sediments and settling particles

For samples collected from 2009 to 2011, THg was analyzed by atomic absorption spectrometry following the procedure described by Szakova et al. 46 using an automatic mercury analyzer (AMA-254). The absolute detection limit was 10 pg and the concentrations obtained for repeated analyses of certified reference material (CRM) never exceeded the range of concentration given for MESS-3 (National Research Council Canada). MeHg was extracted from sediments using HNO₃ leaching/CH₂Cl₂ and measured with a Cold Vapor Atomic Fluorescence Spectrophotometer⁴⁷⁻⁴⁹. The detection limit was 5 pg and the recovery of repeated extraction and analyses of the used CRM (ERM-CC580) were always above 85%. Incubations and analyses for the determination of Hg transformations were carried out according to Rodriguez-Gonzalez et al.⁵⁰. Briefly, IHg and MeHg were extracted from 200 mg of dry sediments or settling particles with HNO₃ (6N) under focused microwave treatment and analyzed by species-specific isotope dilution, gas chromatography (GC) hyphenated to an inductively coupled plasma mass spectrometer (ICP-MS). Methodological detection limits for Hg species were 0.03 ng g⁻¹. The extraction and quantification were validated with a CRM (IAEA-405) and recoveries were 102 ± 7 and 97 ± 4 % for MeHg and IHg, respectively. The concentrations of the added and formed Hg species deriving from the enriched isotopes 199 and 201 were calculated by isotopic pattern deconvolution methodology.

2.3.2. Sulfate-reduction rates

Sulfate (SO₄²⁻) consumption was measured in pore water of sediments and settling particles collected in sediment traps. To extract pore water, sediment core and trap samples were centrifuged (3,500 rpm 25 min). Overlying water after centrifugation was filtered with 0.45 μm Sterivex syringe filters under a N₂-atmosphere. Differences on SO₄²⁻ concentrations between t₀ and t_f were used to calculate sulfate-reduction rates (SRR) in control samples and MoO₄²⁻ amended sediment. SO₄²⁻ values were normalized with the chloride (Cl⁻) concentration that is constant during the incubation period. SO₄²⁻ and Cl⁻ concentrations were measured by ionic chromatography (IC) Dionex, AS19 IonPac column. Analyses were carried on duplicates and the accuracy was tested with the CRM ONTARIO-99 (Environment Canada).

2.3.3. Total organic carbon, mineral carbon, Hydrogen Index and Oxygen Index

Total Organic Carbon (TOC), hydrogen Index (HI) and Oxygen Index (OI) were determined by Rock-Eval® pyrolysis method Model 6 device (Vinci Technologies) following the procedure published by Espitalie, et al.⁵¹. During Rock-Eval® analyses, organic carbon decomposition resulted in 4 main peaks: S1 peak («free» hydrocarbons released during the isothermal phase); S2 peak (hydrocarbons produced between 300 °C and 650 °C); S3 peak (CO₂ from pyrolysis of OM up to 400 °C); and S4 peak (CO₂ released from residual OM below ca. 550 °C during the oxidation step). Mineral carbon decomposition is recorded by the S3' peak (pyrolysis-CO₂ released above 400 °C), and S5 peak (oxidation-CO₂ released above ca. 550 °C). These peaks are used to calculate the amount of TOC and the amount of mineral carbon. In addition, the socalled hydrogen index (HI = S2/TOC) and oxygen index (OI = S3/TOC) are calculated. The HI and OI indices are proportional to the H/C and O/C ratios of the organic matter, respectively, and can be used for OM classification in Van-Krevelen-like diagrams^{51,52}. HI is expressed in mg HC g⁻¹ TOC, and OI in mg CO₂ g⁻¹ TOC. The standard used was IFP 160000 Rock-Eval and the analyses were carried out on 50-100 mg of powdered dry sediment under standard conditions. Analytical precision was better than 0.05 wt.% (1 σ) for TOC, 10 mg HC g⁻¹ TOC (1 σ) for HI, and 10 mg CO_2 g⁻¹ TOC (1 σ) for OI.

2.3.4. Total nitrogen analyses

Total nitrogen content (% N) was analyzed in a CHN Elemental Analyzer (Carlo Erba Flash EA 1112 CHNS/MAS200) using approximately 10 mg of dry powdered sediment. The carbon/nitrogen (C/N) ratio was calculated as the weight ratio of the TOC measured by the Rock-Eval® pyrolysis (see above) and the N content analyzed by CHN Elemental Analyzer. Precision was better than 1% based on internal standard and replicate samples.

2.3.5. Mineral composition diffraction analyses

Bulk mineralogical composition was performed using a X-TRA Thermo-ARL Diffractometer, following the procedure described in Klug and Alexander⁵³ and Adatte et al.⁵⁴. This method for semi-quantitative analysis of the bulk rock mineralogy (obtained by XRD patterns of random powder samples) uses external standards with error margins varying between 5 and 10% for the phyllosilicates and 5% for grain minerals.

2.4. Statistical analyses

Normality was tested using the Shapiro-Wilk test. Annual THg concentration datasets followed a normal distribution in sediments and settling particles. However, MeHg and %MeHg/THg datasets followed a non-normal distribution; therefore the Mann-Whitney rank test was used to assess differences in median values between the two groups (sediments and settling particles). Similarly, correlations between C/N and %MeHg/THg were tested with Spearman rank order correlations. Finally, as Hg-methylation rates were normally distributed, one-way ANOVA tests were performed to compare the results of the three different incubation conditions versus the control group (Holm-Sidak method) Overall the significance level was set to 0.05. All the statistical analyses were performed with SigmaPlot 11.0 software.

3. Results and discussion

3.1. Temporal trends of THg and MeHg concentrations in sediments and settling particles

THg concentrations at NG2 ranged between 174 ± 4 and 270 ± 58 ng g⁻¹ in sediments and from 73.4 ± 0.4 to 257 ± 9 ng g⁻¹ in settling particles (Figure 1). Variations in THg concentrations between sediments and settling particles were not statistically significant (p > 0.05). In contrast, MeHg concentrations were significantly higher (p < 0.05) in settling particles (from 0.62 ± 0.04 to 11.38 ± 0.02 ng g⁻¹) than in sediments (from 0.31 ± 0.03 to 1.67 ± 0.02 ng g⁻¹).

A significant seasonal pattern (p < 0.001) was, however, observed for THg concentrations in settling particles with the lowest values ($< 100 \text{ ng g}^{-1}$) registered during late summer-early fall compared to the winter period showing higher concentrations. MeHg concentrations were more variable throughout the sampling period and, contrary to THg, did not show any seasonal pattern. This contrasts with other studies where a high seasonal variability was reported, for example in estuarine suspended particles⁵⁵. Likewise, the proportion of MeHg to THg (%MeHg/THg), also used as a proxy of net MeHg production¹⁹, was significantly higher in settling particles (0.4 % - 9.6 %) than in sediments (0.2 % to 0.8 %).

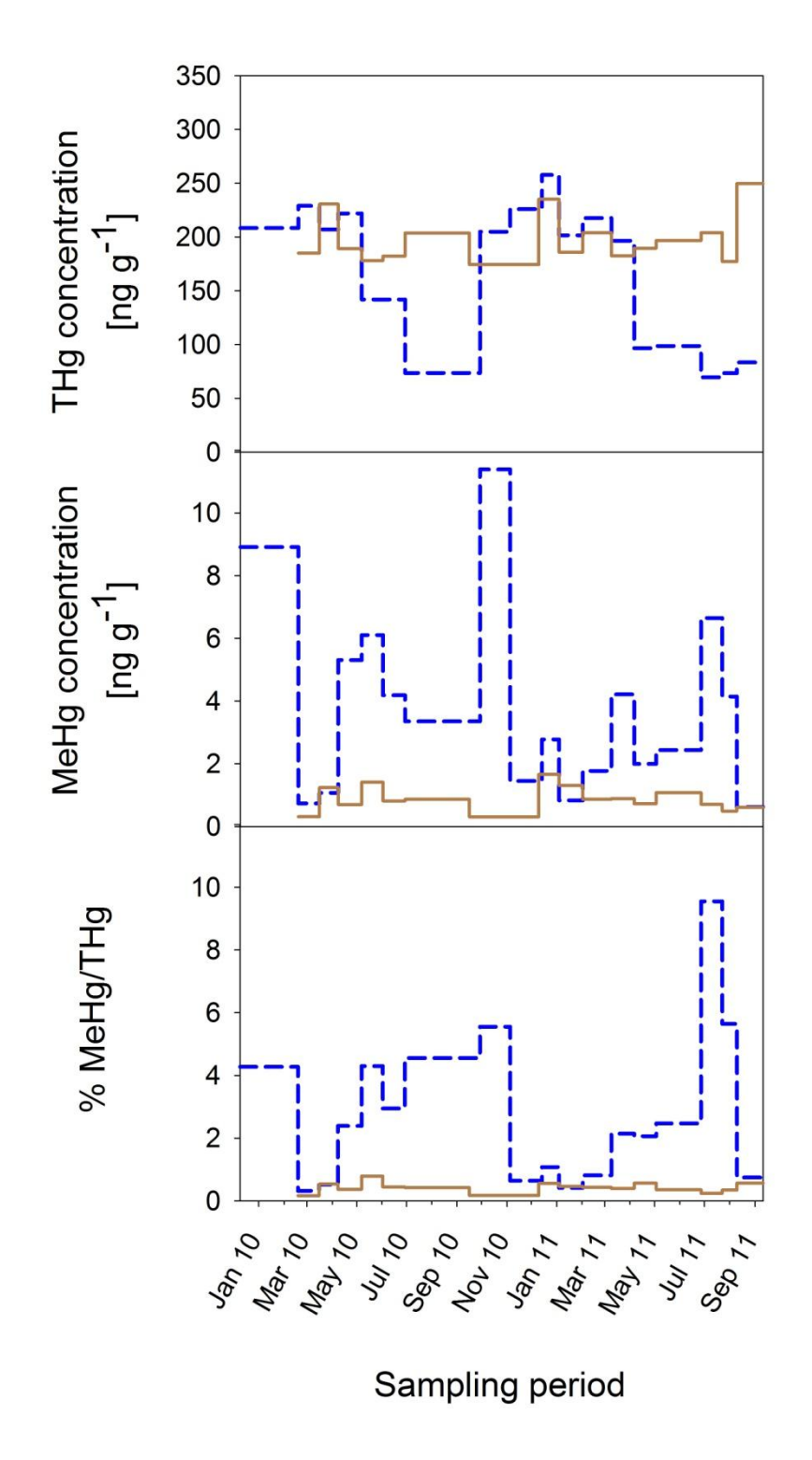


Figure 1. Concentrations of total mercury (THg), methylmercury (MeHg) and MeHg as THg percentage (% MeHg/THg) in settling particles (dash line) and sediments (solid line) at Lake Geneva from December 2009 to September 2011.

Considering a concentration of suspended particles of 0.4 g m⁻³ (lake volume-weighted arithmetic mean) in Lake Geneva⁵⁶, the estimated mass of particles in the whole lake is approximately 35,600 tons. Thus, in view of the concentration of MeHg in suspended particle being equivalent to the concentration in settling particles (3.6 ng g⁻¹), the total amount of MeHg in this compartment is estimated to be around 130 g, accounting for roughly 10 % of the total amount of MeHg estimated be contained in the first cm of the sediments. It thus represents a significant pool of MeHg in this ecosystem and should be considered in further studies to better predict and constrain all sources of MeHg to food webs in aquatic systems.

3.2. THg and MeHg sources for Lake Geneva

Previous studies demonstrated that the sewage water discharges alter sediment characteristics⁴³ and are the main source of pollutants for Vidy Bay^{57,58}. Catchment inputs of THg to Vidy Bay are low compared to the releases of the WWTP^{43,57,58}. In contrast, we have previously demonstrated that MeHg concentrations found in sediment mostly originates from in situ production in sediments⁵⁸ and that the higher Hg methylation rate constants were found closer to the pipe²⁰. In this study, MeHg concentrations measured in fifteen surface sediment samples along a transect from the shore to the deeper part of Vidy Bay (Figure S2), show a clear decrease with distance from the WWTP. In particular, at site EG4 (Figure S2), 530 m away from the outlet pipe, the concentration of MeHg was approximately 30-fold lower than the most contaminated site (EG3) suggesting that at NG2, which was located at 1,100 m from the outlet pipe, there was no effect of the catchment area and/or the WWTP inputs. Furthermore, the MeHg concentration measured in the WWTP sludge before its release was $1.6 \pm 0.2 \text{ ng g}^{-1}$, lower than the MeHg concentrations most often encountered in settling particles (Figure 1). Altogether, it suggests that the MeHg foundin settling particles cannot be explained either by catchment inputs, or by the WWTP releases.

3.3. Hg species transformation rates in sediments and settling particles

The methylation rate constants (k_m) in sediments ranged from 1.0 x 10⁻³ to 6.8 x 10⁻³ day⁻¹ from mid-May to mid-August, without following any particular trend (Figure 2). In contrast, km were about one order of magnitude higher (p < 0.05), in settling particles than in sediments and they also showed an increasing trend over the summer period, from 1.6 x 10^{-2} to 6.5 x 10^{-2} day⁻¹ (Figure 2). These k_m values were similar to those measured in the anoxic hypolimnetic water of some Canadian lakes where k_m ranged between 4.1 x 10⁻³ and 1.5 x 10⁻² day^{-1 3}. On the other hand, MeHg demethylation rate constants (k_d) in sediments and settling particles were on the same order of magnitude (Figure 2). No seasonal trend could be seen in settling particles where k_d ranged from 0.086 to 0.219 day⁻¹ while in sediments k_d increased from 0.064 in spring to 0.330 day⁻¹ for late summer. As a result, the $k_m k_d^{-1}$ ratios were 10-fold higher in settling particles than in sediments from June to August. Even if the bioavailability of added Hg tracers might differ from the natural Hg species, the $k_m k_d^{-1}$ ratios can be compared to the % MeHg/THg among sites and/or samples from the same site⁵⁹. Our results thus clearly show a higher potential for net MeHg production in the settling particles compared to surface sediments, confirming our previous hypotheses based solely on MeHg concentrations and higher proportions of MeHg to THg.

The semi-confined conditions in the sediment traps may have artificially enhanced Hg methylation compared to the open water column. However, redox and O₂ measurements in the sediment traps are very similar to in-situ conditions (Figure S3). In addition, there was indirect evidence that conditions remained oxic during the incubations. For example, the color of the incubated samples indicated that Fe was mainly found as Fe-oxyhydroxides and not as a ferrous-sulfide minerals suggesting a limited accumulation of H₂S. Furthermore, the percentage of ¹⁹⁹MeHg formed from the added ¹⁹⁹IHg was in the same range as the ambient MeHg to IHg ratio found in the traps collected during the period 2009-2011 (3.0 - 12.7 % vs 0.4 - 9.6 %, respectively). This similarity also confirmed the relevance of the incubations compared to *in situ* conditions.

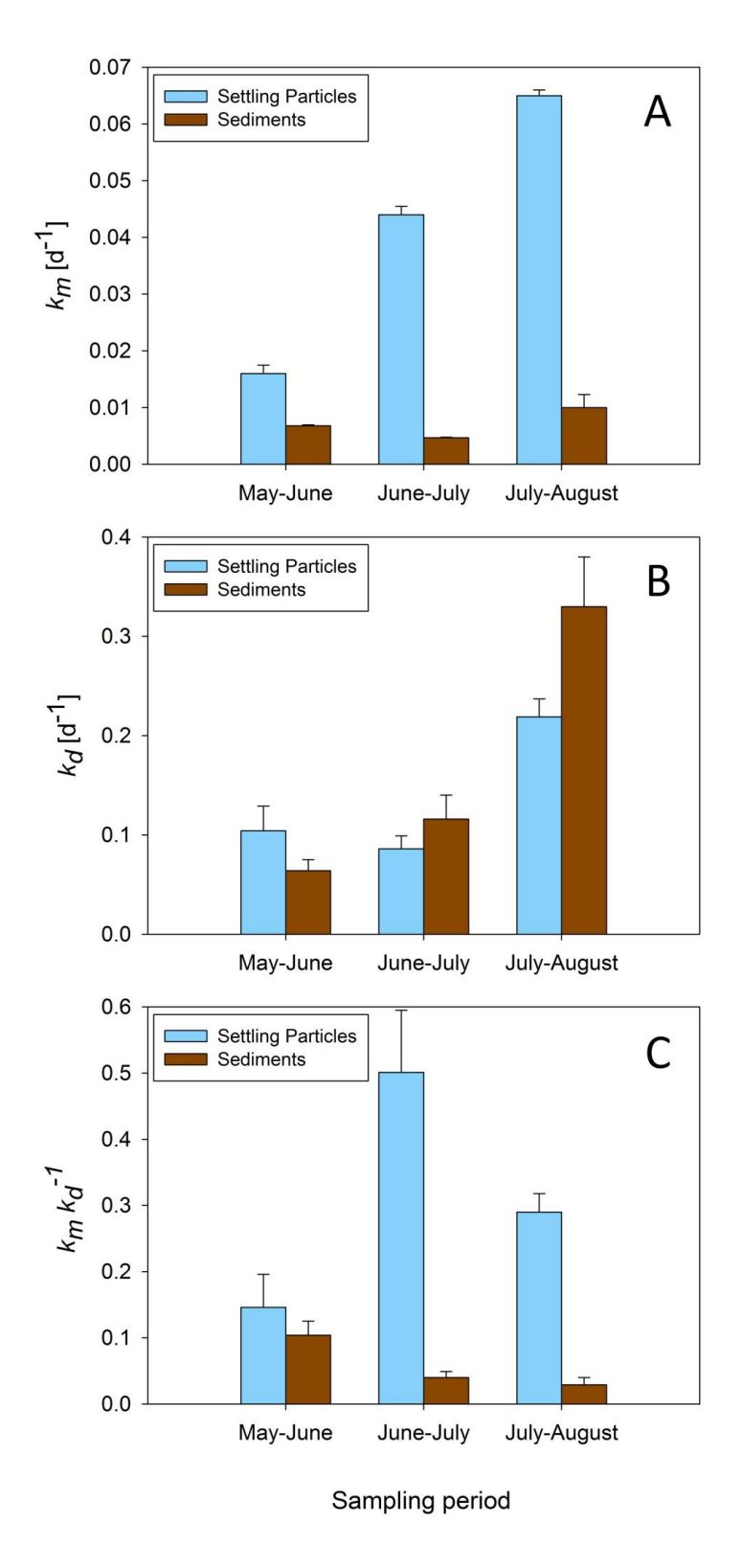


Figure 2. A: Hg methylation (k_m) , B: MeHg demethylation (k_d) rate constants (day^{-1}) and C: net MeHg formation $(k_m k_d^{-1} \text{ ratio})$ of settling particles and surface sediments from mid-May to mid-August 2014.

Our results thus show that methylation of IHg occurs in the water column of Lake Geneva during the time span that particles take to settle out of the water column, which is around one month^{39,56}. Contrary to other lakes where Hg-methylation has been observed in the oxygen depleted water column, Lake Geneva, at 132 m depth, is oxic with~7 mg l⁻¹ of O₂ (Figure S3), implying that both settling particles and surface sediments remain in an oxic environment throughout the year. Our results, along with those obtained from filtered/unfiltered water, cited above^{3,12-16} indicate that settling particles are a potentially important compartment for MeHg production.

3.4. Bacterial anaerobic metabolism contributes to Hg methylation in oxic water column

Despite the fact there are many organisms with the capacity to methylate Hg^{3,4,17}, SRB have been specifically identified as important Hg-methylators in aquatic systems³³⁻³⁵. In this study, molybdate amendments led to an inhibition of around 80% of the Hg-methylation rates in sediments and between 60% and 90% in settling particles (Figure 3). The role of sulfate reduction on Hg methylation in settling particles is further supported by (i) the positive correlation between Hg-methylation rates and sulfate consumption and (ii) the concomitant inhibition of sulphate consumption and Hg-methylation. This study demonstrated the occurrence of biological Hg-methylation in settling particles of Lake Geneva and our results points to an important role of sulfate-reducers in the process; however, iron-reducing bacteria involvement is not excluded, as it was suggested previously in the sediments of Lake Geneva²⁰. The use of direct probing of the recently discovered hgcA and hgcB gene cluster will be tremendously helpful in further studies to characterize the microbial Hg methylating community in settling particles and sediments. As biogeochemical conditions during incubations (O₂ concentrations, temperature and bacterial anaerobic metabolism) were similar for both sediments and settling particles, we rather ascribed differences in MeHg production between the two compartments to OM quality driving both Hg availability and bacterial activity.

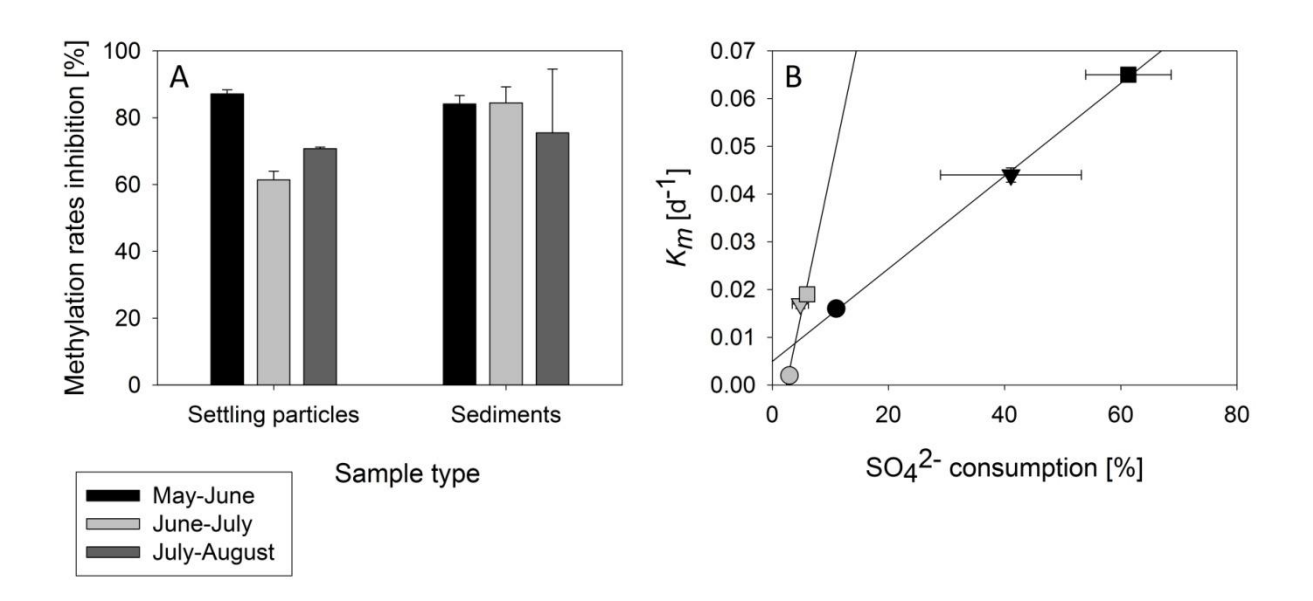


Figure 3. A: percentage of methylation inhibited in settling particles and sediment samples amended with molybdate (MoO_4^{2-}) . B: Sulfate (SO_4^{2-}) consumption in relation with k_m of settling particles; Black symbols represent control settling particles and grey symbols molybdate amended settling particles; Circles correspond to samples of May-June; triangles to samples of June-July; and squares to samples of July-August.

3.5. Organic matter quality favors Hg-methylation in particles compared to sediments

As the sampling station was far from the shore (~2 km) and distant to major river inputs, OM in settling particles originates largely from phytoplankton. This is first confirmed by the abundance of diatoms and *thecamoeba* in the sediment traps (Figure S4). The mineralogy of settling particles and sediments are qualitatively and quantitatively very similar, except for calcite, which is more abundant in settling particles than in sediments, especially from July to September (Figure S5). This increase in calcite in settling particles could be caused either by an enhanced precipitation due to the higher temperatures typically occurring in summer, either by an increase of biological productivity^{60,61}. The negative correlation between calcite and i) phyllosilicates (R²: -0.85) and ii) quartz (R²: -0.82), both from detrital origin, confirms biological in-situ production of calcite (Table S1). Moreover C/N ratios and HI and OI indexes, which are indicators of sources and degrees of biological and

diagenetic alteration⁶², were measured in samples collected from December 2009 to September 2011 (Figure 4). The C/N ratios were higher in 2010 than 2011 in both compartments but overall always higher in sediments than in settling particles, meaning that OM in bulk sediment was either more degraded or more terrestrial than in settling particles. These results are further supported by the HI and OI indexes that can also differentiate the OM of algal origin from the more degraded or terrestrial OM⁶³⁻⁶⁵. HI and OI indexes clearly discriminated OM composition between the settling particles and the sediments collected from 2009 to 2011 (Figure 4) but also in the slurries made in 2014 (Figure S6). In the latter, OM in settling particles was more of algal origin and showed a less-reworked and degraded status than the sedimentary OM. Combined analyses of mineral and OM composition support that OM in settling particles was enriched in algal derived OM and less degraded than in sediments. This energy rich OM can serve as an electron-donor to provide energy and carbon to the Hg methylators and consequently enhance MeHg production in settling particles²¹. A MeHg enrichment in algae of settling particles compared to sediments could also contribute to MeHg concentrations in settling particles, especially over the summer. Several studies showed that Hg uptake by bacteria or phytoplankton microorganisms can be affected by low molecular weight thiols complexing Hg, and/or the degradation state and origin of the OM that binds Hg^{66,67}. In pelagic sea waters, the sinking particulate OM has already been suggested as the main compartment for Hg-methylation¹². In this study we reveal that Hg methylation can also occur in oxic water columns of freshwater ecosystems likely due to the presence of fresh labile OM and micro anoxic environments in settling particles, as it was previously reported in pelagic sea waters¹⁴. Besides the type of OM determining the quality of the electron donors for Hg methylating bacteria, the redox potential within these micro anoxic environments and the formation of dissolved or nanoparticulate mercuric sulfides in these micro-environments likely effect Hg methylation processes in both settling particles and surface sediments⁶⁸.

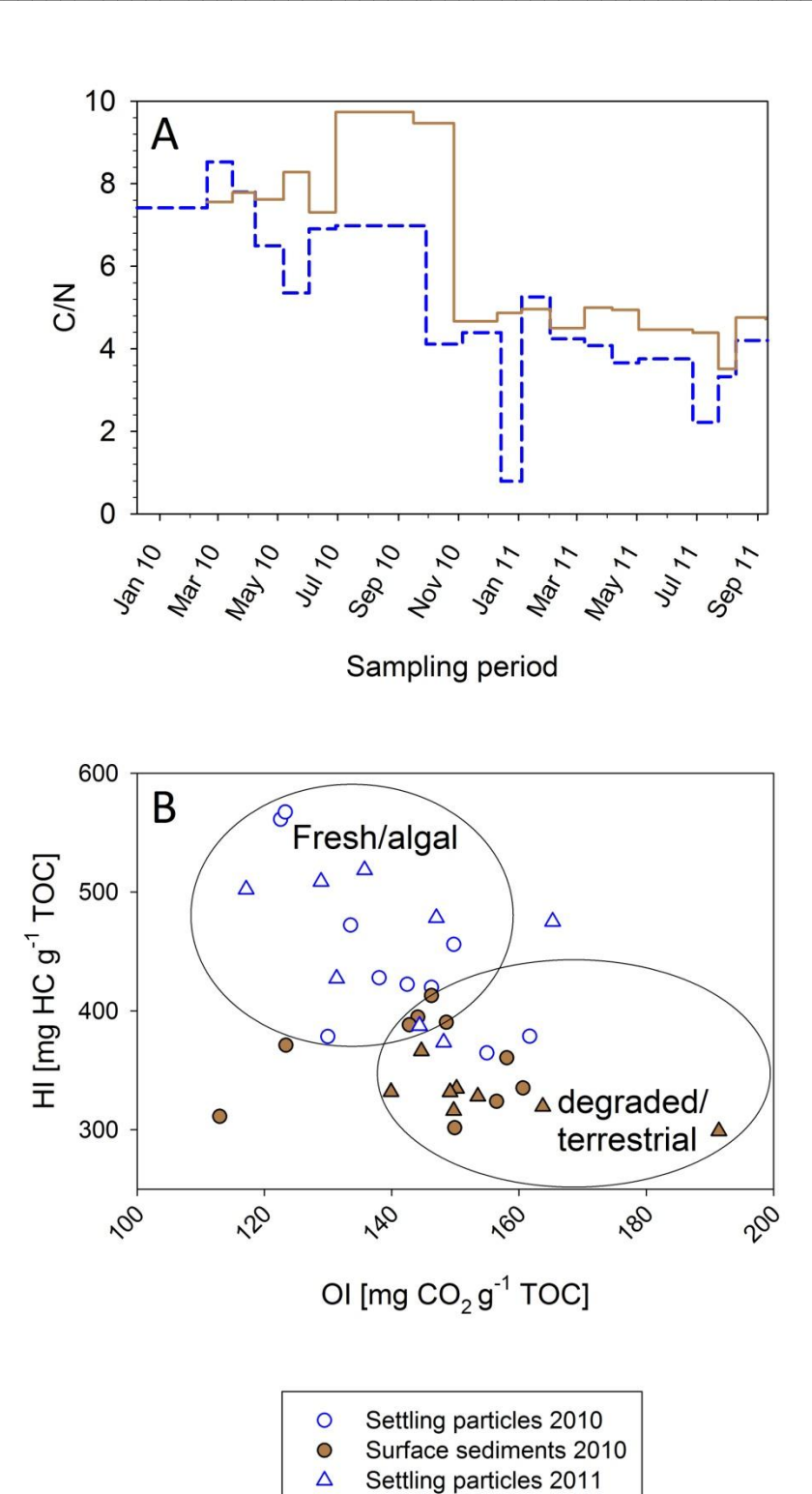


Figure 4. A: C/N ratio measured in settling particles (dash line) and sediments (solid line). B: Hydrogen index (HI) versus oxygen index (OI) in all samples taken at NG2 from December 2009 to September 2011. Blue and brown symbols represent settling particles and sediments respectively.

Surface sediments 2011

3.6. Environmental perspectives

Settling particles in our study consisted of allochthonous material (quartz grains and clay particles) but also of autochthonous components such as diatom frustules, aggregates of organic mucilage (fecal pellet) and organo-mineral flocs (Figure S4). Abrupt changes of the inner physico-chemical conditions, e.g. dissolved oxygen gradients at micrometer scale, have been observed in the sinking organic particles of marine oxic water column⁶⁹⁻⁷¹. Particle association creates a spot in the oxic water column where suboxic or anoxic processes can occur due to the formation of microscale oxyclines^{72,73}. The sulfate-reducing potential by anaerobic microbes in the reducing microzone of such particles has been demonstrated in marine detrital aggregates⁷⁴, and are supposed to be strongly activated by the sharp oxygen gradient occurring in such particles. We suggest that such suboxic/anaerobic microzones also develop in the lake settling particles and that they are ideal for Hg methylation.

Despite our improved understanding of the microbial Hg-methylation, we have only a vague idea of the MeHg sources for aquatic food web and factors that control the efficiency of that methylation. This study demonstrates conclusively that Hg can be methylated within the lake oxic water column to form MeHg to a greater extent than MeHg formed in the sediment, and we suggest that this contribution has so far been underestimated. Our results provide evidence to conclude that higher concentrations of MeHg in settling particles are caused by enhanced in situ MeHg production and by MeHg enrichment in algae. The identification of sources of MeHg has far-reaching implications for central scientific questions in Hg biogeochemistry and should be considered in future biogeochemical Hg cycling models at regional and global scales. In fact, settling particles formed partially by planktonic detritus might be an important source of MeHg for uptake into the food web²⁰. As there are 27 million water bodies larger than 0.01 km² excluding Caspian Sea and around 2,000 larger than 100 km² (i.e. Tanganyika, Victoria, Titicaca, Lake Baikal, the American Great Lakes and large Chinese or Brazilian reservoirs)⁷⁵ the formation of MeHg in the water column of freshwater systems might be thus a global issue.

Acknowledgments

The authors thank Philippe Arpagaus and Neil Graham for their valuable help with sediment and settling particles sampling. Jean-Michel Jaquet for the analyses of electronic microscope. The work was partly funded by Swiss National Foundation (project PDFMP2-123034) and Swedish Research Council (project 2011-7192 grant to AGB). We thank Charles Verpoorter for providing the number of water bodies (and their area) across the globe. We also thank Dolly Kothawala and Prof. Andrew Barry for English editing and manuscript improvement.

Supporting information

Six additional figures (Figures S1-S6, Table S1). This material is available free of charge via the Internet at http://pubs.acs.org. Map of Sampling site; MeHg concentrations in sediments of the Vidy Bay area; Dissolved oxygen temperature and redox profiles in water column; OM microscopy; Mineralogical composition; HI vs OI; Correlation matrix between the different mineralogical components

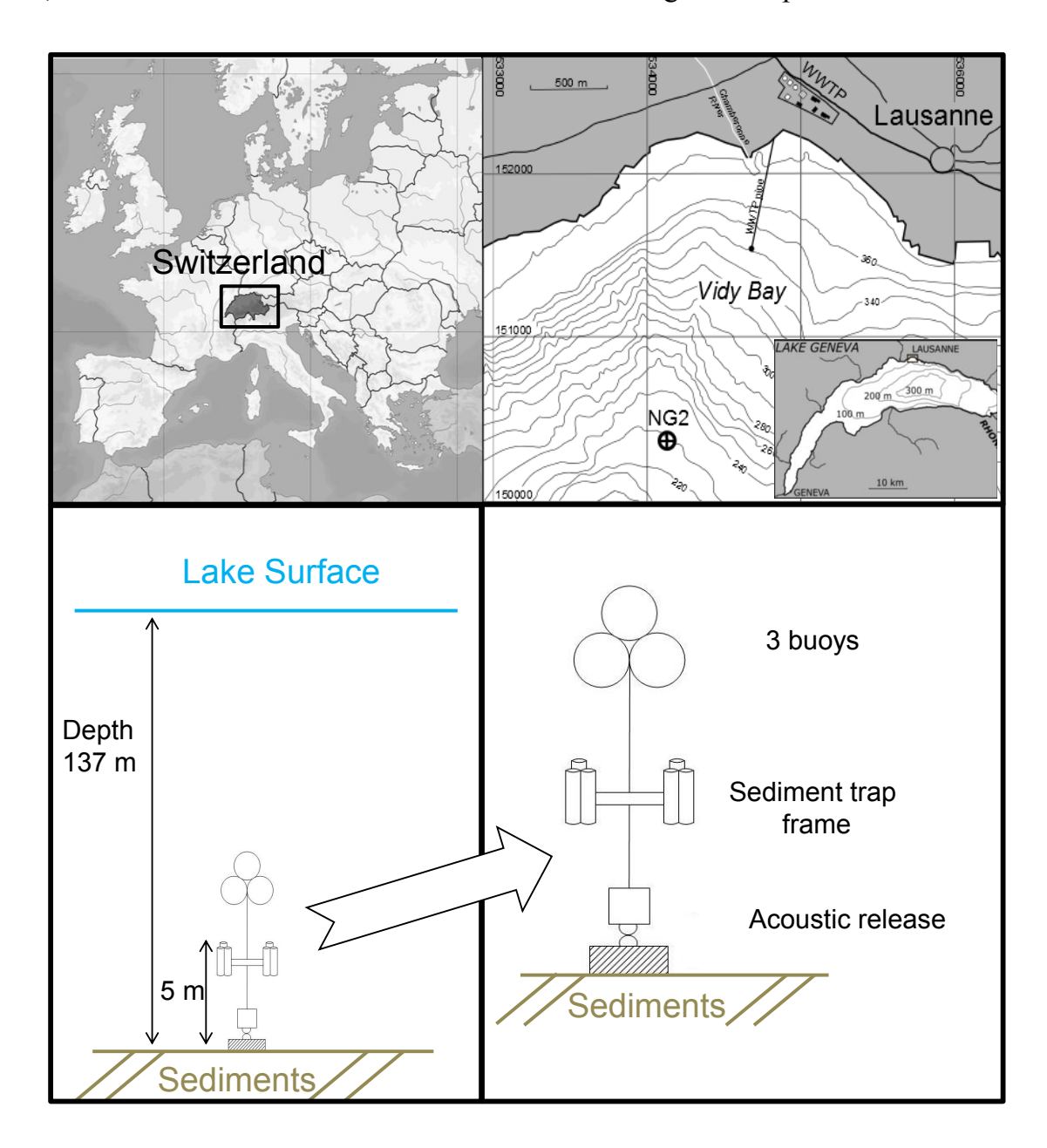


Figure S1. Top: Sampling site location (NG2) in a topographic map Vidy Bay as related to Switzerland and Lake Geneva. Bottom: scheme of the sampling set up and sampling device designed to collect settling particles.

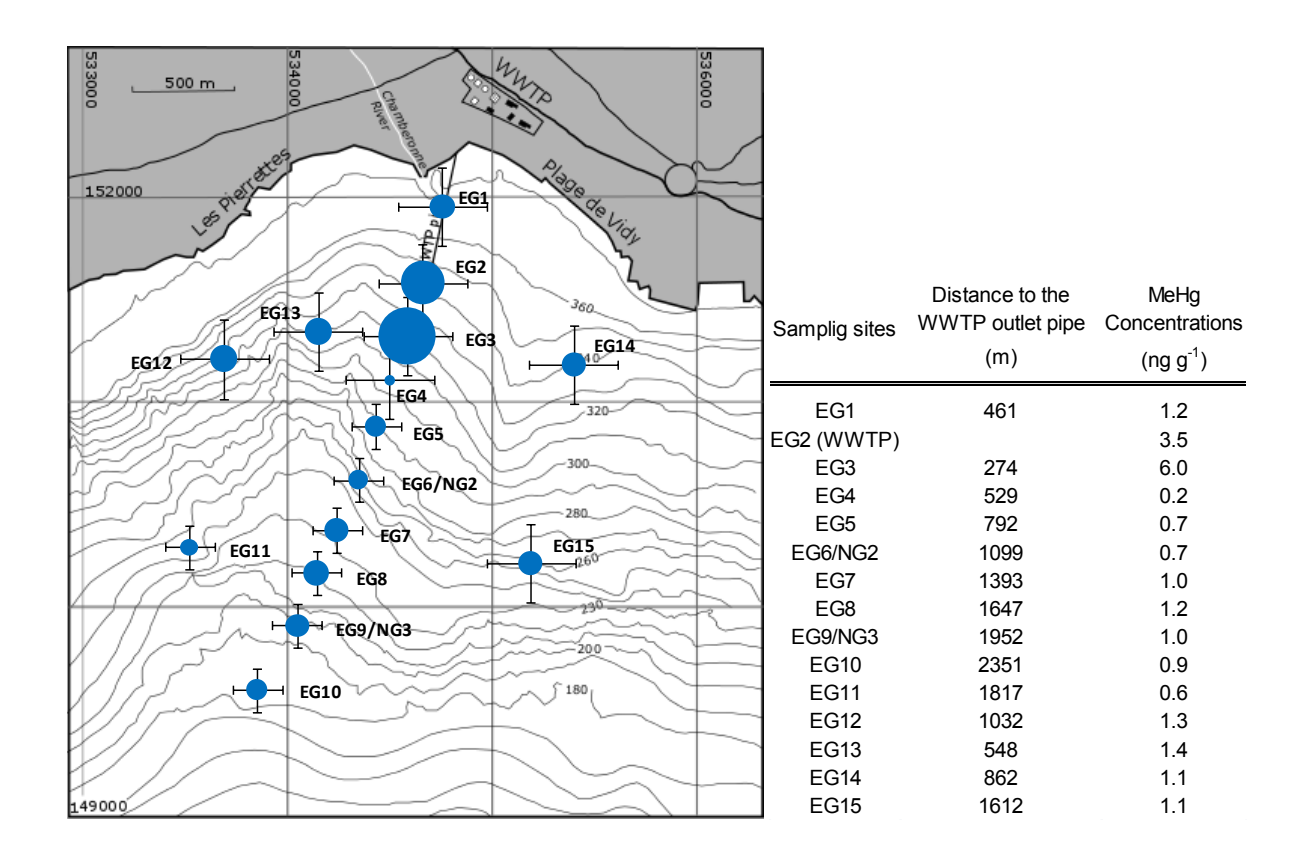


Figure S2. Location map of the study area and sample sites (EG and NG). EG2 represents the point of outlet pipe of sewage treatment plant discharge in the bay and EG6 (NG2) the site where sediment samples were collected and sediment traps deployed. The size of the circles is proportional to the MeHg concentration. Distance to the outlet pipe and MeHg concentrations in sediments are presented in on the right.

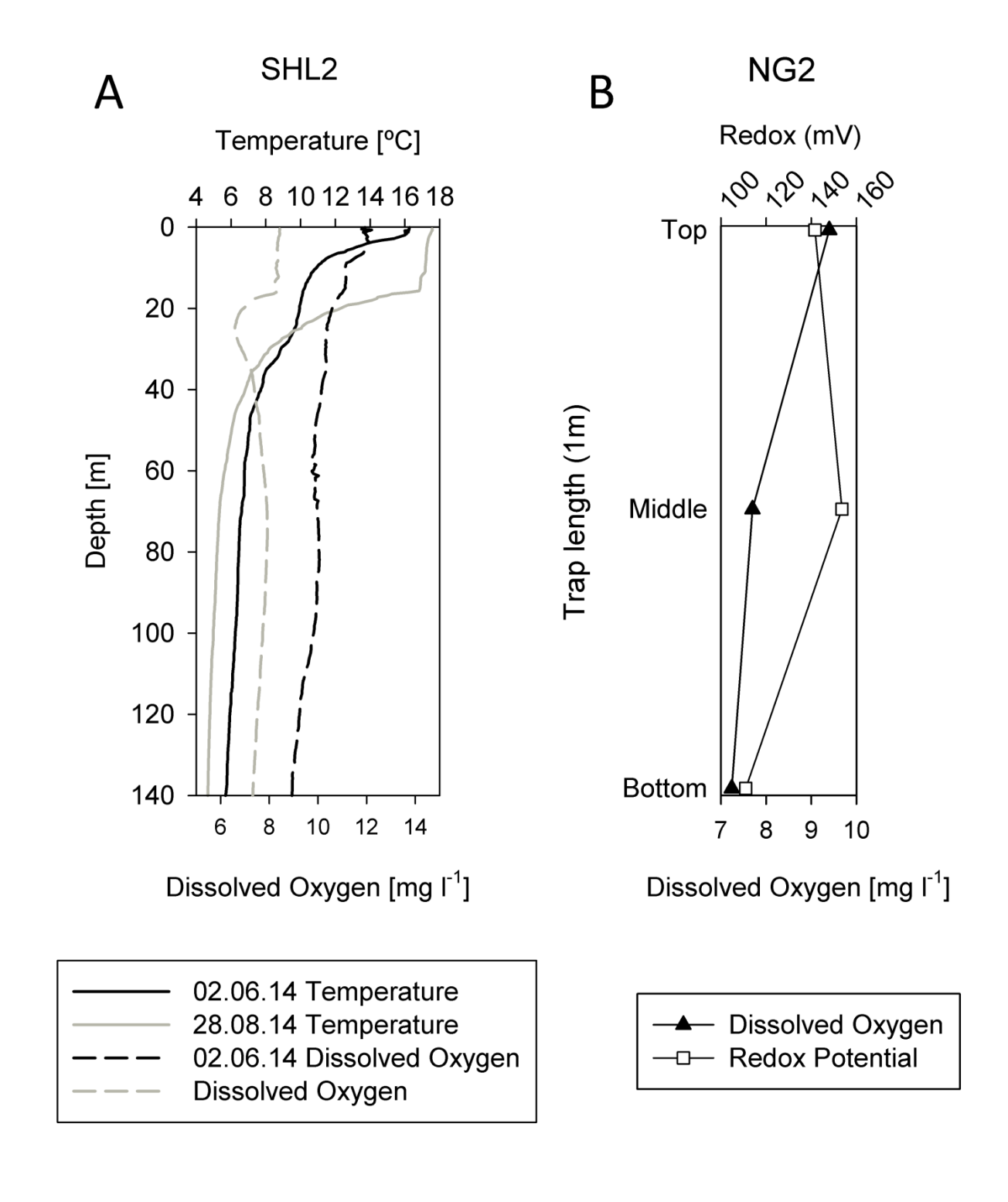


Figure S3. A: Dissolved oxygen and temperature profiles measured in June and August at the center of Lake Geneva (data from CIPEL/INRA). B: Redox and dissolved oxygen measured at three different depths in the sampling traps at NG2, 132 m.

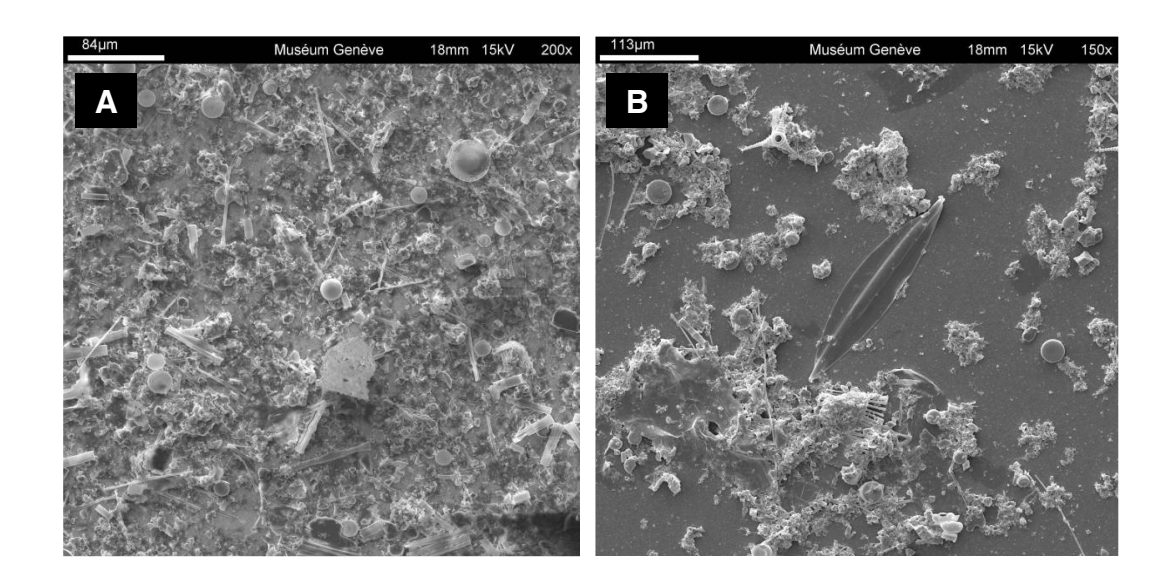
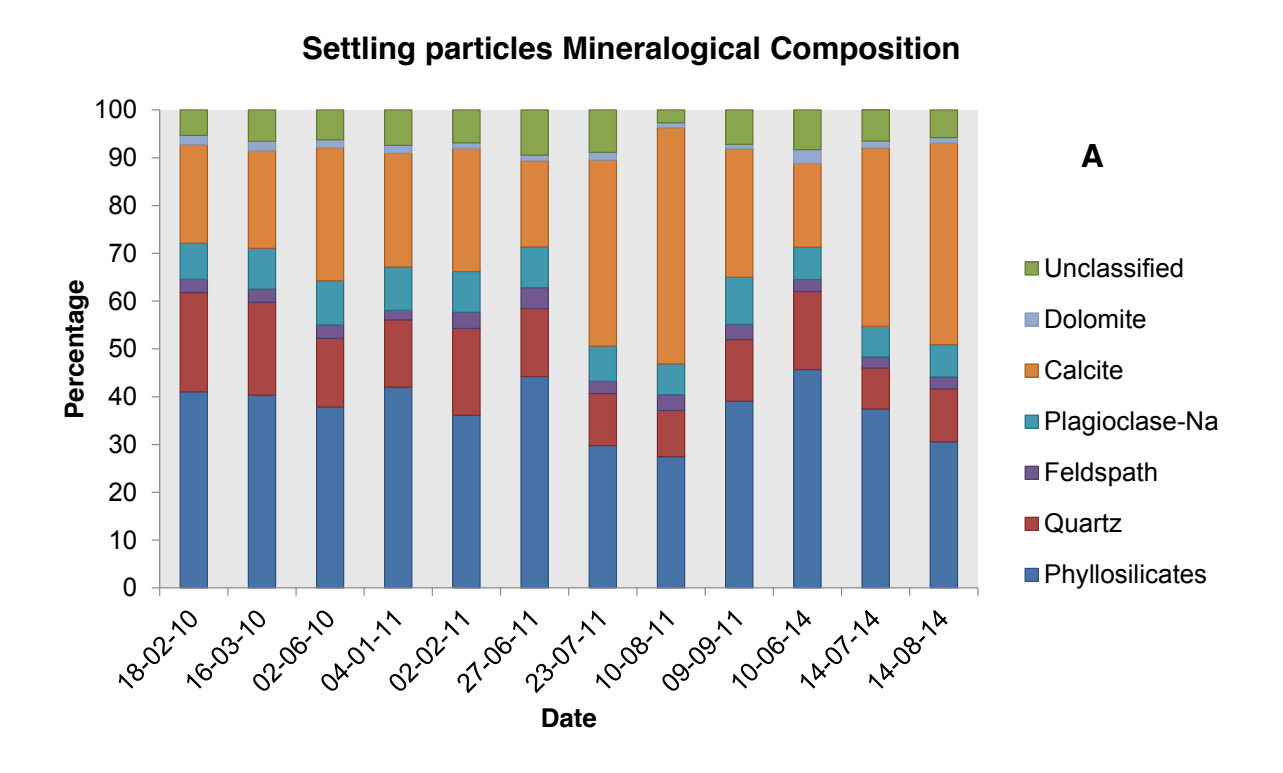
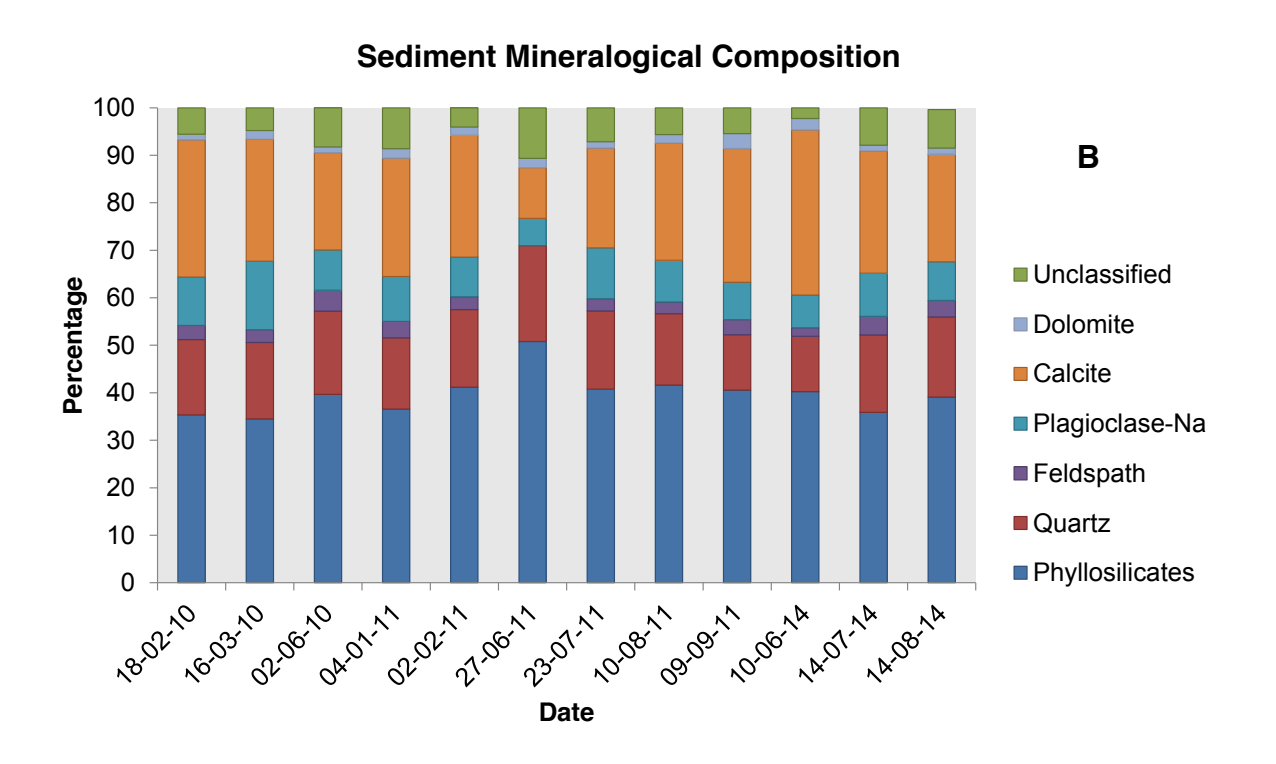


Figure S4. A: May-June: The predominance of diatom frustules as autochtonous component is well visible. Close to the centre, a testate, agglutinated thecamoeba. B: June-July 2014, Organo-mineral flocs (packed by organic mucilage, lower left). Various diatoms (centric, Fragilaria sp.). Staurastrum sp. (Chlorophyta, "tripod"-shaped, upper center).

Imaging was performed with a Jeol® JSM 7001F Scanning Electron Microscope (Jeol Ltd., Tokyo, Japan) with an acceleration voltage of 15 kV following the method described by Jaquet, et al.⁷⁶. Elemental semi-quantitative analyses were done with a JED2300 EDS detector. Brifiely, a dilute suspension of trap sediment was filtered on Millipore® polycarbonate (PC GTTP; 0.2 µm) for SEM+EDS. Filters were air-dried, and no fixation was applied on this first set of samples. Sub-samples of loaded filters were mounted on a conductive support (aluminum stub) with double-sided conductive carbon tape. A coating of gold (ca. 15 nm) or carbon (ca 15 nm) was then deposited on the samples by low vacuum sputter coating prior to imaging.





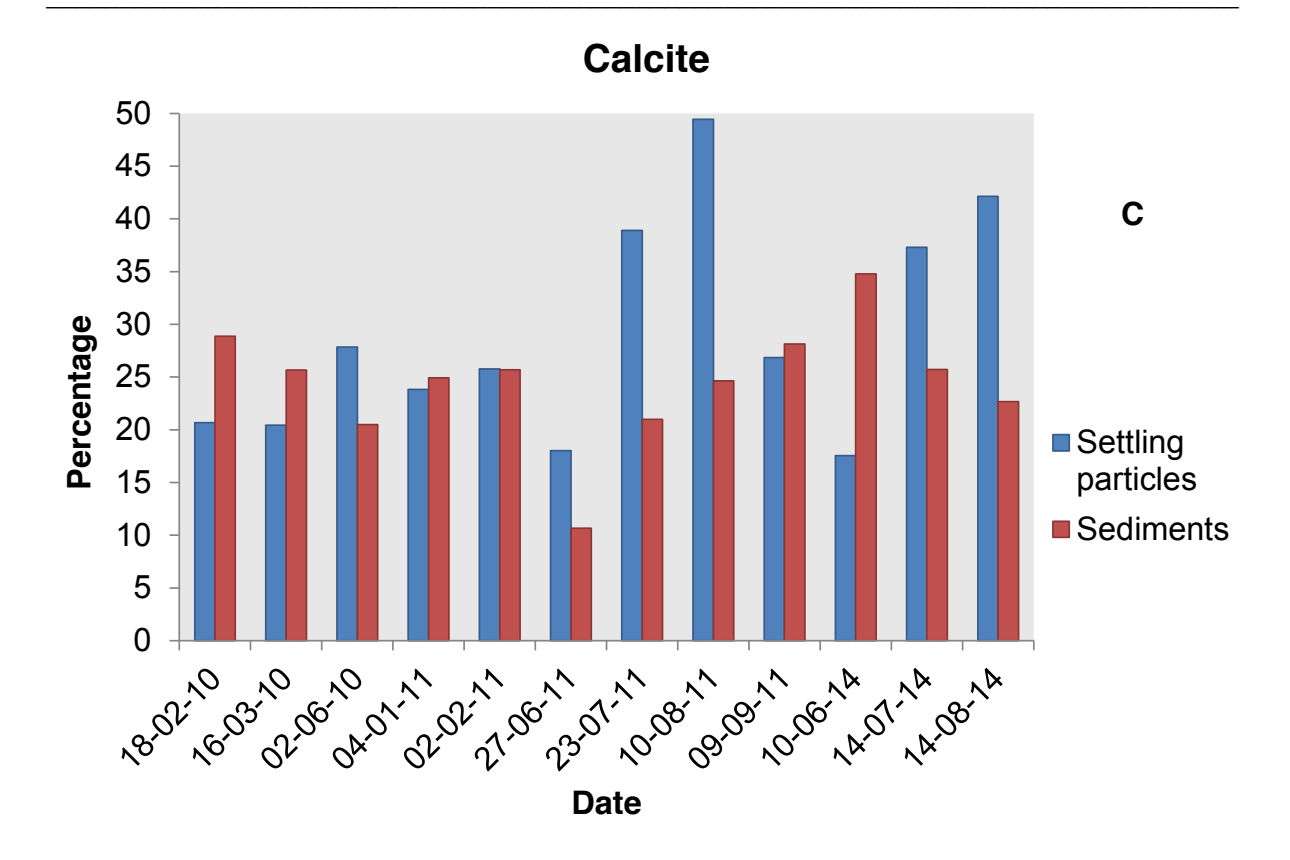


Figure S5. Mineralogical composition of A) settling particles B) sediments and C) percentage of calcite in settling particles (blue) and sediments (red) over time. Briefly, the Vidy Bay mineralogical compositions was dominated by phyllosilicates (mv: 39%, std dev: 3.7%), quartz (mv:18%, std dev: 3.6%), calcite (mv: 23%, std dev: 3.42%) and plagioclase (mv: 9%, std dev: 3.10%). K-Felspaths and dolomite are minor components with mvs of 2.7% and 1.7%, respectively. The non-quantified portion corresponds to poorly crystallized material (iron hydroxydes and sulfides, clay minerals and colloidal material (mv: 6.5%, std dev: 1.65). Calcite was however higher in settling particles than sediments.

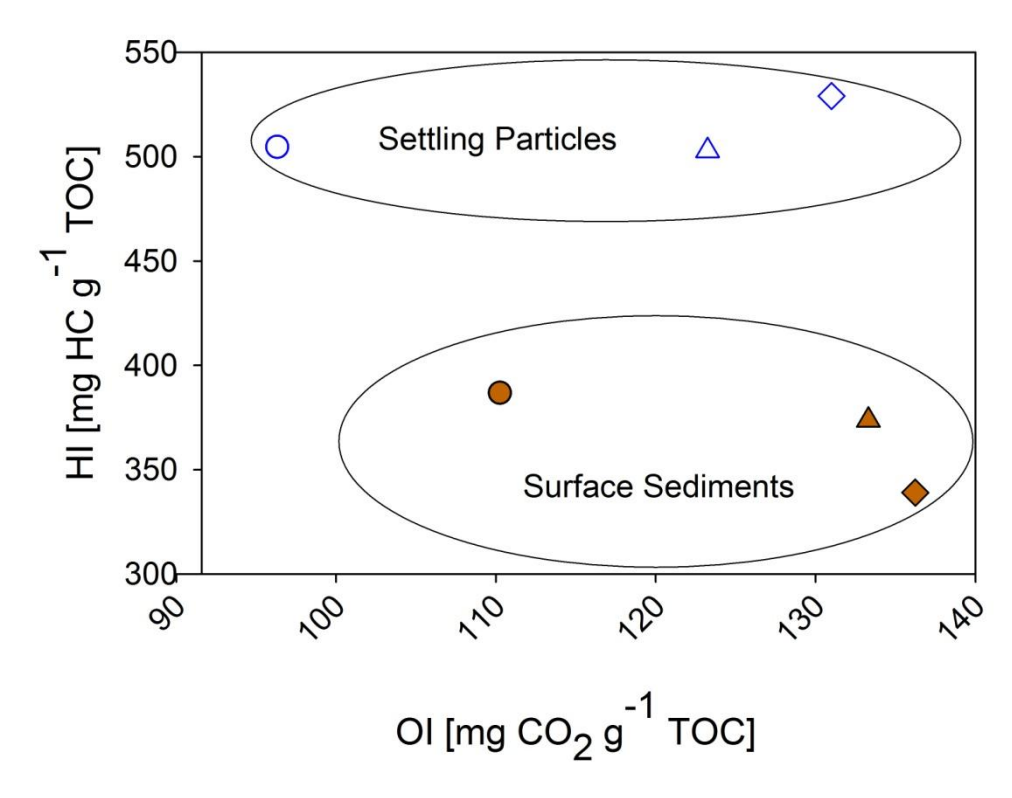


Figure S6. Hydrogen index (HI) versus oxygen index (OI) measurements in the samples used for the determination of Hg methylation and demethylation rate constants. White symbols represent settling particles and black symbols sediment samples. Circles correspond to samples of May-June; triangles to samples of June-July; and squares to samples of July-August.

Table S1. Correlation matrix between the different mineralogical components of Vidy Bay sediments and settling particles.

Pearson Correlation	Phyllosilicates	Quartz	Feldspath-K	Plagioclase-Na	Calcite	Dolomite
Phyllosilicates	1					
Quartz	0.53**	1				
Feldspath-K	-0.36	-0.06	1			
Plagioclase-Na	-0.14	0.22	0.29	1		
Calcite	-0.85**	-0.81**	0.09	-0.21	1	
Dolomite	0.43*	0.05	-0.36	-0.17	-0.24	1

^{**.} Correlation is significant at the 0.01 level (2-tailed).

^{*.} Correlation is significant at the 0.05 level (2-tailed).

References

- 1 AMAP/UNEP. Technical Background Report for the Global Mercury Assessment 2013. (Arctic Monitoringand Assessment Programme, Oslo, Norway/UNEP ChemicalsBranch, Geneva, Switzerland., 2013).
- Mason, R. P. et al. Mercury biogeochemical cycling in the ocean and policy implications. Environ Res 119, 101-117, doi:10.1016/j.envres.2012.03.013 (2012).
- Eckley, C. S. & Hintelmann, H. Determination of mercury methylation potentials in the water column of lakes across Canada. Sci Total Environ 368, 111-125, doi:10.1016/j.scitotenv.2005.09.042 (2006).
- Compeau, G. & Bartha, R. Methylation and Demethylation of Mercury under Controlled Redox, Ph, and Salinity Conditions. Appl Environ Microb 48, 1203-1207 (1984).
- Korthals, E. T. & Winfrey, M. R. Seasonal and Spatial Variations in Mercury Methylation and Demethylation in an Oligotrophic Lake. Appl Environ Microb 53, 2397-2404 (1987).
- Pak, K. R. & Bartha, R. Mercury methylation and demethylation in anoxic lake sediments and by strictly anaerobic bacteria. Appl Environ Microb 64, 1013-1017 (1998).
- Parks, J. M. et al. The Genetic Basis for Bacterial Mercury Methylation. Science 339, 1332-1335, doi:10.1126/science.1230667 (2013).
- 8 Gilmour, C. C. et al. Mercury Methylation by Novel Microorganisms from New Environments. Environ Sci Technol 47, 11810-11820, doi:10.1021/es403075t (2013).
- 9 Ullrich, S. M., Tanton, T. W. & Abdrashitova, S. A. Mercury in the aquatic environment: A review of factors affecting methylation. Crit Rev Env Sci Tec 31, 241-293, doi:Doi 10.1080/20016491089226 (2001).
- Mason, R. P. & Fitzgerald, W. F. Alkylmercury Species in the Equatorial Pacific. Nature 347, 457-459, doi:Doi 10.1038/347457a0 (1990).
- Malcolm, E. G. et al. Mercury methylation in oxygen deficient zones of the oceans: No evidence for the predominance of anaerobes. Mar Chem 122, 11-19, doi:10.1016/j.marchem.2010.08.004 (2010).
- Cossa, D., Averty, B. & Pirrone, N. The origin of methylmercury in open Mediterranean waters. Limnol Oceanogr 54, 837-844, doi:DOI 10.4319/lo.2009.54.3.0837 (2009).
- Sunderland, E. M., Krabbenhoft, D. P., Moreau, J. W., Strode, S. A. & Landing, W. M. Mercury sources, distribution, and bioavailability in the North Pacific Ocean: Insights from data and models. Global Biogeochem Cy 23, doi:Artn Gb2010 10.1029/2008gb003425 (2009).
- Heimburger, L. E. et al. Methyl mercury distributions in relation to the presence of nano- and picophytoplankton in an oceanic water column (Ligurian Sea, Northwestern Mediterranean). Geochim Cosmochim Ac 74, 5549-5559, doi:10.1016/j.gca.2010.06.036 (2010).
- Lehnherr, I., St Louis, V. L., Hintelmann, H. & Kirk, J. L. Methylation of inorganic mercury in polar marine waters. Nat Geosci 4, 298-302, doi:10.1038/NGEO1134 (2011).
- Monperrus, M. et al. Mercury methylation, demethylation and reduction rates in coastal and marine surface waters of the Mediterranean Sea. Mar Chem 107, 49-63, doi:10.1016/j.marchem.2007.01.018 (2007).

- Sharif, A. et al. Fate of mercury species in the coastal plume of the Adour River estuary (Bay of Biscay, SW France). Sci Total Environ 496, 701-713, doi:10.1016/j.scitotenv.2014.06.116 (2014).
- Bouchet, S. et al. MMHg production and export from intertidal sediments to the water column of a tidal lagoon (Arcachon Bay, France). Biogeochemistry 114, 341-358, doi:10.1007/s10533-012-9815-z (2013).
- Podar, M. et al. Global prevalence and distribution of genes and microorganisms involved in mercury methylation. Science Advances 1, doi:10.1126/sciadv.1500675 (2015).
- Bravo, A. G. et al. High methylmercury production under ferruginous conditions in sediments impacted by sewage treatment plant discharges. Water Res 80, 245-255, doi:10.1016/j.watres.2015.04.039 (2015).
- Drott, A., Lambertsson, L., Bjorn, E. & Skyllberg, U. Do potential methylation rates reflect accumulated methyl mercury in contaminated sediments? Environ Sci Technol 42, 153-158, doi:10.1021/es0715851 (2008).
- Jonsson, S. et al. Mercury Methylation Rates for Geochemically Relevant Hg-II Species in Sediments. Environ Sci Technol 46, 11653-11659, doi:10.1021/es3015327 (2012).
- Gray, J. E., Hines, M. E., Goldstein, H. L. & Reynolds, R. L. Mercury deposition and methylmercury formation in Narraguinnep Reservoir, southwestern Colorado, USA. Appl Geochem 50, 82-90, doi:10.1016/j.apgeochem.2014.09.001 (2014).
- Fleming, E. J., Mack, E. E., Green, P. G. & Nelson, D. C. Mercury methylation from unexpected sources: Molybdate-inhibited freshwater sediments and an iron-reducing bacterium. Appl Environ Microb 72, 457-464, doi:10.1128/Aem.72.1.457-464.2006 (2006).
- Cleckner, L. B., Gilmour, C. C., Hurley, J. P. & Krabbenhoft, D. P. Mercury methylation in periphyton of the Florida Everglades. Limnol Oceanogr 44, 1815-1825, doi:10.4319/lo.1999.44.7.1815 (1999).
- Guimaraes, J. R. D., Roulet, M., Lucotte, M. & Mergler, D. Mercury methylation along a lake-forest transect in the Tapajos river floodplain, Brazilian Amazon: seasonal and vertical variations. Sci Total Environ 261, 91-98, doi:Doi 10.1016/S0048-9697(00)00627-6 (2000).
- Mauro, J. B. N. et al. Mercury methylation in macrophytes, periphyton, and water comparative studies with stable and radio-mercury additions. Anal Bioanal Chem 374, 983-989, doi:10.1007/s00216-002-1534-1 (2002).
- Guimaraes, J. R. D. et al. Simultaneous radioassays of bacterial production and mercury methylation in the periphyton of a tropical and a temperate wetland. J Environ Manage 81, 95-100, doi:10.1016/j.jenvman.2005.09.023 (2006).
- Desrosiers, M., Planas, D. & Mucci, A. Mercury Methylation in the Epilithon of Boreal Shield Aquatic Ecosystems. Environ Sci Technol 40, 1540-1546, doi:10.1021/es0508828 (2006).
- Achá, D., Hintelmann, H. & Yee, J. Importance of sulfate reducing bacteria in mercury methylation and demethylation in periphyton from Bolivian Amazon region. Chemosphere 82, 911-916, doi:http://dx.doi.org/10.1016/j.chemosphere.2010.10.050 (2011).
- Eckley, C. S. et al. Mercury methylation in the hypolimnetic waters of lakes with and without connection to wetlands in northern Wisconsin. Can J Fish Aquat Sci 62, 400-411, doi:10.1139/F04-205 (2005).

- Chiasson-Gould, S. A., Blais, J. M. & Poulain, A. J. Dissolved Organic Matter Kinetically Controls Mercury Bioavailability to Bacteria. Environ Sci Technol 48, 3153-3161, doi:10.1021/es4038484 (2014).
- French, T. D. et al. Dissolved Organic Carbon Thresholds Affect Mercury Bioaccumulation in Arctic Lakes. Environ Sci Technol 48, 3162-3168, doi:10.1021/es403849d (2014).
- Harris, R. C. et al. Whole-ecosystem study shows rapid fish-mercury response to changes in mercury deposition. P Natl Acad Sci USA 104, 16586-16591, doi:10.1073/pnas.0704186104 (2007).
- Perrot, V. et al. Higher Mass-Independent Isotope Fractionation of Methylmercury in the Pelagic Food Web of Lake Baikal (Russia). Environ Sci Technol 46, 5902-5911, doi:10.1021/es204572g (2012).
- Watras, C. J., Morrison, K. A., Host, J. S. & Bloom, N. S. Concentration of Mercury Species in Relationship to Other Site-Specific Factors in the Surface Waters of Northern Wisconsin Lakes. Limnol Oceanogr 40, 556-565 (1995).
- Bae, H. S., Dierberg, F. E. & Ogram, A. Syntrophs Dominate Sequences Associated with the Mercury Methylation-Related Gene hgcA in the Water Conservation Areas of the Florida Everglades. Appl Environ Microb 80, 6517-6526, doi:10.1128/Aem.01666-14 (2014).
- Loizeau, J. L. & Dominik, J. The history of eutrophication and restoration of Lake Geneva. Terre et Environnement 50, 43–56 (2005).
- Graham, N. The fate of sediment-bound contaminants: a case study of Vidy Bay (Lake Geneva, Switzerland). Ph.D. Thesis, no. 4760, Universite de Geneve (2015).
- Haller, L., Amedegnato, E., Pote, J. & Wildi, W. Influence of Freshwater Sediment Characteristics on Persistence of Fecal Indicator Bacteria. Water Air Soil Poll 203, 217-227, doi:10.1007/s11270-009-0005-0 (2009).
- Loizeau, J. L., Roze, S., Peytremann, C., Monna, F. & Dominik, J. Mapping sediment accumulation rate by using volume magnetic susceptibility core correlation in a contaminated bay (Lake Geneva, Switzerland). Eclogae Geol Helv 96, S73-S79 (2003).
- Pote, J. et al. Origin and spatial-temporal distribution of faecal bacteria in a bay of Lake Geneva, Switzerland. Environ Monit Assess 154, 337-348, doi:10.1007/s10661-008-0401-8 (2009).
- Gascon Diez, E. et al. Influence of a wastewater treatment plant on mercury contamination and sediment characteristics in Vidy Bay (Lake Geneva, Switzerland). Aquat Sci 76, S21-S32, doi:DOI 10.1007/s00027-013-0325-4 (2014).
- Bloesch, J. Towards a new generation of sediment traps and a better measurement/understanding of settling particle flux in lakes and oceans: A hydrodynamical protocol. Aquat Sci 58, 283-296, doi:10.1007/bf00877472 (1996).
- Savoye, L. & Quentin, P. K., A. Physico-chemical changes in the waters of Lake Geneva, meteorological datas, contributions from the tributaries of Lake Geneva and from the Rhone below Geneva. Rapp. Comm. int. prot. eaux Léman contre pollut. Campagne 2014, 2015, 19 67 (2015).
- Szakova, I., Kolihova, D., Miholova, D. & Mader, P. Single-purpose atomic absorption spectrometer AMA-254 for mercury determination and its performance in analysis of agricultural and environmental materials. Chem Pap-Chem Zvesti 58, 311-315 (2004).
- Liu, B. et al. Insights into low fish mercury bioaccumulation in a mercury-contaminated reservoir, Guizhou, China. Environ Pollut 160, 109-117, doi:DOI 10.1016/j.envpol.2011.09.023 (2012).

- Bloom, N. Determination of Picogram Levels of Methylmercury by Aqueous Phase Ethylation, Followed by Cryogenic Gas-Chromatography with Cold Vapor Atomic Fluorescence Detection. Can J Fish Aquat Sci 46, 1131-1140, doi:Doi 10.1139/F89-147 (1989).
- Cossa, D., Coquery, M., Nakhle, K. & Claisse, D. Total mercury and monomethylmercury analysis in marine organisms and sediments. Analysis Methods in Marine Environment (2002).
- Rodriguez-Gonzalez, P., Bouchet, S., Monperrus, M., Tessier, E. & Amouroux, D. In situ experiments for element species-specific environmental reactivity of tin and mercury compounds using isotopic tracers and multiple linear regression. Environ Sci Pollut R 20, 1269-1280, doi:DOI 10.1007/s11356-012-1019-5 (2013).
- Espitalie, J., Deroo, G. & Marquis, F. Rock-Eval Pyrolysis and Its Applications. Rev I Fr Petrol 40, 563-579 (1985).
- Espitalie, J., Deroo, G. & Marquis, F. Rock-Eval Pyrolysis and Its Applications .3. Rev I Fr Petrol 41, 73-89 (1986).
- Klug, H. P. & Alexander, L. E. X-ray diffraction procedures for polycrystalline and amorphous materials. Harold P. Klug and Leroy E. Alexander. X-Ray Spectrometry 4, 960, doi:10.1002/xrs.1300040415 (1975).
- Adatte, T., Stinnesbeck, W. & Keller, G. Lithostratigraphic and mineralogic correlations of near K/T boundary clastic sediments in northeastern Mexico: Implications for origin and nature of deposition Geological Society of America Special Papers, 211-226 (1996).
- Balcom, P. H., Schartup, A. T., Mason, R. P. & Chen, C. Y. Sources of water column methylmercury across multiple estuaries in the Northeast U.S. Mar Chem, doi:http://dx.doi.org/10.1016/j.marchem.2015.10.012.
- Dominik, J., Schuler, C. & Santschi, P. H. Residence Times of Th-234 and Be-7 in Lake Geneva. Earth Planet Sc Lett 93, 345-358, doi:Doi 10.1016/0012-821x(89)90034-4 (1989).
- Pote, J. et al. Effects of a sewage treatment plant outlet pipe extension on the distribution of contaminants in the sediments of the Bay of Vidy, Lake Geneva, Switzerland. Bioresource Technol 99, 7122-7131, doi:10.1016/j.biortech.2007.12.075 (2008).
- Bravo, A. G., Bouchet, S., Amouroux, D., Pote, J. & Dominik, J. Distribution of mercury and organic matter in particle-size classes in sediments contaminated by a waste water treatment plant: Vidy Bay, Lake Geneva, Switzerland. J Environ Monitor 13, 974-982, doi:10.1039/c0em00534g (2011).
- Tjerngren, I., Karlsson, T., Bjorn, E. & Skyllberg, U. Potential Hg methylation and MeHg demethylation rates related to the nutrient status of different boreal wetlands. Biogeochemistry 108, 335-350, doi:10.1007/s10533-011-9603-1 (2012).
- Hodell, D. A., Schelske, C. L., Fahnenstiel, G. L. & Robbins, L. L. Biologically induced calcite and its isotopic composition in Lake Ontario. Limnol Oceanogr 43, 187-199 (1998).
- Dittrich, M. & Obst, M. Are picoplankton responsible for calcite precipitation in lakes? Ambio 33, 559-564 (2004)
- Tyson, R. V. in Sedimentary Organic Matter (ed Springer) Ch. 22, 384-394 (Chapman & Hall, 1995).
- Ariztegui, D., Chondrogianni, C., Lami, A., Guilizzoni, P. & Lafargue, E. Lacustrine organic matter and the Holocene paleoenvironmental record of Lake Albano (central Italy). J Paleolimnol 26, 283-292, doi:Doi 10.1023/A:1017585808433 (2001).

- Steinmann, P., Adatte, T. & Lambert, P. Recent changes in sedimentary organic matter from Lake Neuchatel (Switzerland) as traced by Rock-Eval pyrolysis. Eclogae Geol Helv 96, S109-S116 (2003).
- Jaccard, T., Ariztegui, D. & Wilkinson, K. J. Assessing past changes in bioavailable zinc from a terrestrial (Zn/Si)(opal) record. Chem Geol 258, 362-367, doi:DOI 10.1016/j.chemgeo.2008.10.037 (2009).
- Schartup, A. T., Ndu, U., Balcom, P. H., Mason, R. P. & Sunderland, E. M. Contrasting Effects of Marine and Terrestrially Derived Dissolved Organic Matter on Mercury Speciation and Bioavailability in Seawater. Environ Sci Technol 49, 5965-5972, doi:10.1021/es506274x (2015).
- 67 Leclerc, M., Planas, D. & Amyot, M. Relationship between Extracellular Low-Molecular-Weight Thiols and Mercury Species in Natural Lake Periphytic Biofilms. Environ Sci Technol 49, 7709-7716, doi:10.1021/es505952x (2015).
- Zhang, T. et al. Methylation of Mercury by Bacteria Exposed to Dissolved, Nanoparticulate, and Microparticulate Mercuric Sulfides. Environ Sci Technol 46, 6950-6958, doi:10.1021/es203181m (2012).
- 69 Alldredge, A. L. & Cohen, Y. Can Microscale Chemical Patches Persist in the Sea Microelectrode Study of Marine Snow, Fecal Pellets. Science 235, 689-691, doi:DOI 10.1126/science.235.4789.689 (1987).
- Ploug, H. Cyanobacterial surface blooms formed by Aphanizomenon sp and Nodularia spumigena in the Baltic Sea: Small-scale fluxes, pH, and oxygen microenvironments. Limnol Oceanogr 53, 914-921, doi:DOI 10.4319/lo.2008.53.3.0914 (2008).
- Klawonn, I., Bonaglia, S., Bruchert, V. & Ploug, H. Aerobic and anaerobic nitrogen transformation processes in N-2-fixing cyanobacterial aggregates. Isme J 9, 1456-1466, doi:10.1038/ismej.2014.232 (2015).
- Karl, D. M., Knauer, G. A., Martin, J. H. & Ward, B. B. Bacterial Chemolithotrophy in the Ocean Is Associated with Sinking Particles. Nature 309, 54-56, doi:Doi 10.1038/309054a0 (1984).
- Woebken, D., Fuchs, B. M., Kuypers, M. M. M. & Amann, R. Potential interactions of particle-associated anammox bacteria with bacterial and archaeal partners in the Namibian upwelling system. Appl Environ Microb 73, 4648-4657, doi:10.1128/Aem.02774-06 (2007).
- Shanks, A. L. & Reeder, M. L. Reducing Microzones and Sulfide Production in Marine Snow. Mar Ecol Prog Ser 96, 43-47, doi:Doi 10.3354/Meps096043 (1993).
- Verpoorter, C., Kutser, T., Seekell, D. A. & Tranvik, L. J. A global inventory of lakes based on high-resolution satellite imagery. Geophys Res Lett 41, 6396-6402, doi:10.1002/2014GL060641 (2014).
- Jaquet, J. M., Nirel, P. & Martignier, A. Preliminary investigations on picoplanktonrelated precipitation of alkaline-earth metal carbonates in mesooligotrophic lake Geneva (Switzerland). J Limnol 72, 592-605, doi:10.4081/jlimnol.2013.e50 (2013).

CHAPTER VI

Discussion and Conclusions

1. General discussion

The main issue addressed in this study was the understanding of the fate of particle-bound contaminants in large lakes, from the shore to the deep lake, using mercury species as tracers of contamination. Vidy Bay, Lake Geneva, was used as case study.

This thesis covers different aspects concerning the accumulation of contaminants, primarily in lake sediments and settling particles. It general goal was to define the fate of pollutants rejected in a contaminated freshwater basin by a domestic-industrial waste water treatment plant (WWTP). Heavy metals, newly called toxic trace metals, and in particular mercury, have been the subject of this study. As there are not many investigations evidencing the impact of WWTP effluents and their fate in lake sediments and particles, the findings of this work could be used to predict their behaviour in future cases of contamination under similar conditions and/or environments.

1.1. Historical and current THg accumulation and fate in sediments and settling particles

It is widely known that sediments act as natural archives of contamination, and sediments of Vidy Bay provide a good example. A sediment core retrieved between the old and the new outlet pipes of Vidy Bay enclosed sediments as old as ca. 1915 AD. The high resolution analyses carried on showed an increase of Pb, Cd, Cu, Zn and Hg even before the implementation of the WWTP, coinciding with the beginning of the global industrialization. With the commissioning of the WWTP, in addition to these five elements, the concentration and enrichment factors of other elements such as Ag and Bi drastically increased. Fe, or even other non-metallic elements such as phosphorus and sulphur, usually considered as detrital, in this area were contained in the effluent of the WWTP. These last elements, either due to a direct pollution because of their use in certain depuration treatments (FeCl₃ to precipitate P), or to their relation to the released organic matter (the case of S) were considered as anthropogenic elements or trace metals.

The concentration of the majority of trace metals dropped in the early 1980's probably due to a combination of a raising awareness on the toxic effects of excessive use of toxic trace metals on a daily basis; and the improvements in the efficiency of the waste water treatment. Nevertheless, Hg showed a peak of concentration in 1986 with a maximum of 11 µg g⁻¹. This high value decreased in the following years, and with the displacement of the outlet pipe of WWTP in 2001, concentrations continued to decrease, tending nowadays to pre-industrial values, meaning that on this site, sediments were not anymore affected by the effluent (Chapter II). However, some of the studied toxic trace metals were still in high concentrations in recent sediments of Vidy Bay affected by the second location of the outlet pipe (Masson and Tercier-Waeber, 2014). In particular, mercury, in most of the sediment cores retrieved in the surroundings of the WWTP, reached (in some sampling sites) 4 and 10 µg g⁻¹ (Chapter III), which is 330 times higher than the 0.03 µg g⁻¹ of the natural background of Lake Geneva sediments (Vernet and Viel, 1984), and exceeded the probable effect concentration (PEC) value. PEC is a sediment quality guideline established at 1.06 µg g⁻¹, above which adverse effects in sediments are expected to frequently occur (MacDonald et al., 2000). In addition, based on the color, texture and structure, the area of surface sediments affected by the sewage water and/or sludge was approximately 1km². This area was classified on 6 different types of sediment (Chapter III), and THg concentrations were measured in each type. No correlations were found between the sediment types and THg concentration. In turn, a correlation was found between THg concentration in the bay and the distance to the WWTP outlet pipe. THg concentration in surface sediments at the reference site of Lake Geneva (SHL2, Fig. 1) is 0.17 µg g⁻¹, considering this value as the current background concentration of the lake, the area considered as contaminated by the WWTP (over ~0.2 µg g⁻¹) was about 3 km². In addition, the THg partition coefficient ($\log K_d$) in Vidy Bay varied from 3.6 to 5.8 l kg⁻¹, which values were similar to those found in other lakes considered as Hg-contaminated. As $\log K_d$ represents the ratio between the THg concentrations in sediments and THg concentrations in the porewater, high values of $log K_d$ suggested diffusion of THg from the sediment to the pore water. On the other hand, overlying water contained between 4 and 40 times more THg when

non-filtered compared to filtered. These results, in Chapter III, provided a first approach of the fate of THg in sediments and suspended particles.

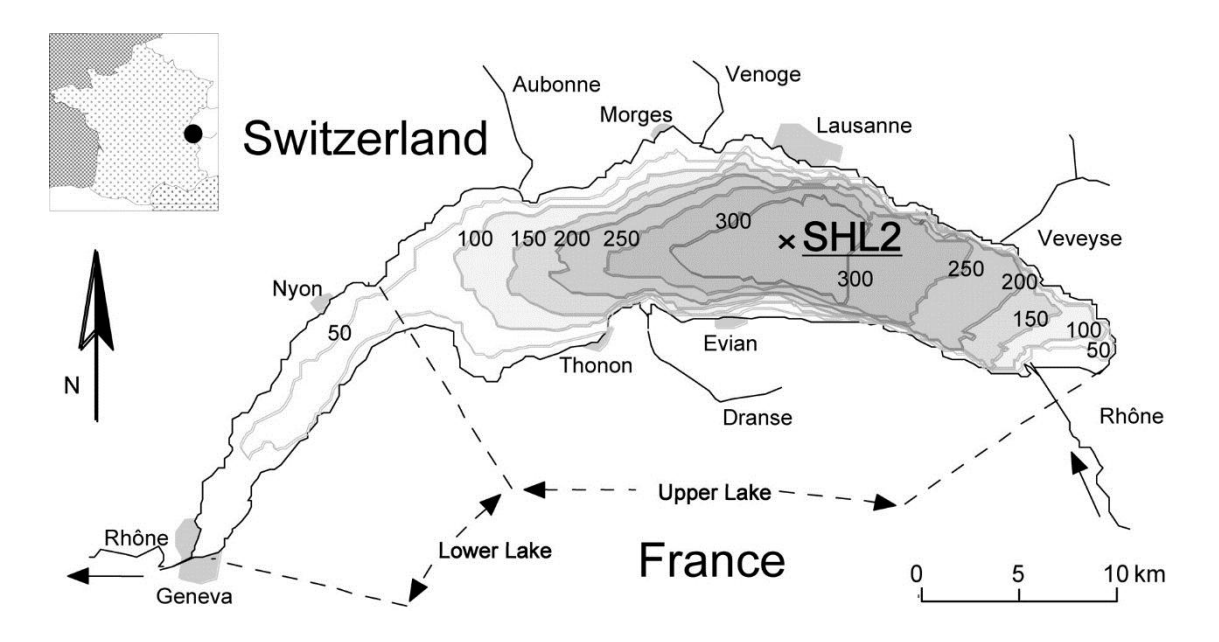


Figure 1. Location of the reference site, SHL2, in a bathymetric map of Lake Geneva.

Source: Anneville et al. (2006).

To better understand the processes between the surface sediments and the water column, settling particles and surface sediments were collected at two sites in the lake, (i) NG2, at around one kilometer to the south of the contaminated zone, and (ii) NG3, outside Vidy Bay, at around two kilometers to the south. At NG2, concentrations and fluxes were higher and more variable than at NG3. This suggested that NG2 was more influenced by the coast (comprising WWTP inputs) than NG3. However, comparing SAR and OM fluxes at NG2 and NG3 to the SAR previously registered in SHL2, it is suggested that, although NG2 is more affected by littoral inputs, NG3 is still influenced by the shore. Moreover, THg fluxes suggested that THg concentrations in sediments traps were strongly influenced by the seasonal trends on sedimentation rates, including temporal patterns of OM and CaCO₃ sedimentation. Thus, overall the lowest THg concentrations were found in summer, and the highest in winter. In contrast MeHg did not follow the same seasonal trends as THg. Generally, the highest MeHg concentrations were observed in summer and they were not subjected to SAR, OM or CaCO₃ fluxes (Chapter IV).

At both sites, the deposition of THg was higher in the bottom traps than in the top ones, supporting the hypothesis that these sites were influenced by sediment resuspension. On average, NG2 had 30% more THg deposition in the bottom than in the top trap; and at NG3, THg fluxes were on average 50% higher in the bottom trap than in the top one. SAR followed the same trend, which implies that the flux of THg was directly linked to particle transport. The fact that at NG2 the proportion of deposited material in the bottom trap was lower than at NG3 could be related to the morphology of the sediment bed. There was a difference of 50 - 60 m depth between the two bottom traps that could be reflected in data, showing more dragged or resuspended material at NG3 bottom, whereas at NG3 top, settling particles seemed to be more authigenic.

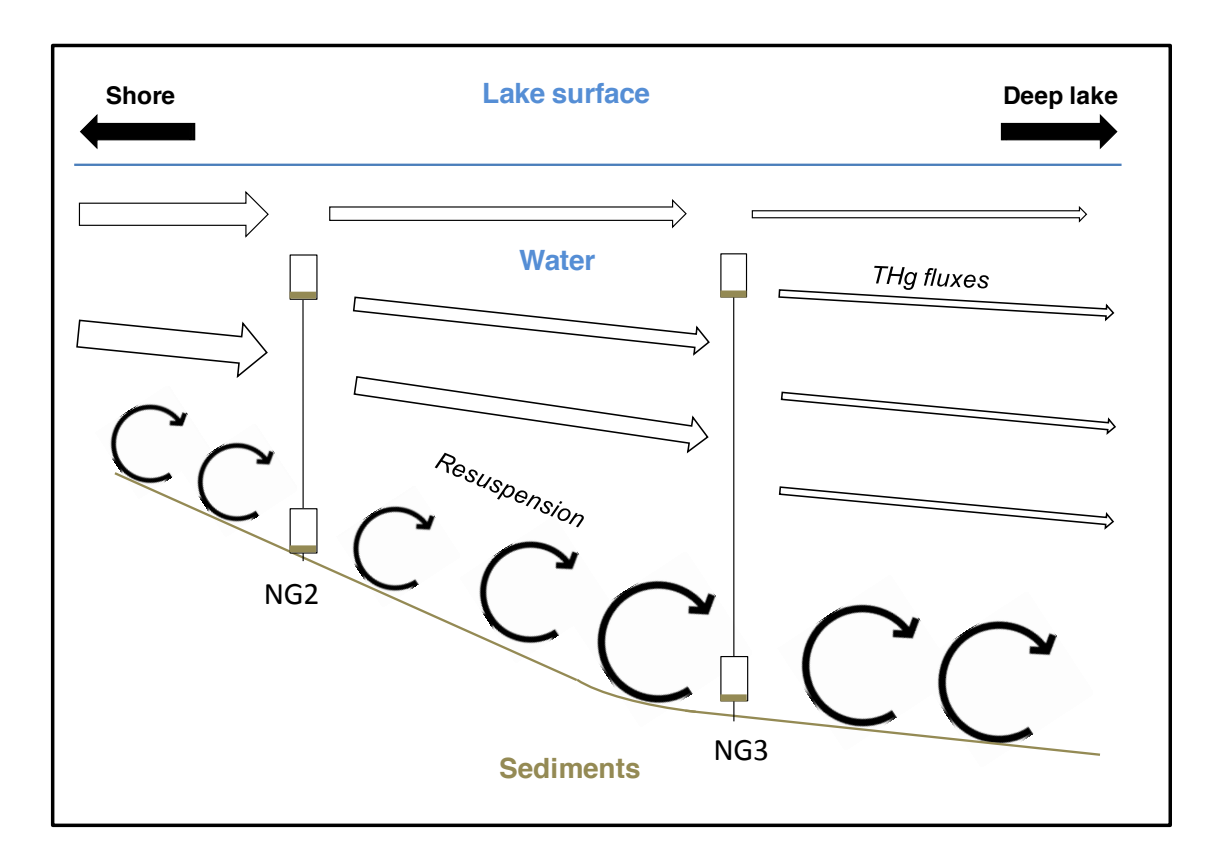


Figure 2. Schema of particle transport from the shore to the deep lake. Size of arrows in the water column symbolize the decrease of the fluxes with the distance shore-deep lake (not to scale).

1.2. MeHg distribution and production in lake compartments

Understanding MeHg behaviour and fate in a freshwater contaminated area was an important part of this work. To do this, several approaches were presented in Chapter III. In such, MeHg was measured in pore waters in the 6 first cm of sediments, founding a MeHg/THg ratio of $0.44 \pm 0.25\%$ in the 0 - 1.5 cm layer that decreases with depth. This approach of methylation process indicated that MeHg primarily occurred in the upper layer (0 - 1.5 cm). On the other hand, in the same sediments, MeHg concentrations were higher in non-filtered overlying waters $(0.14 - 1.7 \text{ ng } 1^{-1})$ than in filtered ones $(0.03 - 0.2 \text{ ng } l^{-1})$, but in any case, exceeding the $0.05 \text{ ng } l^{-1}$ found in the water column in the centre of the lake (Bravo, 2010). These results suggested that particles in the water column were good carriers of MeHg. In order to better understand the role of settling particles in MeHg production and fate, they were collected at NG2 and NG3 during almost two years, similarly to THg discussed above and in Chapter IV. Although MeHg is supposed to be bound to settling particles and organic matter, MeHg concentrations and fluxes, and MeHg/THg ratios measured in settling particles did not show any similarity with THg, OM fluxes and SAR patterns. This pointed to a possible formation of MeHg in these particles that reside in the oxic water column of Lake Geneva. This is a critical question; Hg-methylating microbes have an anaerobic metabolism, and Hg-methylation is known to occur in oxic-suboxic sediments, thus, higher concentrations of MeHg were expected to be found in sediments than in settling particles. In turn, MeHg concentrations in settling particles largely exceeded the concentrations found in sediment, with higher values in summer. Since settling particles are richer in OM during summer time (Graham, 2015), the high content of fresh planktonic OM was supposed to enhance the activity of the heterotrophic bacteria involved in the Hg-methylation processes (Heimburger et al., 2010; Schartup et al., 2015). Results of Chapter V suggested that Hg methylation occurred elsewhere than in sediments, probably within the particles settled in the traps. Recently, other authors worked on filtered and unfiltered lake waters to answer this question, indicating that mercury methylation likely occurred in suspended particles of the hypolimnion (Eckley et al., 2005). Neverthelss, none of them measured potential methylation rates directly in settling particles. This study showed 10-fold potential

methylation rates in settling particles than in surface sediments, and it showed to be inhibited in ~80% in presence of molybdate, indicating that sulfate-reducing bacteria (SRB) would be well involved in the process of Hg methylation of both, sediments and settling particles (Fleming et al., 2006). As these bacteria are anaerobic, the high methylation rates found in settling particles could be mainly explained by the combination of two aspects; (i) by the differences on C/N ratio, and HI and OI, as proxies of the quality of the organic OM. Higher C/N ratios were observed in sediments than in settling particles, which means that the OM was fresher than in sediments. HI and OI values confirmed this, settling particles showed high HI values and low OI values (and vice-versa in sediments), pointing to an algal content in OM in settling particles, and more terrestrial in sediments. Thus, theoretically, MeHg should be bound to the planktonic settling particles which should be of easier uptake for SRB (Schartup et al., 2015). (ii) Settling particles would be formed by aggregates with particular physico-chemical conditions creating gradients of dissolved oxygen at micrometer scale, allowing SRB-survival in low oxygen microzones (Shanks and Reeder, 1993) and consequently being able to methylate. Finally, it is important to note that the high concentrations and fluxes of MeHg were found much more mitigated in sediments, suggesting either a degradation of this molecule from the production to the sedimentation, or a possible influence of a sampling artefact in the methylation process. Further studies are needed to completely understand the role of sediment traps in MeHg and/or the formation and degradation of MeHg in these ecosystems.

2. Conclusions

This work showed the importance of particle-bound contaminant behavior in a freshwater system and the key factors affecting the fate of pollutants reaching the lake from the shore. A high-resolution multi-proxy study was critical to determine the history of mercury contamination in Vidy Bay. In general all the trace metals reached their maximum values just after the implementation of the WWTP in 1964, mercury also increased from this date; however its maximum contamination peak corresponded to 1986. The inputs of the WWTP also changed the sedimented OM providing HI and OI values that are typical of algal-rich sediments. THg concentrations showed that the most contaminated area of Vidy Bay was the closest to the outlet pipe since the concentration on sediments and pore waster was distance-dependent. In these sediments, THg partition coefficient (sediment-pore water); and THg and MeHg concentrations in non-filtered overlying waters were significantly high, showing an interaction between the sediment boundary layer and particles in the water column. Thus, mercury concentrations and fluxes in suspended particles were studied, showing that THg particulate inputs from the shore decreased towards the deep lake, and, although the distal site was at almost 3 km of the shoreline, it was still affected by littoral inputs. THg resuspension was noticed 5m above the sediments. This process was of greater magnitude in the deeper sites likely due to the inputs caused by the depth gradient between sites. THg was a good tracer of contamination in freshwater particles.

On the other hand, as predicted by non-filtered overlying water measurements, settling particles were highly charged on MeHg. Furthermore, MeHg concentrations of settling particles largely exceeded the concentration in surface sediments that were supposed to be the propitious sub-oxic environment for Hg-methylation processes. Indeed, significantly higher potential methylation yields were measured in settling particles than in sediments. These differences in the methylation processes were ascribed to differences on the quality of OM between settling particles and sediments. It was observed that OM in settling particles was fresher or more algal-like than in sediments, which can readily be up-taken by microorganisms responsible for Hg-methylation.

However, Hg-methylation in the oxic freshwater column remains poorly understood. Although redox and dissolved O₂ measurements in the sediment traps did not show drastic changes compared to the water column conditions, the sediment traps might have artificially enhanced Hg methylation compared to the open water column due to their configuration. The particular biochemical behavior of MeHg and its dependence of microorganisms to be synthetized, MeHg could not be used for tracing the transport of particle-bound contaminants.

3. Perspectives

In order to have a better idea of the actual quality and origin of the organic matter in sediments affected by the effluent of the WWTP, it is suggested to further complete OM analysis by carrying out more measurements by transmission electron microscope (TEM) in sediments as those studied in Chapter II.

Regarding Hg fluxes, it would be interesting the measure THg (and MeHg) fluxes in sediments at NG3 to better understand why at NG2 and NG3, the concentrations of THg is similar in sediments, but different in settling particles.

Finally, to better constrain the role of settling particles on Hg-methylation processes further experiments should be carried out. One of the main artifacts of the experiments used in this study was that sediment traps could have induced micro anoxic environments themselves. A good way to exclude this possible effect of the traps would be sampling enough volume of water and centrifuge on-site, and then particles should be immediately frozen to avoid induced methylation. At the same sample site, different sediment layers should be collected at 0 - 1.5 cm and 1.5 - 3 cm depth. Amendments with specific mercury isotopes should be performed in both, settling particles and sediments, to determine the potential rates of mercury methylation. This would avoid the possible artifact of the traps and would help to balance the importance of MeHg formation in each compartment for a better understanding of Hg cycle in

freshwater lakes. One of the disadvantages of this experiment would be that particles would likely be damaged during the centrifugation.

References

- ANNEVILLE, O., MOLINERO, J. C. S., S., BALVAY, G. & GERDEAUX, D. 2006. Long-term changes in the copepod community of Lake Geneva. *Journal of plankton research*, 29, 49-59.
- BRAVO, A. G. 2010. *Mercury methylation and trophic transfer in contaminated freshwater systems*. Ph.D. Thesis, no. 4276, Universite de Geneve.
- ECKLEY, C. S., WATRAS, C. J., HINTELMANN, H., MORRISON, K., KENT, A. D. & REGNELL, O. 2005. Mercury methylation in the hypolimnetic waters of lakes with and without connection to wetlands in northern Wisconsin. *Canadian Journal of Fisheries and Aquatic Sciences*, 62, 400-411.
- FLEMING, E. J., MACK, E. E., GREEN, P. G. & NELSON, D. C. 2006. Mercury methylation from unexpected sources: Molybdate-inhibited freshwater sediments and an iron-reducing bacterium. *Applied and Environmental Microbiology*, 72, 457-464.
- GRAHAM, N. 2015. The fate of sediment-bound contaminants: a case study of Vidy Bay (Lake Geneva, Switzerland). Ph.D. Thesis, no. 4760, Universite de Geneve.
- HEIMBURGER, L. E., COSSA, D., MARTY, J. C., MIGON, C., AVERTY, B., DUFOUR, A. & RAS, J. 2010. Methyl mercury distributions in relation to the presence of nanoand picophytoplankton in an oceanic water column (Ligurian Sea, North-western Mediterranean). *Geochimica Et Cosmochimica Acta*, 74, 5549-5559.
- MACDONALD, D. D., INGERSOLL, C. G. & BERGER, T. A. 2000. Development and evaluation of consensus-based sediment quality guidelines for freshwater ecosystems. *Archives of Environmental Contamination and Toxicology*, 39, 20-31.
- MASSON, M. & TERCIER-WAEBER, M. L. 2014. Trace metal speciation at the sediment-water interface of Vidy Bay: influence of contrasting sediment characteristics. *Aquatic Sciences*, 76, S47-S58.
- SCHARTUP, A. T., NDU, U., BALCOM, P. H., MASON, R. P. & SUNDERLAND, E. M. 2015. Contrasting Effects of Marine and Terrestrially Derived Dissolved Organic Matter on Mercury Speciation and Bioavailability in Seawater. *Environmental Science & Technology*, 49, 5965-5972.
- SHANKS, A. L. & REEDER, M. L. 1993. Reducing Microzones and Sulfide Production in Marine Snow. *Marine Ecology Progress Series*, 96, 43-47.
- VERNET, J. P. & VIEL, M. 1984. Métaux lourds dans les sédiments lacustres. *Comission Internationale pour la Protection des Eaux du Léman Contre la Pollution.*, Synthèse des travaux 1957-1982, Lausanne, 227-238.